Deciphering the Interaction Between *Leishmania* and *Leishmania RNA Virus 1*

Andrea Lafleur

Department of Microbiology and Immunology

McGill University, Montreal, Canada

March 2023

A thesis submitted to McGill University in partial fulfillment of the requirements of the degree of Master of Science.

TABLE OF CONTENTS

TABLE OF FIGURES

Chapter 1. Literature Review and Research Objectives

Chapter 2. Methods, Results and Discussion

TABLE OF TABLES

Chapter 1. Literature Review and Research Objectives

Chapter 2. Methods, Results and Discussion

Appendix

ABSTRACT

The protozoan parasite *Leishmania* is the causative agent of leishmaniasis – a neglected tropical disease responsible for an annual 1.5-2 million new cases and 70,000 deaths globally. Northward vector migration and increased incidence of drug resistance pose an important threat to global health. Endogenous infection of species of the *Viannia* subgenus by the *Totiviridae Leishmania RNA Virus 1* (LRV1) is predictive of the development of severely disfiguring mucocutaneous leishmaniasis and of first-line treatment failure. Recently, we have shown that LRV1 hijacks leishmanial exosomal pathways to acquire a viral pseudo-envelope while exiting the cells, facilitating its uptake by other naive *Leishmania* of the *Viannia* subgenus (ex. *L. v. panamensis*). However, the impact of the acute infection of *L. v. panamensis* by LRV1 remains uncharacterized. We hypothesized that LRV1 modulates parasitic pathogenesis and that *L. v. panamensis* utilizes antiviral mediators to control viral infection. We further suspected that the parasite would overcome viral infection through ancestral antiviral immune mechanisms retained over the course of evolution. Herein, exosome-enveloped LRV1 was isolated by filtration/ultracentrifugation and was characterized by Nanoparticle Tracking Analysis and Transmission Electron Microscopy. Following PCR validation of LRV1 presence in extracellular vesicle preparations, exosomes were directly inoculated in *L. v. panamensis* culture and infection was established. Assessment of proteomic landscapes of naïve and infected *L. v. panamensis* was conducted by LC-MS/MS, revealing that LRV1 significantly modifies the parasite's proteome, enriching key fitness and virulence assets, which were further corroborated with functional assays. In addition, clearance of LRV1 by *L. v. panamensis* was attained over a 10-week course of infection, during which the proteomic landscape was altered accordingly, and disease severity in a murine model directly correlated with viral load. Findings stemming from this project suggest a complex

Leishmania/LRV1 interaction and could lead to elucidation of mechanisms regulating viral infection in infected hosts, including the presence of pathogen-associated pattern receptors.

RESUME

Le parasite protozoaire *Leishmania* est l'agent causal de la leishmaniose – une maladie tropicale négligée responsable de 1,5 à 2 millions de nouveaux cas et de 70 000 décès annuellement à travers le monde. La migration des vecteurs facilitée par les changements climatiques, et l'incidence accrue de la résistance aux agents thérapeutiques constituent une menace importante pour la santé globale. L'infection d'espèces du sous-genre *Viannia* par l'endosymbionte d'origine totivirale *Leishmania RNA Virus 1* (LRV1) est prédictive du développement de la *leishmaniose* cutanéo-muqueuse, une pathologie particulièrement défigurante, et de l'échec des traitements de première ligne. Récemment, nous avons montré que LRV1 utilise les voies exosomales du *Leishmania* pour acquérir une pseudo-enveloppe virale, facilitant l'infection d'autres *Leishmania* naïfs du sous-genre *Viannia* (ex. *L. v. panamensis*). Cependant, l'impact de l'infection aiguë de *L. v. panamensis* par LRV1 demeure non caractérisé. Nous avons donc émis l'hypothèse que LRV1 module la pathogenèse parasitaire et que *L. v. panamensis* produit des médiateurs antiviraux pour contrôler l'infection virale. Nous suggérions également la possibilité que le parasite surmonterait l'infection virale grâce à des mécanismes immunitaires antiviraux ancestraux conservés au cours de l'évolution. Dans notre étude, des exosomes contentant du LRV1 ont été isolés par filtration/ultracentrifugation et ont été caractérisés par analyse de nanoparticules et par microscopie électronique à transmission. Après validation de la présence du LRV1 dans nos préparations de vésicules extracellulaires par PCR, les exosomes ont été directement inoculés dans des cultures de *L. v. panamensis*, permettant l'établissement de l'infection. La caractérisation du protéome de *L. v. panamensis* naïf et infecté a été effectué par LC-MS/MS, révélant que LRV1 module significativement le protéome du parasite, enrichissant les médiateurs de virulence et d'aptitude à la survie, qui ont ensuite été corroborés par des tests fonctionnels. De plus,

l'élimination du LRV1 par *L. v. panamensis* a été atteinte au cours d'une période de 10 semaines, au cours de laquelle le protéome a été modulé, et la sévérité de la maladie dans un modèle murin était directement corrélée à la charge virale. Les résultats de cette étude suggèrent une interaction complexe entre *Leishmania* et LRV1 et pourraient conduire à l'élucidation des mécanismes de régulation de l'infection virale chez les hôtes infectés, y compris la présence de récepteurs qui pourraient reconnaitre des motifs moléculaires associés à des pathogènes.

ACKNOWLEDGMENTS

First and foremost, I would like to express my deepest gratitude to my supervisor, Dr. Martin Olivier, for his continued support and mentorship throughout the entirety of my McGill career, first as a volunteer in the lab, then as an Honours student, and finally to the completion of my master's degree. Your dedication to science and the advancement of knowledge is admirable. Thank you for welcoming me into your lab and giving me the opportunity to learn and grow as a scientist. To my advisory committee, Dr. Selena Sagan, and Dr. Janusz Rak, thank you for your support of this project and for your invaluable feedback and advice. Though our meetings took place virtually, your investment in my progress and your insight into the project were much appreciated.

I would like to extend my sincere thanks to both past and present lab members for their support and friendship throughout my years in the lab. Many thanks to Dr. Alonso Da Silva Lira Filho and to Caroline Martel for being my first mentors and for teaching me indispensable laboratory skills. I am also thankful to Aretha Chan, Andrea Vucetic, Nada Al-Emadi, Fio Vialard and Dr. Mohamed Daoudi for welcoming me into the lab at various points throughout my undergraduate degree. Thanks should also go to Dr. Emanuella Fajardo for her help in starting the project, and to Sabrina Sgro and Dr. Marine Leroux for our collaborative work. I would like to express my deepest appreciation to Line Larivière for her support throughout my graduate degree, and for being such a warm presence in the lab. I owe special thanks to Carlos Villalba-Guerrero for his assistance with *in vivo* experiments, to George Dong for his expertise on extracellular vesicles, to Édouard Charlebois for his help with qPCR, and to Dr. Victoria Wagner for her knowledge of leishmanial drug resistance. Thank you for your guidance and, above all, for your friendship. I would be remiss

in not mentioning Morgane Brouillard-Galipeau and Myriam Beaulieu, who contributed immensely to the positive lab environment.

I'd like to thank my parents, Catherine, and Philippe, for fostering my curiosity and for their unwavering support, and my sister, Emilie, for believing in me and for giving me a safe space to vent. Thank you for your interest in my project, and for all the proofreading you did and practice presentations you attended; I owe my success to you. I'd also like to thank Chauncey for his companionship, especially during the height of the pandemic; your presence is missed.

Thanks must also go to my grandmother Marika, whose passion for science encouraged my own, and to my uncle Andy, who gifted me my very first microscope. I would also like to thank my grandparents Margaret, Bill, and Robert who watched over me throughout this journey.

Lastly, I'd like to thank Arundhati Nair, Nicole Giroux, Julia Foody, Stephanie Da Silva, Gabrièle Fontaine, Florence Cardinal, Sarah Assalian and Sanoussy Diallo, whose friendship was invaluable over the past few years.

PREFACE

This thesis was written in accordance with McGill University's Graduate and Postdoctoral Studies (GPS) Thesis Guidelines. The candidate has chosen to present their thesis as a manuscript-based (article-based) thesis: "As an alternative to the traditional format, a thesis may be presented as a collection of scholarly papers of which the student is the first author or co-first author. […] A manuscript-based master's thesis must include the text of one or more manuscripts published, submitted or to be submitted for publication" and "contain additional text that connects the manuscript(s) in a logical progression from one chapter to the next, producing a cohesive, unitary focus, and documenting a single program of research."

All work towards this thesis was performed under the supervision of Dr. Martin Olivier. The candidate is the first author of the manuscript presented in Chapter II, which will be submitted for publication. Author contributions are as described:

The project was designed and conceptualized by MO. *In vitro* experiments were performed by AL. *In vivo* experiments were prepared by MO and AL and carried out by MO and CV. NTA was performed by AL, and TEM imaging was performed by AL and GD. Sample preparation for LC-MS/MS proteomics and phosphoproteomics, bioinformatic analysis and data curation and analysis were completed by AL. In addition, comprehensive review of the literature and all writing in this master's thesis was performed by AL.

LIST OF ABBREVIATIONS

2-CMA	2′C-Methyladenosine
AGO	Argonaute
AIDS	Acquired Immunodeficiency Syndrome
Akt	Protein Kinase B
AP-1	Activator Protein 1
ASC	Apoptosis-Associated Speck-Like Protein Containing A CARD
ATP	Adenosine Triphosphate
BIRC	Baculoviral IAP Repeat Containing
BLAST	Basic Local Alignment Tool
BMDM	Bone Marrow-Derived Macrophage
CCL	C-C Motif Ligand
cDNA	Complementary DNA
CL	Cutaneous Leishmaniasis
CPA	Cysteine Protease A
CPB	Cysteine Protease B
CPC	Cysteine Protease C
CR3	Complement Receptor 3
CRISPR	Clustered Regularly Interspaced Short Palindromic Repeats
Csp1	Cryspovirus 1
DALY	Disability-Adjusted Life Year
DCFDA	Dichlorofluorescein Diactetate
DCL	Diffuse Cutaneous Leishmaniasis
DENV	Dengue Virus

dsRNA	Double-Stranded RNA
EBOV	Ebola Virus
EBV	Epstein-Barr Virus
EF1a	Elongation Factor 1 Alpha
eIF2a	Eukaryotic Initiation Factor 2 Alpha
ESCRT	Endosomal Sorting Complexes Required for Transport
EV	Extracellular Vesicle
FACT	Facilitates Chromatin Transcription Protein
GIPL	Glycoinositolphospholipids
GLV	Giardia Lamblia Virus
GO	Gene Ontology
GP63	Glycoprotein 63
GPI	Glycosylphosphatidylinositol
GPX	Glutathione Peroxidase
H_2O_2	Hydrogen Peroxide
HCMV	Human Cytomegalovirus
HCV	Hepatitis C Virus
HIV	Human Immunodeficiency Virus
IFN	Interferon
IgG	Immunoglobulin G
IL	Interleukin
iNOS	Inducible Nitric Oxide Synthase
IRF3	Interferon Regulatory Factor 3
JAK/STAT	Janus Kinase and Signal Transducer and Activator of Transcription
kDNA	Kinetoplast DNA

KMP11	Kinetoplast Membrane Protein 11
LACK	Receptors For Activated Kinase C
LAMB	Liposomal Amphotericin B
LC-MS/MS	Liquid Chromatography Tandem Mass Spectrometry
LMIC	Low- And Middle-Income Country
LPG	Lipophosphoglycan
LR	Leishmania Recidivans
LRV1	Leishmania RNA Virus 1
LRV2	Leishmania RNA Virus 2
M1	Classically Activated Macrophage
M2	Alternatively Activated Macrophage
MAPK	Mitogen-Activated Protein Kinase
MCL	Mucocutaneous Leishmaniasis
MF	Miltefosine
MIP	Macrophage Inflammatory Protein
MIPT3	Microtubule-Interacting Protein Associated with Traf3
mtDNA	Mitochondrial DNA
MVB	Multivesicular Body
NET	Neutrophil Extracellular Trap
NF-κB	Nuclear Factor Kappa-Light-Chain-Enhancer of Activated B Cells
NK	Natural Killer
NKG2D	Killer Cell Lectin Like Receptor K1
NLRP	NOD-, LRR- And Pyrin Domain-Containing Protein
NLV1	Lepsey Narna-Like Virus 1
NO	Nitric Oxide

NTA	Nanoparticle Tracking Analysis
NTD	Neglected Tropical Disease
NW	New World
OPB	Oligopeptidase B
OW	Old World
PCR	Polymerase Chain Reaction
PKA	Protein Kinase A
PKC	Protein Kinase C
PKDL	Post-Kala-Azar Dermal Leishmaniasis
PM	Paromomycin
PPG	Proteophosphoglycan
PPI	Protein-Protein Interaction
PRDX	Peroxiredoxin
PserNV1	Pser Narna Virus 1
PSG	Promastigote Secretory Gel
PTM	Pentamidine
PTP1B	Protein Tyrosine Phosphatase 1B
RISC	RNA-Induced Silencing Complex
RNAi	RNA Interference
ROS	Reactive Oxygen Species
SARS-CoV2	Severe Acute Respiratory Syndrome Coronavirus 2
Sb(III)	Trivalent Antimonials
Sb(V)	Pentavalent Antimonials
SDM	Schneider's Drosophila Medium
SHP-1	Src Homology Region 2 Domain-Containing Phosphatase-1

SKP1	S-Phase Kinase Associated Protein 1
SNARE	SNAP-Receptor
SOD	Superoxide Dismutase
ssRNA	Single-Stranded RNA
STAT-1	Signal Transducer and Activator of Transcription 1
SUMO1	Small Ubiquitin-Like Modifier 1
TCPTP	T-Cell Protein Tyrosine Phosphatase
TEM	Transmission Electron Microscopy
TGF	Transforming Growth Factor
Th1	T Helper Type 1
Th17	T Helper Type 17
Th2	T Helper Type 2
TIR	Toll/Interleukin-1 Receptor
TLR	Toll-Like Receptor
TNF	Tumor Necrosis Factor
TrCP	F-Box/WD Repeat-Containing Protein 1A
TRDX	Tryparedoxin
TRIF	TIR-Domain-Containing Adapter-Inducing Interferon-B
tRNA	Transfer RNA
TVV	Trichomonas Vaginalis Virus
TXN	Thioredoxin
VL	Visceral Leishmaniasis
VPS	Vacuolar Protein Sorting
WHO	World Health Organization

CHAPTER 1. LITERATURE REVIEW AND RESEARCH OBJECTIVES

1.1 LEISHMANIA

Leishmaniasis is a vector-borne parasitic infection caused by the intracellular trypanosomatid *Leishmania.* With an estimated annual burden of 1.5-2 million cases and 70,000 deaths worldwide, most of which occur in tropical and subtropical regions, leishmaniasis has been recognized as a neglected tropical disease (NTD) by the World Health Organization (WHO) since 2012 [1,2]. In recent years, emerging drug resistance and northward migration of phlebotomine sandflies have highlighted the public health risk posed by leishmaniasis, underscoring the need for better insight into the parasite's pathophysiology for eventual development of effective therapeutics.

1.1.1 Taxonomy and Cellular Physiology

The genus *Leishmania* belongs to the order *Kinetoplastida* and the family *Trypanosomatidae* (Summarized in Figure 1) [3]. This group of parasitic protozoa includes 39 distinct species, more than 20 of which are pathogenic to humans [3,4]. *Leishmania* species have classically been characterized according to their geographical distribution, wherein Old World (OW) species are endemic to the Eastern hemisphere, and New World (NW) species are native to the Western hemisphere, though the practicality of this classification is challenged by the expansion of endemic regions [5].

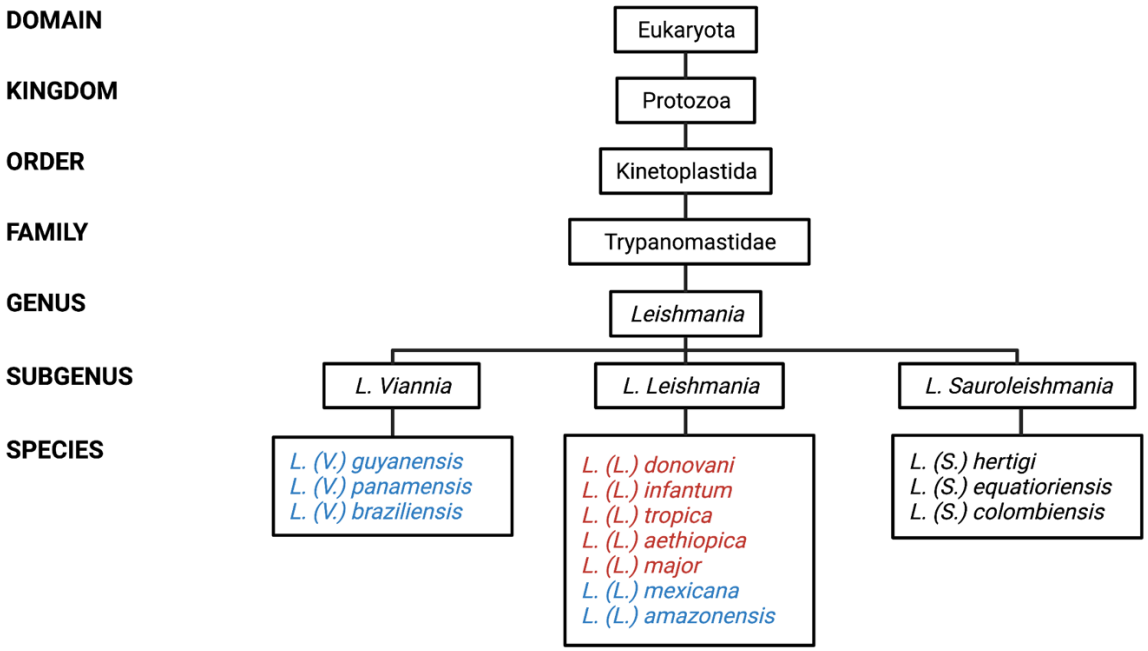

Figure 1. Hierarchal taxonomic classification of the Leishmania genus. For *L. Viannia* and *L. Leishmania* subgenera, NW species are identified in blue, and OW species are identified in red. Adapted from Maurício, 2018 [3].

Leishmania have two major cellular morphologies: the promastigote and the amastigote. While promastigotes are characterized by an elongated ovoid cell body and a long flagellum, which permits cell motility, amastigotes are smaller, rounder, and are immotile due to their short flagellum, which barely extends from the cell body [6]. Though these forms may seem vastly different, their overall subcellular architecture is constant (Summarized in Figure 2). *Leishmania* subcellular structure is comprised of organelles that are highly conserved between eukaryotes, including a nucleus, a mitochondrion, and a Golgi apparatus, as well as structures that are characteristic of *Trypanosomatidae*, like the flagellum, the flagellar pocket and the kinetoplast [6]. Anterior to the nucleus is the flagellar pocket, an invagination of the cellular membrane around the base of the flagellum, which acts as a key interface for endocytosis and exocytosis [6]. The flagellum extends from the basal body, which is connected to the kinetoplast – a network of

concatenated mitochondrial DNA (kDNA or mtDNA), made up of minicircles (0.5-3kb) and maxicircles (30-40kb), which makes up 10-30% of total cellular DNA [6]. The *Leishmania* genome is haploid, and nuclear genetic material is variable between species, ranging from 29-36 Mb organized onto 34-36 chromosomes [7]. Chromosomal DNA displays high gene density on both strands and includes polycistronic gene clusters that heavily rely on trans-splicing and RNA editing for gene expression [8]. Despite this prokaryotic-like transcription process, *Leishmania* genes themselves are mostly orthologous to other eukaryotes, considering biological pathways are highly conserved throughout the eukaryotic phylogenetic tree [9].

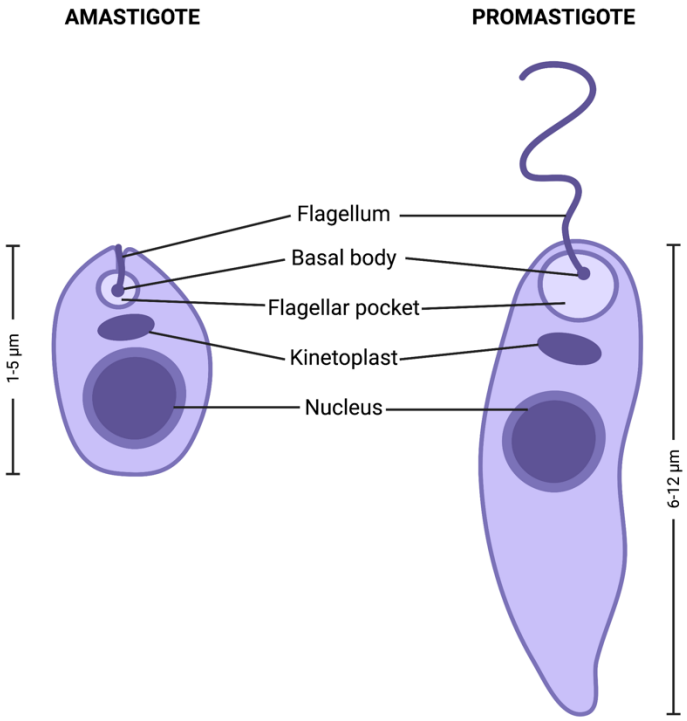

Figure 2. *Leishmania* amastigote and promastigote morphology. Adapted from Sunter and Gal, 2017 [6].

Important functional differences have accumulated between species of the *Leishmania* genus since their divergence, enabling subclassification according to three distinct subgenera: *L. (Leishmania), L. (Viannia),* and *L. (Sauroleishmania).* Notably, while species of the *L. (Viannia)* lineage have

retained genes for RNA interference (RNAi), including *Argonaute* (AGO) and *Dicer*, this is not the case for species of the other subgenera [10]. Additionally, though both *L. (Leishmania)* and *L. (Viannia)* are pathogenic to mammals, *L. (Sauroleishmania)* primarily infects reptiles and is therefore not a focus of this literature review [11].

1.1.2 Clinical Features

Leishmaniasis has a wide range of clinical presentations, largely dependent on the species causing the primary infection, in addition to environmental and host-related factors (Summarized in Figure 3) [12]. Visceral leishmaniasis (VL), or kala-azar, is the most severe pathological form of the disease, with fatality rates up to 95% if left untreated [12]. Caused predominantly by species of the *L. (Leishmania) donovani* complex (*L. donovani* and *L. infantum*), VL is characterized by a systemic infection that predominantly affects the liver and spleen [13]. The most common clinical manifestation of VL includes persistent fever and splenomegaly [14]. In 5-10% of VL cases in India, and in up to 50% of VL cases in Sudan, post-kala-azar dermal leishmaniasis (PKDL), which presents as nodular dermal rashes, develops several months to several years following treatment [15–17]. Though often self-healing, PKDL skin lesions remain a reservoir for transmission [14].
The most common form of disease is cutaneous leishmaniasis (CL), which usually presents as a small erythema at the site of the sandfly bite that ulcerates over subsequent weeks and months [1]. CL can be caused by multiple species of the *L. (Leishmania)* and *L. (Viannia*) subgenera, and lesions are often localized and self-limiting within several months of disease onset [1]. 1-10% of infections caused by *L. (Viannia*) species (*L. v. guyanensis*, *L. v. braziliensis* and *L. v. panamensis)* progress to mucocutaneous leishmaniasis (MCL) 1-5 years after resolution of the primary cutaneous lesion [18]. MCL is characterized by destructive and disfiguring lesions of the

nasopharyngeal mucosa, and often requires aggressive treatment regimens. Opportunistic secondary bacterial infections are common and incur significant mortality [1]. Other complications of CL include widespread non-ulcerating lesions caused by *L. amazonensis, L. aethiopica* or *L. mexicana* in diffuse cutaneous leishmaniasis (DCL), and re-activation and expansion of resolved *L. tropica* lesions in *Leishmania* recidivans (LR) [14,19,20].

Figure 3. Clinical manifestations of leishmaniasis. PKDL and MCL images are reproduced from Burza *et al.* [14], DCL and CL images are reproduced from Mann *et al.*[13], VL image is reproduced from the WHO/PAHO [21], and LR image is reproduced from Gitari *et al.* [20].

1.1.3 Epidemiology

Leishmaniasis is a NTD that is endemic to 98 countries, the majority of which are low and middle income countries (LMICs) in Africa, Asia, and South and Central America (Summarized in Figure 4) [13,22]. Globally, there are an estimated 12 million cases of leishmaniasis, with a further 1.5-2 million new cases and 70,000 deaths reported annually [14,23]. Due to low numbers of mandatory reporter countries and a high proportion of subclinical or asymptomatic infections, these numbers are widely underreported [23]. In fact, seroprevalence of VL-causing *L. donovani* ranges from 7-

63% in endemic regions, indicating high rates of asymptomatic infection [14,24]. Along with mortality, leishmaniasis incurs significant morbidity, with some estimates as high as 2.4 million disability-adjusted life years (DALYs), and important health expenditure for both individuals and healthcare systems [25].

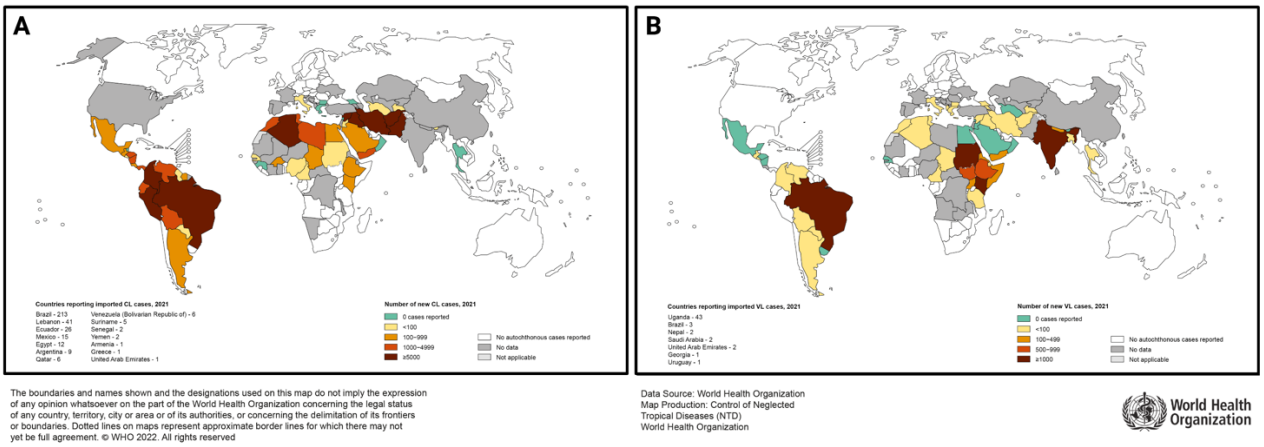

Figure 4. Global distribution of reported leishmaniasis cases. Maps representing endemicity of A) CL and B) VL for 2021. Reproduced from the WHO [12].

While CL is endemic to 70 countries, over 90% of global cases occur in Afghanistan, Algeria, Brazil, Pakistan, Peru, Saudi Arabia and Syria [1]. In the Eastern hemisphere, CL is caused only by *L. (Leishmania)* species, while in the Western hemisphere, infection etiology includes both *L. (Leishmania)* and *L. (Viannia)* species [1]. *L. (Viannia) braziliensis* alone is responsible for up to 300,000 CL infections, with major reservoirs in domestic and stray dog populations in Central and South America [14]. Though almost all reported cases of leishmaniasis involve vector transmission, rare vector-independent infections have occurred congenitally, via blood transfusion, through organ transplantation and drug-users sharing needles [14,26–29].

In endemic regions, the incidence of CL increases until the age of 15, after which immunity is acquired and risk of infection declines [14]. Leishmaniasis is also more prevalent in males than in females – a sex bias that is likely occupational, with males more frequently employed in positions

with longer vector exposure [1,30]. Other risk factors include poor housing conditions, which can be conducive to sandfly resting and mating, and the presence of peridomestic animals, which can act as reservoirs [1,31].

Both immunosuppressive therapeutics and infection by HIV, which are major causes of immune compromisation, increase the risk of leishmaniasis development by up to 100 times and up to 2300 times, respectively [23]. HIV/*Leishmania* co-infection dramatically precipitates AIDS development, as both pathogens target macrophages and DCs [14,32]. Immune compromisation is also a significant risk factor for CL-associated complications, with up to 68% of HIV/*Leishmania* co-infected patients developing MCL [30].

Over 350 million individuals currently live in regions endemic to leishmaniasis and are at risk of contracting the disease [1,14]. While cases of VL have declined in recent years, CL infection incidence continues to rise – a trend that will only accelerate in the advent of climate change and urbanization. Geographical distribution of leishmaniasis is dependent on the vector's ecological niche, which has historically been limited to humid and forested habitats [33]. Deforestation and transformation of these environments has increased proximity between humans and sandflies, increasing risk of infection [33]. Ambient temperature is an important climatic indicator of vector spread, as several phlebotomine sandfly species are unable to survive in temperatures below 10-15˚C for sustained periods of time [34]. Global average temperature increase and rearrangement of climates pose the risk of endemic region expansion [35]. Northward migration of phlebotomine sandflies is already apparent, with CL now endemic to Texas and Oklahoma and additional sporadic *Leishmania* infections reported throughout the southern United States [36]. Establishment of leishmaniasis in Central and Northern Europe is expected by 2061-2080, given current vector control and mitigation strategies [34]. As climate change inflates the incidence of natural disasters

and causes climate migration, epidemic potential of leishmaniasis increases, with previous outbreaks reported in displaced populations following floods, landslides, earthquakes and cyclones [37]. Thus, leishmaniasis poses an important threat to global health, and while already well-established in some regions, will likely emerge in the global North in coming years [33]. As has become clear with other zoonotic diseases, a "One Health" approach using coordinated efforts to target the health of populations, animals, and of ecosystems will be crucial for the control of leishmaniasis [38].

1.1.4 Life cycle

Leishmania parasites have a digenic lifecycle, requiring alternation between a phlebotomine sandfly vector and a mammalian host (Summarized in Figure 5). *Phlebotomus* (in the OW) or *Lutzomyia* (in the NW) sandflies become infected with *Leishmania* when they take a bloodmeal from a mammalian reservoir – most frequently a human, rodent or canid [1]. Rather than from the blood itself, it is the tissue damage from the feeding process that causes sandflies to ingest parasitized tissue-resident cells [39]. The rapid shift in temperature and pH due to vector uptake causes the immotile amastigotes present within the bloodmeal to transform into procyclic promastigotes – a form which, while remaining somewhat ovoid, short and only partially motile, is extremely proliferative [39]. Over several days, haptonomad promastigotes then migrate throughout the sandfly's digestive tract, attaching to epithelium of the midgut (species of *L. (Leishmania)*) or the hindgut (species of *L. (Viannia)*) [40,41]. Within the midgut, parasites produce promastigote secretory gel (PSG), a thick gel-like substance composed of filamentous proteophosphoglycan that forms a scaffold for the promastigotes near the sandfly's proboscis, thus concentrating them prior to egestion [39]. Finally, parasites undergo metacyclogenesis, during

which their flagella extend to about twice the length of their bodies, proliferation decreases and critical virulence factors for infection are upregulated [41,42].

Upon their next bloodmeal, sandflies inoculate highly infective and motile metacyclic promastigotes into the mammalian host's dermis. Along with the parasites, the sandfly's inoculum contains PSG and saliva, both of which have established roles in the potentiation of infection [39]. Immediately following inoculation, neutrophils are recruited to the site of infection, where they release neutrophil extracellular traps (NETs) and internalize parasites [43]. While their short lifespan prohibits parasitized neutrophils from acting as final hosts to *Leishmania*, their propensity for apoptosis is fundamental to their "Trojan horse" function [44]. Apoptotic neutrophils recruit macrophages which, in turn, phagocytose the dying cells along with their internalized parasites [42]. *Leishmania* are trafficked into the host cell's phagosome, which undergoes acidification following fusion with the lysosome – a process that causes promastigotes to differentiate into amastigotes [45]. Within this cellular structure, coined the parasitophorous vacuole, parasites divide rapidly, eventually leading to bursting of the host cell [45]. Parasites are released into the surrounding tissue, subsequently coated with IgG, then internalized by phagocytic cells through a direct interaction with Fc receptors [46]. Successful infection of a mammalian host establishes a reservoir from which sandflies can ingest parasitized cells and recommence the parasite's life cycle [22].

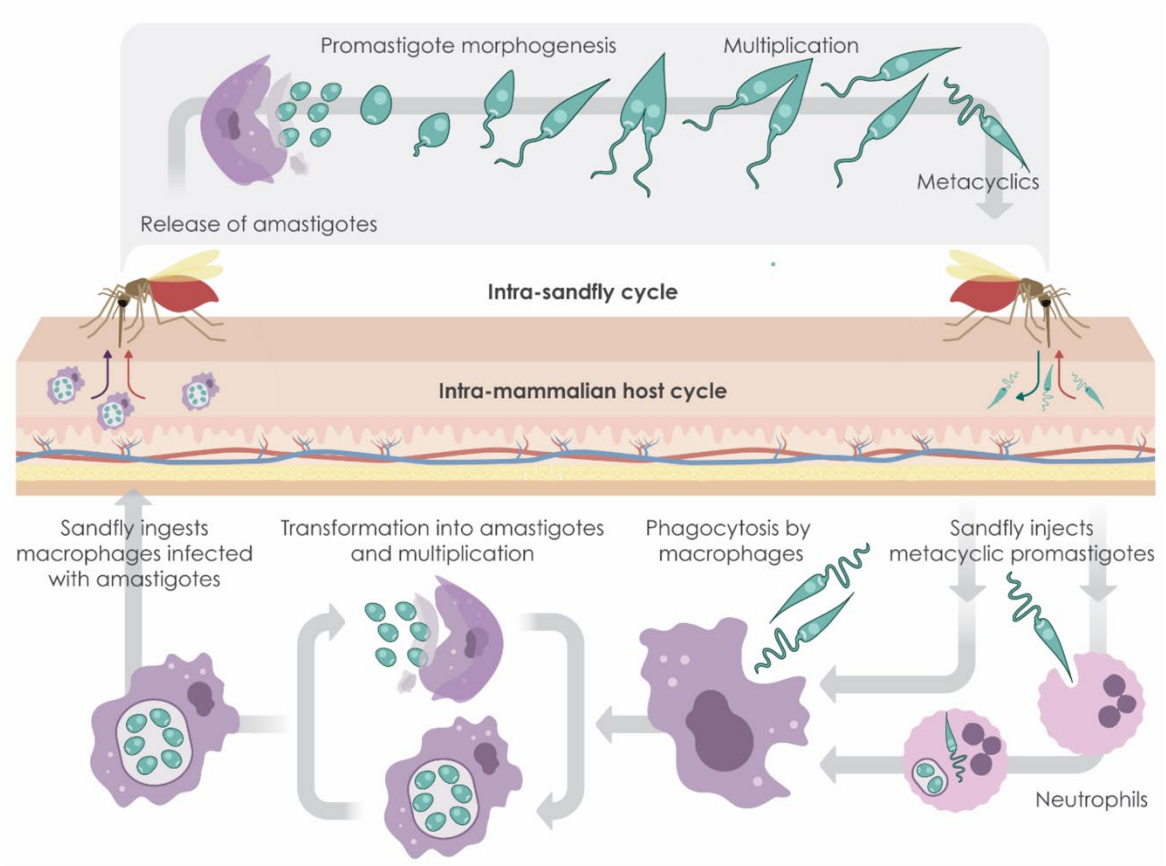

Figure 5. Digenic life cycle of Leishmania. Adapted from Olivier *et al.* [47].

1.1.5 Immunopathogenesis of CL and MCL

The immunopathogenesis of CL is dependent on complex interactions between the innate and adaptive immune systems, culminating in either parasitic clearance, acute or chronic infection. Immediately following parasite internalization, inactivated macrophages attempt to control infection through an initial burst of reactive oxygen species (ROS) [43]. Various cells at the site of infection release the chemokines MIP-1α, MIP-1β, MIP-2, which recruit additional inflammatory cells [48]. An adaptive immune response is initiated following phagocytosis of parasites by dendritic cells, which migrate to primary lymphoid tissues where they process then present *Leishmania* antigens to naïve T cells (Th0) [45]. Naïve T cells then differentiate into T helper type 1 or type 2 (Th1/Th2) effector $CD4^+$ T cells – a decision point that determines the

course of *Leishmania* infection [43]. While a balanced Th1/Th2 response is required for infection control, the Th1 response, characterized by the production of proinflammatory cytokines (IL-12, IFNγ and TNF), promotes the clearance of *Leishmania* infection and is the primary phenotype associated with disease resolution [14,43,49]. In contrast, the Th2 response induces the production of anti-inflammatory cytokines (IL-4, IL-10, IL-13 and TGFβ) – a process that, while potentially protective against excessive tissue damage, enables parasitic persistence within host cells [14]. The presence of Th17 lymphocytes, which are IL-17-producing $CD4^+$ T cells, contributes to immunopathogenesis through its inflammatory mediators. High levels of IL-17 have been reported to induce hyperinflammation and tissue damage and are inversely correlated to the regulatory cytokine IL-10 [50,51].

Macrophages are both the canonical host cell for *Leishmania* and important effectors in parasitic clearance. Macrophages can be classically activated (M1) or alternatively activated (M2) – a designation based on Th1/Th2 phenotypes whereby M1 macrophages are pro-inflammatory and associated with intracellular pathogen clearance, and immunomodulatory M2 macrophages play a role in disease progression [52]. The presence of Th1 or Th2 cytokines in the cellular microenvironment is the main driver of a respective M1 or M2 macrophage polarization, though IFNγ produced by NK cells may cause M1 polarization at early timepoints post-infection [50,52]. In addition, IL-12 produced by M1 macrophages can stimulate T cell differentiation into Th1, underscoring the crosstalk between innate and adaptive immune cells for the establishment of a sustained response [52]. While the initial oxidative burst in naïve macrophages is often insufficient to kill parasites, the production of microbicidal mediators by M1 macrophages plays an essential role in parasite clearance [43,50]. Along with robust generation of ROS, the expression of

inducible nitric oxide synthase (iNOS) following stimulation by Th1 cytokines prompts the production of highly leishmanicidal nitric oxide (NO) [50].

The role of the inflammasome in parasitic clearance or persistence is more elusive. While several groups have reported that the upregulation of IL-1β and sustained NLRP3 inflammasome activation can trigger NO-mediated parasitotoxic activity, other studies have revealed that the inflammasome promotes pathology and parasitic growth [53–56]. The propensity for parasites to activate or inhibit the inflammasome for survival is potentially dependent on the species of *Leishmania* causing infection and the stage of infection [57].

In the context of localized CL, a properly coordinated Th1 response often culminates in the resolution of infection [50]. Though most parasites are cleared, a low number persist subclinically, enabling continuous antigen presentation and generation of a memory response [50]. However, recurrence by reactivation may occur, often progressing to a more severe form of disease, as is the case with DCL [14].

While Th1 may be considered to be the major effector of parasite clearance, it has a small "window of protective immunity" [58]. In fact, excessive skewness of the Th1/Th2 response towards an inflammatory phenotype can be pathological [51]. This is the case for MCL, which is characterized by excessive production of the pro-inflammatory cytokines IFNγ and TNFα [50].

Though the etiology of parasitic dissemination in MCL remains poorly elucidated, hallmarks of the condition include unregulated inflammatory cascades and cytotoxicity [50]. Over the course of lesion ulceration, the ratio of $CD4^+$ to $CD8^+$ T cells has been reported to shift in favour of the latter [50,59]. Rather than expressing IFNγ like their counterparts, these $CD8^+$ T cells express high levels of granzyme and the NKG2D-activating receptor, directly inducing cell death within lesions [50,60]. Studies of MCL biopsies have indicated abnormally large populations of neutrophils and

Th17 cells, as well as high levels of IL-17-inducing cytokines, likely potentiating the hyperinflammatory phenotype [61]. The accumulation of plasma cells and B cells in lesions and increased antileishmanial antibody titers have also been reported to contribute to apoptosis and tissue damage [62]. Altogether, both cellular and humoral mediators directly causing lesion ulceration are increasingly well established.

Heterogenous infection outcomes are a product of both host susceptibility and parasitic virulence. While large-scale genome-wide associative studies have correlated IL-6 and CCL2 polymorphisms to increased risk of MCL in humans, the capacity for parasites to modulate the immune response is crucial in pathogenesis [51].

1.1.6 Parasitic Virulence

To establish infection and chronicity, *Leishmania* have evolved a wide array of virulence factors that abrogate or modulate host immune functions [63]. While some virulence factors are secreted, others are membrane-bound, forming an integral part of the glycocalyx – a gel-like meshwork of glycosylated proteins and glycans that creates an additional physical barrier around the cell membrane [64]. Membrane-bound virulence factors, most notably lipophosphoglycans (LPGs), proteophosphoglycans (PPGs), glycoinositolphospholipids (GIPLs) and the glycoprotein 63 (GP63), share a common transmembrane domain: the glycosylphosphatidylinositol (GPI) anchor [63]. LPG mediates host cell internalization by directly binding to complement receptor CR3, integrin receptor p150/95 and mannose receptors – a process that circumvents classical triggering of inflammatory cascades in macrophages [64]. LPG and GIPL both prevent lysosomal fusion and vacuolar acidification through the inhibition of host protein kinase C (PKC), a potent regulator of the cell cycle and antimicrobial production [65]. PPG similarly inhibits macrophage function,

significantly reducing lipopolysaccharide-mediated TNFα production [65]. In addition, both Kinetoplast membrane protein 11 (KMP11), which forms a complex with LPG, and the leishmanial homolog of receptors for activated kinase C (LACK) have been shown to mildly suppress IFNγ production and induce the production of Th2 cytokines [66].

The zinc-dependent metalloprotease GP63, or leishmanolysin, has multiple immunomodulatory functions to aid with parasitic survival [65]. Among these are the degradation of the extracellular matrix for parasitic migration, the cleavage of lytic complement factor C3b to iC3b, which aids with opsonization and internalization, and the interaction with fibronectin receptors at host cell surfaces [65,67]. GP63 proteolytic activity has also been shown to activate host protein tyrosine phosphatases (SHP-1, PTP1B and TCPTP), which render macrophages refractory to IFNγ stimulation and dampen toll-like receptor (TLR) and JAK/STAT mediated inflammatory signaling [65]. Interestingly, while leishmanial EF1α has also been reported to inhibit IFNγ signaling and downstream NO production, this is not a function shared by its mammalian counterpart [65].

Both cysteine proteases (CPA, CPB, CPC) and the serine protease oligopeptidase B (OPB) have well established roles in the modulation of macrophage function, particularly through the cleavage of the host transcription factors NF-κB, STAT-1 and AP-1 [64]. OPB also regulates the virulence factor enolase, which, in addition to being an important metabolic enzyme, binds host plasminogen, likely facilitating parasitic entry into macrophages [68].

Other enzymes of the *Leishmania* secretome act as virulence factors, notably arginase and the functional catalase analogs peroxiredoxin and tryparedoxin, which all enable the parasite to overcome toxicity of the oxidative burst (NO and ROS), among other functions [64]. The host's reserves of L-arginine, which is the required substrate for NO production by iNOS, are depleted by the parasite's arginase, which hydrolyzes L-arginine into L-ornithine [64]. In addition to

detoxifying ROS, both tryparedoxin and peroxiredoxin have been shown to potentiate Th2 responses to VL, suppressing parasite clearance potential [69].

Collectively, these virulence factors, which are conserved among most *Leishmania* species but may vary in expression levels, enable parasites to survive within the hostile host environment.

1.1.7 Treatments and Drug Resistance

Due to the complex nature of *Leishmania* parasites, no effective prophylaxis has been developed to date [70]. Few novel chemotherapeutics have been developed for leishmaniasis in the past 50 years, and treatment regimens are expensive, highly toxic, and of decreasing efficacy due to emerging drug resistance [71].

While CL is often self-healing, treatment can be used to reduce scarring and decrease the risk of parasitic dissemination [1]. Identification of the causative species of *Leishmaniasis* can be beneficial to diagnosis and clinical treatment. However this requires a biopsy or aspirate, culturing of material, or other molecular methods (i.e. PCR) for identification – all of which are dependent on technical equipment and funding which may not be readily accessible in all endemic regions [1]. First-line treatment protocols for CL and MCL usually require intravenous or intramuscular administration of pentavalent antimonials (Sb(V)), though other therapeutics are commonly used throughout endemic regions (Summarized in Table 1) [1]. Antimonial treatment displays significant toxicity, with severe side effects including pancytopenia, peripheral neuropathy and nephrotoxicity [30,72]. While the direct activity of Sb(V) remains unclear, it is its metabolized counterpart, trivalent antimony (Sb(III)), which is responsible for antileishmanial activity [1]. Primary resistance to antimony has been reported in up to 15% of patients treated with pentavalent antimonials [73].

Table 1. *Leishmania*a species endemicity and common therapeutics.

Species	Clinical Presentation	High-Burden Endemic Regions	Common Treatments
Leishmania (L.) donovani	VL and PKDL	India*, Bangladesh*, Ethiopia, Sudan, and South Sudan	Systemic Sb, LAMB, and MF can be used for both VL and PKDL. Prolonged MF treatment regimens (>6 weeks) are required for PKDL.
Leishmania (L.) infantum	VL, PKDL and CL	China, Southern Europe, Brazil, south and central America	Systemic Sb, LAMB, and MF can be used for both VL and PKDL. Prolonged MF treatment regimens (>6 weeks) are required for PKDL, and CL can be treated using thermotherapy**.
Leishmania (L.) tropica	CL and LR	Eastern Mediterranean, the Middle East, northeastern and southern Africa	Intralesional Sb and thermotherapy** can be used for CL. Prolonged systemic Sb therapy is required for LR treatment.
Leishmania (L.) aethiopica	CL and DCL	Ethiopia and Kenya	Intralesional Sb is frequently used for CL. Prolonged systemic Sb therapy is required for DCL treatment.
Leishmania (L.) major	CL	Iran, Saudi Arabia, north Africa, the Middle east, central Asia, and west Africa	Intralesional Sb and PM can be used to treat CL.
Leishmania (L.) mexicana	CL and DCL	South America	Intralesional PM and thermotherapy** can be used to treat CL, and systemic MF can be used to treat both CL and DCL.
Leishmania (L.) amazonensis	CL and DCL	South America	Intralesional PM and thermotherapy** can be used to treat CL, and systemic MF can be used to treat both CL and DCL.
Leishmania (V.) braziliensis	CL and MCL	South America	Systemic Sb and LAMB or thermotherapy** can be used to treat CL. Systemic Sb, PTM, LAMB, or a combination thereof is used to treat MCL.
Leishmania (V.) guyanensis	CL and MCL	South America	Intralesional Sb, or systemic Sb, PTM or MF can be used to treat CL. Systemic Sb, PTM, LAMB, or a combination thereof is used to treat MCL.
Leishmania (V.) panamensis	CL and MCL	South America	Intralesional Sb, or systemic Sb, PTM or MF can be used to treat CL. Systemic Sb, PTM, LAMB, or a combination thereof is used to treat MCL.

CL, cutaneous leishmaniasis; DCL, diffuse cutaneous leishmaniasis; LAMB, Liposomal Amphotericin B; LR, *Leishmania* recidivans; MCL, mucocutaneous leishmaniasis; MF, Miltefosine; PKDL, post-kala-azar dermal leishmaniasis; PM, Paromomycin; PTM, Pentamidine; Sb, Antimonials; VL, visceral leishmaniasis.

*Pentavalent antimonials are not advised as a first-line treatment for VL/PKDL in the Asian subcontinent due to widespread resistance.

**Thermotherapy consists of localized and topical heat application.

Data source: Burza *et. al* [14] and Reithinger *et. al*. [1].

Pentamidine, which targets the parasite's kinetoplast, can be used as both a first-line treatment or following antimony treatment failure [74]. While effective against CL, pentamidine cures lesions at a slower rate than Sb(V), increasing the risk of MCL development [74]. Other common treatment regimens for CL and MCL include the second-line drugs Miltefosine, Paromomycin, Amphotericin B, or a combination thereof, though resistance has emerged to all major antileishmanials [72]. Drug resistance mechanisms remain a major field of study and have enabled the characterization of a significant number of implicated genes (Summarized in Table 2). Notably,

recent evidence establishes a role for extracellular vesicles in the horizontal transfer of resistance genes [75].

Table 2. *Leishmania* genes associated to drug resistance and treatment failure.

Gene Name	Gene Symbol	Drug Targeted	Effect on Drug Resistance
*ATP-binding cassette transporter C3	ABCC3	Antimonials [76]	Upregulation of ABCC3 increases efflux of antimonials [76].
*ATP-binding cassette transporter G2	ABCG2	Antimonials [77]	Upregulation of ABCG2 increases efflux of antimonials [77].
*ATP-binding cassette transporter G4	ABCG4	Miltefosine [78]	Upregulation of ABCG4 competitively imports phosphatidylcholine rather than miltefosine [78].
*ATP-binding cassette transporter G6	ABCG6	Miltefosine [79]	Upregulation of ABCG6 increases efflux of miltefosine [79].
*ATP-binding cassette transporter I4	ABCI4	Antimonials [80]	Upregulation of ABCI4 increases efflux of antimonials [80].
*Multidrug resistance 1/ P-glycoprotein	MDR1/ ABCB1	Amphotericin B, Miltefosine [81]	Upregulation of MDR1 decreases influx of amphotericin B and miltefosine [82].
*Pentamidine resistance protein 1	PRP1	Pentamidine [83]	Upregulation of PRP1 increases efflux of pentamidine [83].
14-3-3 protein	14-3-3	Antimonials [84]	Upregulation of 14-3-3 increases antimony resistance through an unknown mechanism [84].
Amino acid permease	AAP3	Antimonials [85]	Upregulation of AAP3 increases import of arginine, a substrate for the synthesis of reduced thiol, which detoxifies antimony [85].
Antimony Resistance Marker of 56kDa	ARM56	Antimonials [86]	Upregulation of ARM56 increases antimony resistance through an unknown mechanism [86]
Antimony Resistance Marker of 58kDa	ARM58	Antimonials [86]	Upregulation of ARM58 increases antimony resistance through an unknown mechanism [86]
Aquaglyceroporin 1	AQP1	Antimonials [87]	Downregulation of the AQP1 channel disrupts uptake of antimonials [88].
Aquaglyceroporin 2	AQP2	Pentamidine, Melarsoprol [89]	Downregulation or mutation of AQP2 disrupts uptake of pentamidine and melarsoprol [89].
C24-Methyltransferase	ERG6/ SCMT	Amphotericin B [90,91]	Downregulation of ERG6 decreases affinity the parasite membrane for Amphotericin B and subsequent uptake [92].
Calcineurin	CaN	Antimonials [93].	Downregulation of CaN decreases antimony-mediated apoptosis [93].
Dihydrofolate-reductase-thymidylate synthase	DHFR-TS	Methotrexate [94]	Upregulation of DHFR-TS increases folate metabolic pathways, circumventing methotrexate antifolate activity [94].
DNA Topoisomerase 1B	TOP1B	Topotecan [95]	Mutations in TOP1B inhibit targeting of the gene by topotecan [95].
Elongation factor 1B	EF1B	Antimonials [96]	Upregulation of EF1B increases antimony detoxifying *S*-transferase activity [96].
Folate transporter 1	FT1	Methotrexate [97]	Downregulation of FT1 decreases methotrexate influx [97].
Glutathione synthase	GSS	Antimonials [98]	Upregulation of GSS enhances production of glutathione, a necessary precursor to antimony detoxification [98].
Heat shock protein 23	HSP23	Antimonials [99]	Upregulation of HSP23 increases antimony resistance through an unknown mechanism [99].
Heat Shock protein 83	HSP83	Antimonials [84,100]	Upregulation of HSP83 decreases antimony-mediated apoptosis [84,100].
Histone 1	H1	Antimonials [101]	Upregulation of H1 increases antimony resistance through an unknown mechanism [101].
Histone 2A	H2A	Antimonials, Miltefosine, Amphotericin B [101,102]	Upregulation of H2A increases multidrug resistance through an unknown mechanism [102].
Histone 4	H4	Antimonials [84]	Upregulation of H4 increases antimony resistance through an unknown mechanism [84].
Kinetoplastid membrane protein 11	KMP11	Antimonials [84]	Downregulation of KPM11 changes the activity of AQP1 and increases efflux of antimonials [84].
Lathosterol Oxidase	LSO	Amphotericin B [92]	Downregulation or deletion of LSO decreases affinity the parasite membrane for Amphotericin B and subsequent uptake [92].

Map Kinase 1	MAPK1	Antimony [103]	Downregulation of MAPK1, a negative regulator of ABC transporters, increases efflux of antimonials [103].
Miltefosine transporter	MTF	Miltefosine [104]	Upregulation of MTF increases efflux of miltefosine [104].
Multidrug resistance protein A	MRPA	Antimonials [84]	Upregulation of MRPA increases efflux of antimonials [84].
Phosphoglycerate kinase B	PGKB	Antimonials [101]	Upregulation of PGKB increases pyruvate uptake and decreases drug-induced oxidative stress [101].
Phosphoglycerate kinase C	PGKC	Antimonials [101]	Upregulation of PGKC increases pyruvate uptake and decreases drug-induced oxidative stress [101].
Protein 299	P299	Antimonials, Miltefosine [84]	Upregulation of P299 increases antimony resistance through an unknown mechanism [84]
Pteridine reductase 1	PTR1	Antimonials [105]	Upregulation of PTR1 maintains pools of tetrahydropteridine and decreases drug-induced oxidative stress [105].
S-adenosylmethionine synthase	MAT2	Methotrexate [94]	Upregulation of MAT2 increases folate metabolic pathways, circumventing methotrexate antifolate activity [94].
Sec13	Sec13	Miltefosine [106]	Upregulation of Sec13 increases miltefosine resistance through an unknown mechanism [106]
Spermidime synthase	SRM	Antimonials [98]	Upregulation of SRM enhances production of glutathione, a necessary precursor to antimony detoxification [98].
T-complex protein-1 γ	TCP1γ	Miltefosine [107]	Upregulation of TCP1γ protects against miltefosine-mediated oxidative stress [107].
Trypanothione reductase	TryR	Antimonials [108]	Upregulation of TryR protects parasites against antimony-mediated oxidative stress [108].
Trypanothione synthase	TryS	Antimonials [98,109]	Upregulation of TryS increases synthesis of trypanothione, a precursor for antimony detoxification [82].
Ubiquitin	Ubiquitin	Antimonials [85]	Upregulation of ubiquitin increases antimony resistance through an unknown mechanism [84].
γ-glutamylcysteine synthetase	GHS	Antimonials [84]	Upregulation of GHS enables conjugation with antimonials and detoxification [84].

*Gene is a member of the ATP-binding cassette (ABC) transporter family [110]

1.2 EXTRACELLULAR VESICLES

Extracellular vesicles (EVs) are a heterogenous group of non-replicative membranous structures released ubiquitously by eukaryotic and prokaryotic cells [111]. They can be classified within one of the three major subtypes – exosomes, ectosomes or apoptotic bodies – according to size, biogenesis, content and function [111,112]. Apoptotic bodies are the largest EVs, ranging from 50-5000 nm in diameter, and originate from the dissociation of the plasma membrane from the cytoskeleton during apoptosis [112]. As by-products of cell death, their contents are randomly packaged and fully recapitulative of the apoptotic cell, promoting the migration of phagocytes for clearance [112,113]. Ectosomes, or microvesicles, fall in between 100-1000 nm in size, and are formed by the outward budding of the cell's plasma membrane [112]. While initially thought to

be a mechanism by which cells release unwanted materials, ectosomes have since been shown to play a role in intercellular communication [113].

Exosomes are the smallest EVs (30-150 nm) – a characteristic that enables rapid diffusion and stability in the extracellular environment, explaining their immense biological significance [112]. Exosome biogenesis utilizes the endosomal sorting complexes required for transport (ESCRT) pathway, whereby vesicles are formed by the inward budding of the early endosome, which then matures into a multivesicular body (MVB) [112]. The MVB subsequently fuses with the plasma membrane, releasing exosomes into the extracellular environment, where they are able to circulate and penetrate nearby or distal recipient cells through direct fusion or endocytosis [112]. Exosomal cargo, which includes nucleic acids, proteins, lipids and metabolites, is only partially recapitulative of its cell of origin [112]. Protein sorting into exosomes is highly regulated and is dependent on the physiological state of the cell from which the exosomes derive [111].

1.2.1 Exosomes in Health and Disease

Exosomes have been identified in almost all biological fluids, including plasma, breast milk, urine, amniotic fluid, saliva and semen, in both homeostatic and disease contexts [114] .The primary function attributed to exosomes is that of cell-to-cell communication, with well-established roles in immunity, oncogenesis, cardiovascular disease and neurodegenerative disease [115].

Numerous studies have established the expression of major histocompatibility complexes class I and II, adhesion and co-stimulatory molecules in exosomes derived from antigen-presenting cell-derived exosomes, which are capable of activating $CD4^+$ and $CD8^+$ T cells [115,116]. Similarly, exosomes produced by NK cells display cytotoxic activity, and macrophage exosomes can trigger innate inflammatory cascades [115,117]. Dysregulation of these processes can be pathogenic, with

tumor exosomes containing oncogenes and displaying immunosuppressive properties that significantly reduce anti-tumor immunity [115,118,119]. Exosomes have also been shown to mediate the transport and dissemination of misfolded proteins in both Parkinson's and Alzheimer's disease and to modulate angiogenesis and coagulation in cardiovascular disease – exerting effects that can be either protective or pathogenic depending on cells of origin and cargo [120].

In addition to their undeniable role in noncommunicable disease, exosomes are crucial to the pathogenesis of infectious disease. Many viruses have evolved mechanisms to hijack host ESCRT machinery to promote transmission and immune evasion [121]. Exosome membranes, which are composed of lipids and integrated membrane proteins, provide protection of viral cargo from degradation in the extracellular environment and maintain low immunogenicity [121]. Furthermore, biocompatibility of EV membranes facilitates uptake by target cells and permits diffusion through biological barriers [121]. Utilizing exosomes for viral pathogenesis can be done by modulating host cargo, including viral elements, or a combination thereof. Viruses including HIV, EBV, HCV, EBOV and, more recently, SARS-CoV2 have all been reported to manipulate host ESCRT machinery for delivery of viral RNA and proteins to diverse target cells [122–126]. Even more strikingly, however, is the capacity for certain non-enveloped viruses, such as Hepatitis A and Hepatitis E, to completely encapsulate themselves within exosomes, forming a pseudo-envelope [127,128]. In fact, it has been suggested that this may be a mechanism by which some viruses have gained their envelope over the course of evolution [129].

Though viruses lack the necessary cellular structures to produce EVs themselves, prokaryotic and eukaryotic pathogens can, themselves, produce exosomes that interact with host cells. Gram-negative bacteria secrete immunogenic outer membrane vesicles, and eukaryotic pathogens have retained the ESCRT pathway to produce exosomes, which can be either immunostimulatory or

immunoinhibitory, in a pathogen-dependent manner [130–132]. For example, while EVs produced by the pathogenic fungus *Cryptococcus neoformans* induce the production of TNF and IL-10, culminating in macrophage activation and NO production, *Trypanosoma cruzi* exosomes generate an anti-inflammatory response, which enables parasitism of visceral organs [133,134]. Exosomes produced by the closely-related *Trypanosomatidae Leishmania*, mostly secreted at the flagellar pocket, have also been shown to exacerbate disease [135].

1.2.2 *Leishmania* Exosomes

Prior to the parasite's entry into a mammalian host, exosomes are constitutively produced by *Leishmania* promastigotes within the sandfly midgut [135]. Exosomes are then co-egested with the infectious inoculum during the sandfly's bloodmeal, whereby they immediately exert immunomodulatory effects on the host (Summarized in Figure 6) [135]. In fact, a temperature shift from 25˚C to 37˚C, mimicking that of the transmission from the sandfly to the mammalian host, has been shown to induce a substantial increase in leishmanial exosome production, indicating a key role in early infection [136]. When administered alone, *Leishmania*-derived exosomes exert an immunomodulatory effect on monocytes, inhibiting IFN- γ signaling and TNF-α production, and inducing IL-10 [137,138]. *In vivo* studies have corroborated these immunomodulatory effects, showing increased IL-10 in the spleen and higher frequencies of IL-4-producing $CD4^+$ T cells [139]. When co-injected with parasites, however, exosomes have been reported to induce IL-17a rather than IL-10, likely leading to the infiltration of neutrophils and tissue damage [61,140]. This induces a hyperinflammatory phenotype, causing a 3- to 4-fold increase in lesion volume comparatively to parasites alone [135].

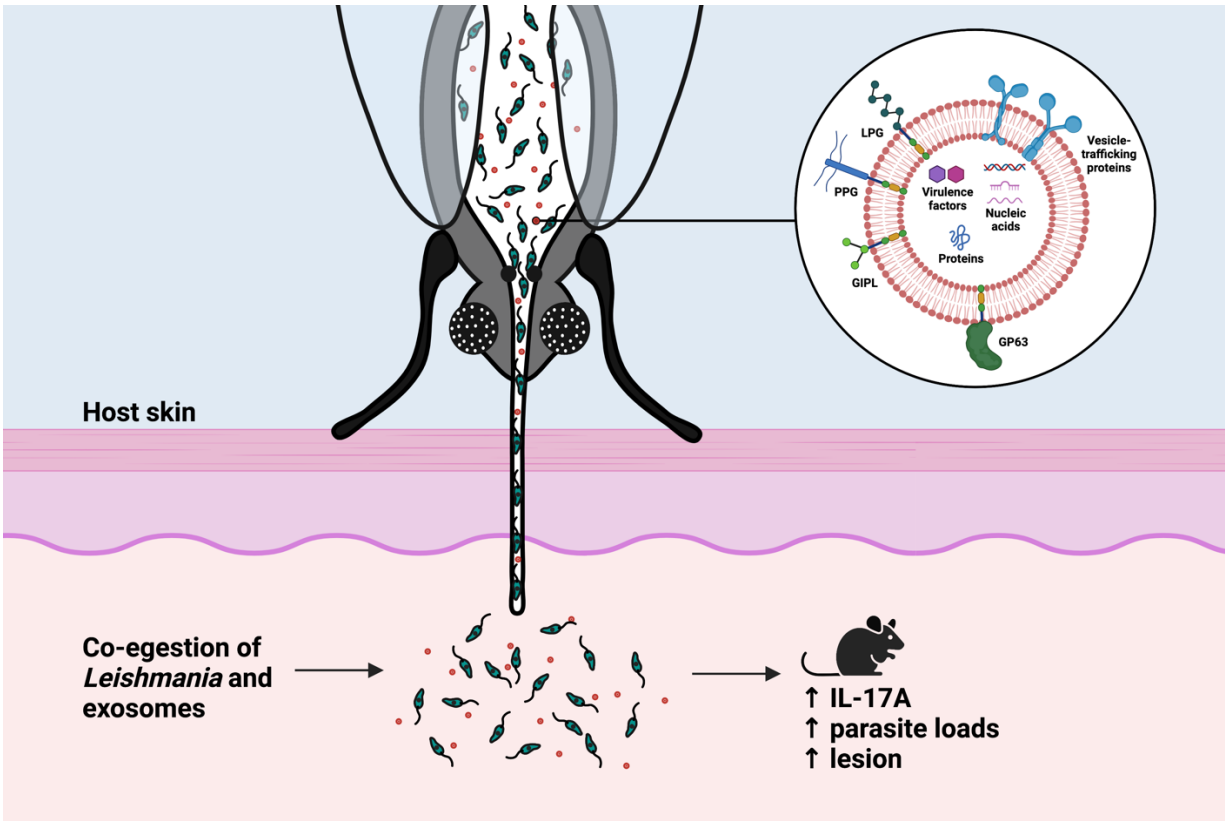

Figure 6. *Leishmania* exosome secretion and co-egestion. Adapted from Atayde *et al.* [135].

The effect of leishmanial exosomes is largely a function of their cargo, including its exoproteome. Rapid diffusion of exosomes at the site of inoculation and subsequent uptake by potential host cells occur prior to infiltration by the parasites themselves [141]. Virulence factors that are transported by EVs can therefore pre-emptively modulate these cells to establish permissive environments for eventual parasitic infection [141]. This was further illustrated by exosomes derived from GP63 knockout *L. amazonensis*, which, when used to stimulate macrophages *in vitro*, showed an increase in pro-inflammatory and antiparasitic cytokines [142,143]. In a murine footpad infection model, these exosomes were unable to elicit their characteristic lesion swelling, establishing an important role for GP63 in leishmanial exosome function [142,143]. In addition to

promoting parasitic survival and inducing disease exacerbation, leishmanial EVs have recently been shown to act as mediators of horizontal gene transfer for drug resistance genes [75].

1.3 Viruses of Protozoa

Viruses are obligate intracellular parasites that require host cell machinery for replication [144,145]. To complete their infectious cycles, they have two effective options; the first requires the killing of the host and rapid spread, while the second circumvents the lytic cycle in favour of endosymbiosis, wherein the virus exists either neutrally within the host or provides it with a fitness advantage [144,145]. As a form of mutualism, endosymbiotic interactions confer evolutionary advantages to both the host and the infectious agent, whereby the infectious agent is protected from extracellular microbicidal factors and the host may gain functions or resistance to environmental stressors [145]. In fact, Eukaryogenesis is thought to have occurred through successive endosymbiotic infections of viral and bacterial origin, which gave rise to the nucleus and the mitochondrion, respectively [146,147].

Viruses are capable of parasitizing living organisms all along the evolutionary spectrum, from prokaryotes to complex organisms [144,145]. Unicellular protozoa are no exception, with recent advances in imaging, molecular and sequencing technologies enabling the characterization of several endogenous viruses or virus-like particles within these ancient eukaryotes (Summarized in Table 3) [148]. Of these, the viral family *Totiviridae* is particularly notable as it encompasses most of the viral endosymbionts identified in pathogenic protozoa that have been associated with parasitic disease exacerbation and drug resistance [148].

Table 3. Viral endosymbionts of protozoa. Adapted from Lafleur and Olivier [149].

Protozoon	Viral endosymbiont	Virus type	Effect on pathogenesis
Cryptosporidium spp.	Csp1 [150]	*Partitiviridae* (dsRNA)	Increase [150]
Trichomonas vaginalis	TVV [151]	*Totiviridae* (dsRNA)	Increase [152]
Leptomonas seymouri	NLV1 [153]	*Narnaviridae* (ssRNA+)	Unknown
Phytomonas spp.	PserNV1 [154]	*Narnaviridae* (ssRNA+)	Unknown
Giardia spp.	GLV [155]	*Totiviridae* (dsRNA)	Decrease [156]
Leishmania (Viannia)	LRV1 [54]	*Totiviridae* (dsRNA)	Increase [56,157]
Leishmania (Leishmania)	LRV2 [158]	*Totiviridae* (dsRNA)	Unknown

(+) ssRNA, positive single-stranded RNA; Csp1, *Cryspovirus 1*; dsRNA, double-stranded RNA; GLV, *Giardia lamblia virus*; LRV1, *Leishmania RNA Virus 1*; LRV2, *Leishmania RNA Virus 2*; NLV1, *Lepsey Narna-like virus 1*; PserNV1, *Pser Narna virus 1*; TVV, *Trichomonas vaginalis virus.*

1.3.1 Totiviruses

Totiviruses can be morphologically characterized as isometric particles of approximately 40 nm in diameter, lacking a viral envelope [159]. Their monosegmented double-stranded RNA (dsRNA) genomes encode only a capsid protein and RNA-dependent RNA polymerase [159]. *Totiviridae* are thought to have evolved from a branch of (+) single-stranded RNA viruses that contains *Narnaviridae* – another major group of protozoan endosymbiotic viruses identified within the flagellates *Leptomonas seymouri* and *Phytomonas spp.* [159]. Several *Totiviridae* genera have been characterized within protozoa, including *Giardiavirus, Trichomonavirus,* and *Leishmaniavirus* [159]. Intriguingly, viral endosymbionts of the *Totiviridae* family have been associated with exacerbated pathology in the context of parasitic infection, despite being unable to establish infection in mammalian hosts [148].

This phenomenon was first described in the context of the sexually-transmitted infection trichomoniasis, caused by *Trichomonas vaginalis* [151,152]. When infected by the totivirus *Trichomonas vaginalis virus* (TVV), the parasite expresses significantly higher levels of the immunogenic virulence factor P270, which aids in host immune evasion [151,152]. The TVV

genome has also been reported to interact with mammalian endosomal TLR3, inducing a TRIF-dependent inflammatory response and subsequent tissue damage, which has been associated with increased risk of preterm birth and HIV susceptibility [152,160,161].

Giardia spp., the causative agent of the diarrhoeal infection giardiasis, can similarly become infected by the totivirus *Giardia lamblia virus* (GLV) [155]. GLV-infected *Giardia* induces greater pro-inflammatory cytokine production than its uninfected counterpart, while maintaining similar levels of TLR9 stimulation *in vitro* [162]. This finding suggests a TLR3-dependent mechanism, though no direct evidence of GLV dsRNA interaction with endosomal TLR3 has been published to date [156,162]. In addition, some reports indicate that GLV-induced inflammation may be protective against *Giardia* infection, in contrast to TVV [144,156].

Two distinct *Leishmaniavirus*es circulate within different species of *Leishmania*: *Leishmania RNA virus 1* (LRV1) has been reported in the isolates of the *L. Viannia* species *L. v. braziliensis* and *L. v. guyanensis*, and *Leishmania RNA virus 2* (LRV2) has been identified in *L. major* and *L. aethiopica*. Establishment of stable endosymbiotic infection by LRV1 is hypothesized to require function RNA interference pathways, whereby the viral load is maintained under a lytic threshold by LRV1-specific silencing RNAs [163]. While this potentially explains the propensity of LRV1 to infect the *L. Viannia* subgenus, the more recent discovery of LRV2 in the *L. Leishmania* subgenus may refute this theory. Due to their phylogenetic proximity, two additional viruses have been identified as LRV3 and LRV4, though they infect *Blechomonas spp.,* an ancestral clade of trypanosomatids [164]. The interaction between *Leishmania* and LRV1 is of particular interest due to its role in disease progression and chronicity.

1.3.2 LRV1-Mediated Immunopathogenesis

The endogenous virus LRV1 is prevalent in both *L. v. guyanensis* and *L. v. braziliensis*, with positivity rates of 44% and 34.5% from respective clinical isolates [165]. Notably, no LRV1-positive isolates of *L. v. panamensis* have been characterized thus far [166].

LRV1 infection of *Leishmania* has been associated with leishmaniasis treatment failure, symptomatic relapse, and parasitic metastasis. Cohort studies of human *L. v. guyanensis* and *L. v. braziliensis* infections have indicated that, while 76-100% of LRV1-negative (LRV1-) infections are resolved with first-line treatments, 27-53% of LRV1-positive (LRV1+) infections require extended therapeutic regimens and the use of second-line drugs [167–169]. The presence of LRV1 has also been shown to be predictive of disease relapse, with up to 30% of LRV1-positive infections displaying disease reactivation in the 12 months following initial treatment [167].

Studies by Fasel *et al.* have determined that MCL lesions in humans display high LRV1 positivity rates, and that parasites causing metastasized lesions in golden hamster infections express greater levels of the virus than non-metastasizing parasites [170]. Thus, it is hypothesized that LRV1 infection of *Leishmania* can control the progression and severity of MCL [170,171].

Mechanistically, LRV1-mediated hyperpathogenesis is dependent on the interaction between the viral dsRNA genome and mammalian endosomal TLR3, which triggers inflammatory signal transduction [170]. When stimulated with LRV1, TLR3 knockout macrophages cannot reproduce this pro-inflammatory cytokine and chemokine production [170]. Similarly, LRV1-infected *Leishmania* does not induce its characteristic hyperinflammatory phenotype in TLR3 knockout mice, once again exemplifying the pathogenic importance of this LRV1:TLR3 interaction [170].

Downstream of TLR3, several pathways converge to produce the ideal environment for parasitic persistence and metastasis. Stimulation of TLR3 triggers a canonical antiviral immune response,

culminating in the production of type I interferons [172]. This, in turn, downregulates the receptor for IFN-γ on macrophages, rendering them partially unresponsive to antiparasitic signaling [172]. Parasitic metastasis has also been shown to occur almost solely in the absence of IFN-γ, while the inverse correlation is observed with IL-17A [168]. Akt signaling and the micro-RNA miR-155, which has also been associated to Th17 development, have been associated to increased lifespans in macrophages [173]. Moreover, inhibition of caspase-11 and IL-1β maturation by LRV1 hinders inflammasome assembly and activation in a TLR3-dependent manner [56,174]. Subversion of the inflammasome, which is directly associated with MCL disease severity, is also achieved by degradation of NLRP3 and ASC via autophagy [54]. Together, these pathways create an ideal environment for parasitic proliferation and dissemination.

It follows that, as a key mediator of virulence and disease progression, LRV1 is an interesting therapeutic target for MCL. While a 2017 study showed protection against severe lesion development in mice following immunization with recombinant LRV1 capsid protein conjugated with a Th1-polarizing adjuvant, no follow-up studies are currently published [175]. Treatment with RDRP inhibitors, including the adenosine analog 2′-C-methyladenosine (2-CMA), can be used to eliminate LRV1 *in vitro* [176–178]. Though this provides an important tool for laboratory work by enabling the generation of genetically identical LRV1- and LRV+ strains, no *in vivo* studies exploring 2-CMA antiviral potential have been published thus far.

1.3.3 LRV1 and Exosomes

Transmission of viruses of the *Totiviridae* family has, until recently, been presumed to only occur vertically during cellular division, with the exception of GLV – a more robust virion capable of withstanding the extracellular environment [179]. The discovery of complete virions within

LRV1-infected *L. v. guyanensis*-derived exosomes, however, has caused a paradigm shift, providing evidence of horizontal transmission [157]. In a seminal paper published by Atayde *et al.* in 2019, authors showed that LRV1 hijacks leishmanial ESCRT machinery to form a pseudo-envelope – a mechanism that has been previously reported in several mammalian unenveloped viruses [157]. Encapsulation within exosomes, approximately 30% of which contain the virus, enables non-lytic viral shedding and dissemination [157]. In this study, purified exosome preparations from an isolate of *L. v. guyanensis* endogenously infected with LRV1 were inoculated into cultures of the closely-related species *L. v. panamensis*, prompting acute infection of the parasite [157]. Notably, inoculation of the unenveloped virus alone was insufficient for the establishment of LRV1 infection in other parasites, underscoring the role of the exosomal membrane in endocytosis and viral pathogenesis (Summarized in Figure 7) [157]. The role of EVs was further corroborated by the exacerbation of murine footpad lesions induced by the co-inoculation of *L. v. panamensis* with exosome-enveloped LRV1 – a phenotype that could not be replicated by the parasite and unenveloped virus [157]. LRV1 infection of *L. v. panamensis* was followed over a two-week period, during which viral RNA integrated into leishmanial polysomes and the translational efficiency of key genes, including the virulence factor GP63, was significantly altered [157]. These changes affected the course of leishmaniasis development, as illustrated by the increased lesion thickness induced by LRV1-infected *L. v. panamensis* comparatively to its uninfected counterpart [157]. Though notable changes to the parasite's transcriptome and virulence can be inferred, the nature of these changes remains uncharacterized [157].

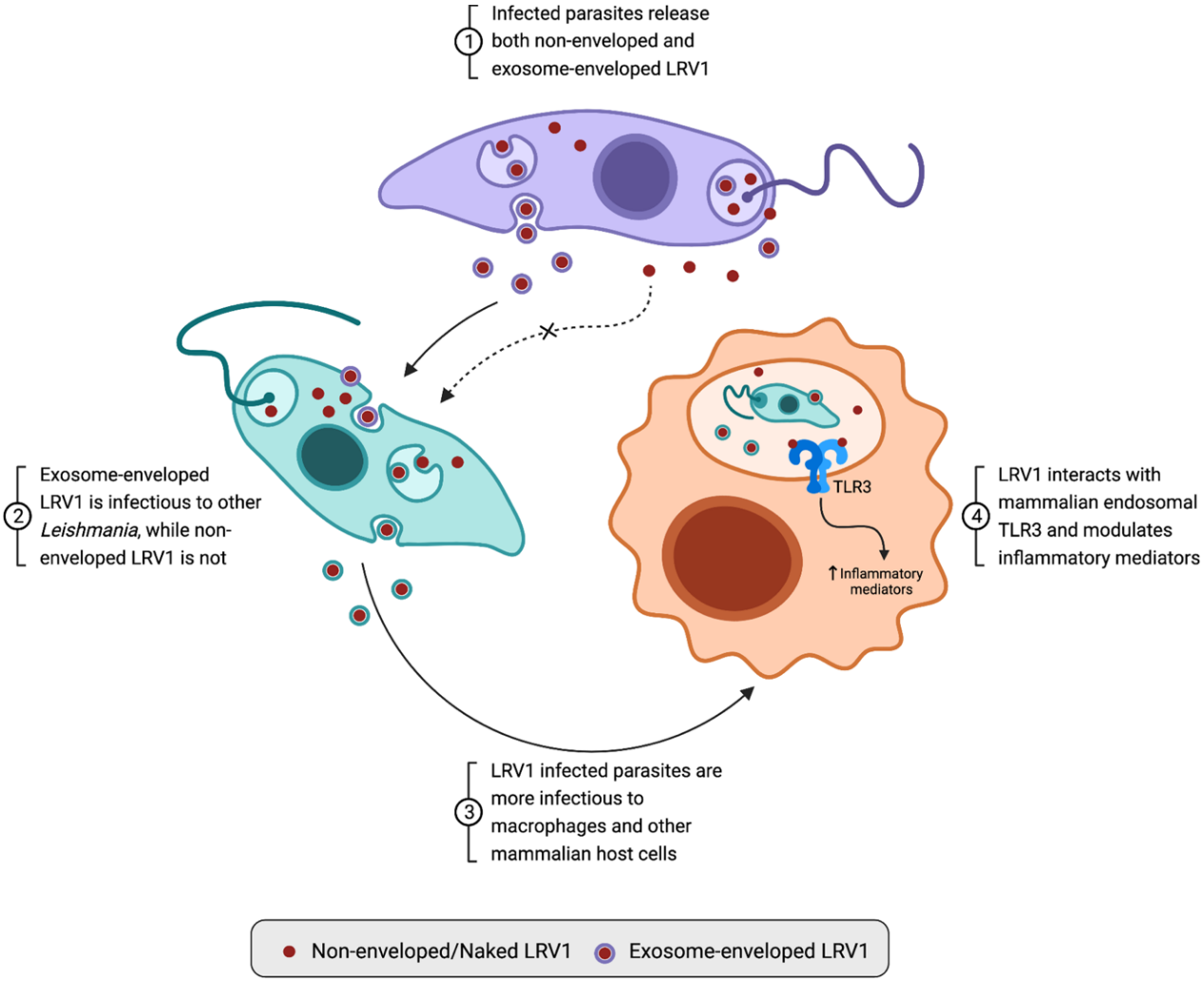

Figure 7. Hijacking of the leishmanial exosomal pathway by LRV1. Reproduced from Lafleur and Olivier [149].

1.4 Objectives of Research and Rationale

Infection of *Leishmania (Viannia)* by *Leishmania* RNA virus 1 (LRV1) is an important risk factor in the development of mucocutaneous leishmaniasis, as observed in both human cohort studies and murine models. While the interaction between endogenously LRV1-infected *Leishmania* and its mammalian host has been well-described, the effect of LRV1 infection on *Leishmania* remains unclear. The acute infection of *L. v. panamensis* by exosome-enveloped LRV1 provides an interesting model, whereby we can compare the parasite to its uninfected, or wildtype, isogenic counterpart. Evidence of viral RNA integration into leishmanial ribosomal machinery and subsequent modulation of leishmanial genes, which we published in 2019, indicates an interesting *Leishmania/LRV1* host-pathogen interaction. Moreover, observations of a decrease in LRV1 expression in *L. v. panamensis* over several weeks suggests potential restriction mechanisms and evolutionarily-conserved antiviral cascades. Drawing from our previous findings, we posed the following research question: "How does LRV1 infection affect *Leishmania panamensis* survival, fitness, and infectivity?" We hypothesized that LRV1 infection of *L. v. panamensis* would affect parasitic pathogenesis by modulating key mediators of virulence, and that *L. v. panamensis* would upregulate antiviral mediators to control viral infection. We further suspected that, over a course of several weeks, *L. v. panamensis* would overcome LRV1, during which parasitic virulence would be altered accordingly. To determine the validity of these hypotheses, we proposed the following research objectives:

Objective 1. Characterize the impact of acute LRV1 infection on *L. v. panamensis* survival, fitness, and infectivity.

Objective 2. Identify potential mechanisms of antiviral immunity and modulation of parasitic function over the course of LRV1 infection.

CHAPTER 2. METHODS, RESULTS AND DISCUSSION

2.1 PREFACE TO THE ARTICLE

The results of this research project will be submitted in the form of a manuscript for publication. The paper focuses on research objectives described in section 1.4, pertaining to the investigation of the host-pathogen interaction between *L. v. panamensis* and LRV1 during 1) established acute infection, and 2) over the course of infection resolution. The methods and results presented in this manuscript aim to elucidate the effect of LRV1 course of infection on parasitic virulence, fitness, and infectivity, using a combination of bioinformatic analysis, *in vitro* and *in vivo* work.

2.2 AUTHOR CONTRIBUTIONS

The project was designed and conceptualized by MO. *In vitro* experiments were performed by AL. *In vivo* experiments were prepared by MO and AL and carried out by MO and CV. NTA was performed by AL, and TEM imaging was performed by AL and GD. Sample preparation for LC-MS/MS proteomics and phosphoproteomics, bioinformatic analysis and data curation and analysis were completed by AL.

Deciphering the Interaction Between *Leishmania* and *Leishmania RNA Virus 1*

Andrea Lafleur[1,2], George Dong[1,2], Carlos Villalba-Guerrero[1,2], Vyacheslav Yurchenko[3], Martin Olivier[1,2*]

[1]Department of Microbiology and Immunology, Faculty of Medicine and Health Sciences, McGill University, Montréal, Québec, Canada.

[2]Infectious Diseases and Immunity in Global Health, Research Institute of McGill University Health Centre, Montréal, Québec, Canada.

[3]Life Science Research Centre, Faculty of Science, University of Ostrava, Ostrava, Czech Republic

Correspondence: martin.olivier@mail.mcgill.ca

Keywords: *Leishmania*, Leishmaniasis, Mucocutaneous leishmaniasis, LRV1, *Totiviridae*, Endosymbiotic virus

2.3 ABSTRACT

Leishmania are ancient protozoan parasites that have retained multiple higher eukaryotic pathways over the course of evolution. Notably, the parasite's exosomal pathway is exploited by the *Totiviridae Leishmania RNA Virus 1* (LRV1) to form a viral pseudo-envelope, facilitating transmission and uptake by other *Leishmania* cells. Endosymbiotic infection of *Leishmania* by LRV1 is associated with progression of primary lesions to highly disfiguring mucocutaneous leishmaniasis and to first-line therapeutic treatment failure. Herein, we investigated the effect of LRV1 infection on the fitness and infectivity of *L. v. panamensis*, an unnatural host to the virus. Extracellular vesicles derived from LRV1-bearing *L. v. guyanensis* were isolated, characterized by transmission electron microscopy and nanoparticle tracking analysis, and used to acutely infect *L. v. panamensis*. Bioinformatic analysis of the infected *L. v. panamensis* proteome revealed a remarkable increase in translational and metabolic pathways to promote viral replication, along with a notable increase in mediators of virulence. Moreover, *L. v. panamensis* was shown to overcome LRV1 infection over a 10-week time course, suggesting a role for ancient antiviral mechanisms to eliminate the virus, particularly ROS-mediated antiviral activity, RNA-mediated silencing of the viral dsRNA genome, and potentially conserved antiviral pathogen-associated pattern-recognition signaling via a TLR3-like cascade. Furthermore, mice infected with *L. v. panamensis* at earlier time-points of their LRV1 course of infection developed a more severe disease. Overall, this work provides evidence that the interaction between *Leishmania* and LRV1 confers additional virulence and survival assets to parasites, which decrease following the elimination of the virus, and suggests the presence of ancestral antiviral immunity.

2.4 INTRODUCTION

Leishmania is the causative agent of leishmaniasis, a neglected tropical disease with an annual burden of 1.5-2 million cases and 70,000 deaths worldwide – the majority of which occur in the global South [1]. *Leishmania* are ancient vector-borne protozoan parasites, with a digenic life cycle involving developmental stages in both a sandfly vector and a mammalian host [14]. Transmission occurs when a female phlebotomine sandfly takes a blood meal from a mammalian host – most frequently a human, rodent, or canid [14]. Within the mammalian host, *Leishmania* primarily infect and persist within macrophages, altering canonical parasitotoxic signaling and ROS/NOS-mediated killing [43,63]. Clinical presentation of leishmaniasis is dependent on the species of *Leishmania* and is designated as either visceral (VL), cutaneous (CL), or mucocutaneous (MCL) – the latter of which involves the development of highly disfiguring lesions to the nasopharyngeal mucosa [14]. Mucosal involvement is characteristic of infection by species of the *Viannia* subgenus, occurring in 5-10% of CL cases up to five years following resolution of the primary lesion [73].

Several species of the *Viannia* subgenus, including *L. v. guyanensis* and *L. v. braziliensis*, harbour the endogenous totivirus *Leishmania RNA Virus 1* (LRV1) [180,181]. LRV1 is a non-enveloped isometric virus of approximately 40 nm in diameter, which encompasses a monosegmented double-stranded RNA (dsRNA) genome encoding the capsid protein and an RNA-dependent RNA polymerase (RdRp) [159].

LRV1 infection of *Leishmania* is predictive of the development of MCL and has been associated to symptomatic relapse and parasitic metastasis, in both epidemiological studies and rodent models [49,170]. LRV1 is thought to contribute to the hyperinflammatory phenotype that is characteristic of MCL by interaction of the viral dsRNA genome with mammalian endosomal TLR3,

culminating in inflammatory cascades and exacerbation of lesions [49,54,170]. The presence of LRV1 has also been associated to first-line treatment failure [167,169].

While initially thought to be transmitted only vertically during cell division, we recently showed that horizontal transmission of LRV1 occurred through the leishmanial endosomal sorting complex required for transport (ESCRT) pathway [157]. This pathway is responsible for the biogenesis of exosomes, a subset of small extracellular vesicles containing biologically active cargo, which reflect the state of the cells from which they are derived and modulate recipient cell function [113]. *Leishmania* have retained the exosomal pathway through evolution, with secretion dependent on multivesicular bodies (MVBs) and the flagellar pocket. Leishmanial exosomes have been shown to be produced within the sandfly midgut, co-egested as part of the infectious inoculum during the sandfly's bloodmeal and modulate host cell functions to create a permissive environment for parasitic replication and persistence [48,135,141–143]. In addition to the mediation of pathogenesis, leishmanial extracellular vesicle machinery can be hijacked by LRV1 to encapsulate virions within exosomes, forming a pseudo-envelope [157]. Presence of the exosomal envelope is necessary for LRV1 transmission and enables rapid diffusion and uptake by naïve parasites [157]. Exosome-enveloped LRV1 derived from endogenously infected *L. v. guyanensis* can be isolated and used to infect the closely related parasite *L. v. panamensis* [157]. This acute infection of an unnatural host to the virus induces important functional changes to the parasite and culminates in eventual viral elimination after a 10-week course of infection. Herein, we provide evidence that LRV1 increases *L. v. panamensis* fitness and infectivity, and that ancestral antiviral immune cascades may be utilized by parasites to overcome viral infection. This research explores mechanisms whereby the *Leishmania*/LRV1 host-pathogen interaction provides parasites with additional virulence and survival assets, leading to exacerbation of leishmaniasis.

2.5 MATERIALS AND METHODS

Leishmania Promastigote Culture

Leishmania species used in this study include *Leishmania v. panamensis* strain MHOM/87/CO/UA140; *L. v. guyanensis* strain MHOM/BR/75/M5313 metastatic clone 21 (Lvg^{LRV1+}) [182]; and 2-CMA-treated *L. v. guyanensis* strain MHOM/BR/75/M4147 (Lvg^{LRV1-}), generously provided by Dr. Vyacheslav Yurchenko (University of Ostrava, Czech Republic). 2-CMA treatment was performed as previously described, using six consecutive passages of parasites in Schneider's Drosophila Medium (SDM) supplemented with 10% FBS, 100 U ml^{-1} penicillin, 100 µl ml^{-1} streptomycin, and 10 mM 2-CMA [177]. Though Lvg^{LRV1+} was previously identified as the *Lutzomyia* isolate WHI/BR/78/M5313 from Brazil, sequencing indicates it is identical to the laboratory strain MHOM/BR/75/M4147, the gold standard for *L. v. guyanensis* research (See Supplemental Table 1) [181].

Promastigotes were cultured at 25 ˚C, 5% CO_2 in SDM supplemented with 10% heat-inactivated fetal bovine serum (Wisent, St-Bruno, Canada), 2 mM L-glutamine, 100 U ml^{-1} penicillin, 100 µl ml^{-1} streptomycin and 5mg/ml Hemin in unvented cell culture flasks. Parasites were passaged every 3-4 days to maintain logarithmic growth.

Species were validated using Sanger Sequencing (Genome Quebec, Montreal, Canada) of PCR amplicons for GP63 and AGO1 (primer sequences available in table 1), and mapped to *Leishmania* genomes using NCBI Basic Local Alignment Search Tool (BLAST) [183].

Extracellular Vesicle Purification

Extracellular vesicle purification was performed as previously described [184]. Briefly, late log phase promastigotes were washed twice with PBS to remove serum, resuspended in RPMI 1640

without phenol red (Life Technologies) at a concentration of $1x10^8$ parasites/mL, then subjected to a four-hour incubation at 37˚C, 40 RPM.

Parasites and aggregates were pelleted at 2,555 g then 8,500 g, and supernatant was filtered through a 0.45μm and a 0.22 μm filter to remove debris and larger extracellular vesicles. The filtrate was transferred to 13.2mL Thinwall Polypropylene tubes (Beckman Coulter, Brea, CA, USA) and completed with exosome buffer (137mM NaCl, 20mM HEPES, pH 7.5). Tubes were placed in SW 32.1 Ti swinging buckets (Beckman Coulter), then centrifuged at 100,000 x g for 70 minutes. The supernatant was then discarded, before pooling content from all tubes, completing remaining volume with exosome buffer, and repeating ultracentrifugation. Supernatant was discarded, and extracellular vesicles were resuspended in approximately 400 μL of exosome buffer, aliquoted, and frozen at -80˚C.

Nanoparticle Tracking Analysis (NTA)

Concentration and size of extracellular vesicles were assessed by nanoparticle tracking analysis (NTA) [184]. Extracted extracellular vesicles were diluted in exosome buffer at a 1:50 ratio, and samples were infused into a Nanosight NS300 (Malvern Panalytical) at the Centre for Applied Nanomedicine, RI-MUHC, Canada. Three distinct 30-second videos were taken, during which samples were maintained at 37˚C. Particle concentrations and size distributions were calculated using NTA 3.4 Build 3.4.4 software.

Transmission Electron Microscopy (TEM)

TEM for the visualization of EV morphology was performed as previously described [184]. Fomvar carbon grids (Mecalab, Montréal, QC, Canada) were subjected to 20 seconds of glow discharge at 20 V to prepare grid surfaces for hydrophobic extracellular vesicle samples. 10 μL of purified extracellular vesicles were deposited on the surface of the carbon grids for one minute.

Once EVs adhered, grids were fixed with 1% glutaraldehyde, washed 3 times, and stained with 1% uranyl acetate. Grids were then visualized using an FEI Tecnai-12 120kV transmission electron microscope and AMT XR80C CCD Camera (Facility for Electron Microscopy Research, McGill University, Montréal, Canada).

Nucleic Acid Isolation and Purification

Nucleic acids from whole parasites were extracted and purified using TRIzol reagent (Invitrogen) and purified using Ethanol precipitation with 0.1 volumes of 3M Sodium Acetate. RNA from extracellular vesicles was isolated using the miRNeasy Micro kit (Qiagen). Sample concentration and purity was determined using a NanoDrop spectrophotometer.

Polymerase Chain Reaction (PCR)

RNA was reverse-transcribed into cDNA using Superscript III Reverse Transcriptase and random hexamers (Invitrogen). PCR was performed with standard amounts of cDNA and primers (sequences available in Table 1) using *Taq* 2X Master Mix (New England BioLabs). The thermocycling protocol was performed using a T100 Thermal Cycler (Bio-Rad) and was as follows: 95˚C for 30 seconds (initial denaturation), then 30 cycles of 95˚C for 15 seconds, 60˚C for 30 seconds, and 68˚C for 1 minute (denaturation, annealing and extension), followed by 68˚C for 5 minutes (final extension).

Table 1. Primers for PCR and qPCR

Target	Gene Name	Primer sequence (5'–3')	Product Length (bp)
α-Tubulin	LbrTUBA	F – ACACCGAGTTCGTGATGTCC R – CAGGTGGTGTCGTCTCTGAC	190
LRV1 ORF3	LRV1gp3	F – CGGACATTGCTGATATCATGGC R – GCTCTCACCCCACAAATCTAGC	296
Argonaute 1	LbrAGO1	F – GTCCACAAGCATGACGGGATTAACC R – CGTCCAGCTGCAGTACATCCATCAT	743
Leishmanolysin	LbrGP63	F – CGGCGAACATTGTGTCGCGCTA R – CGCCGCGTCGGAGAAGACGTTG	725

Real-Time Quantitative PCR (RT-qPCR)

RT-qPCR was performed with standard amounts of RNA and primers (primer sequences available in Table 1) using Luna® Universal One-Step RT-qPCR Kit (New England BioLabs). The thermocycling protocol was performed using a CFX96 Touch Real-Time PCR Detection System (Bio-Rad) and was as follows: 55°C for 10 minutes (reverse transcription), 95˚C for 1 minute (initial denaturation), then 40 cycles of 95˚C for 10 seconds followed by 60˚C for 30 seconds (denaturation and extension). Melt curves were obtained between 65-95˚C and results were analyzed using the ΔΔCt method.

Protein Isolation and Purification

Parasite samples were lysed using 8M Urea/Thiourea and three freeze-thaw cycles and dosed with the Bradford Protein Assay Kit (Bio-Rad). EVs were diluted in deionized water and dosed with the Micro BCA Protein Assay Kit (Thermo Scientific) for optimal sensitivity to lower protein concentrations. Sample concentration was determined using an Infinite 200 Pro spectrophotometer (Tecan) and interpolation with a BSA standard curve.

***Leishmania* Infection with LRV1**

Promastigotes were counted using a hemocytometer, washed twice with PBS, and adjusted to a concentration of $5x10^7$ parasites/mL in completed SDM. 10 μg of exosomes were inoculated into 5mL of parasite culture in a T25 unvented cell culture flask. Parasites were cultured at 26 ˚C, 5% CO_2 and passaged every 3-4 days to maintain logarithmic growth.

***Leishmania* Survival Assays**

Promastigotes were counted using a hemocytometer, washed twice with PBS, and adjusted to a concentration of $1x10^6$ parasites/mL in completed SDM with increasing concentrations of potassium antimonyl tartrate trihydrate (Sigma) or hydrogen peroxide (Thermo Scientific). Every

2 days, aliquots of cultures were transferred to 96-well plates and optical density at 600nm was determined using an Infinite 200 Pro spectrophotometer (Tecan) to monitor growth.

***Leishmania* Mitochondrial ROS Accumulation Assays**

5 x 10^6 promastigotes were transferred to amber Eppendorfs and washed twice with Hepes-NaCl (21 mM HEPES, 137 mM NaCl, 5 mM KCl, 0.7 mM Na2HPO4·7H2O, 6 mM glucose, pH 7.4). Parasites were resuspended in 500uL Hepes-NaCl containing 25 μg/mL H_2DCFDA (Thermo Scientific), and incubated at room temperature for 30 minutes, protected from light. Parasites were then washed twice with Hepes-NaCl and resuspended in a final volume of 500 μL. 200μL aliquots were transferred to 96-well plates and read at excitation/emission of 485nm/535nm using an Infinite 200 Pro spectrophotometer (Tecan). Fluorescence was normalized with the number of living parasites by manual counting. Experiments were performed with at least three independent biological replicates, each of which included two technical replicates.

Gelatin Zymography Assays

Protease activity of GP63 was assessed using 10% SDS-PAGE with 1mg/mL gelatin. Gels were loaded with 5 or 10 μg of protein using a non-reducing loading buffer (4% SDS, 20% glycerol, 0.01% bromophenol blue, 125 mM Tris-HCl). Electrophoresis was performed at a constant voltage of 100V for one hour. Following electrophoresis, gels were washed twice with washing buffer (2.5% Triton X-100 in 50mM Tris pH 7.4, 5mM $CaCl_2$, 1μM $ZnCl_2$) for 30 minutes on a shaker at room temperature, then rinsed with deionized water and incubated in renaturation buffer (1% Triton X-100 in 50mM Tris pH 7.4, 5mM $CaCl_2$, 1μM $ZnCl_2$) overnight at 37˚C. After incubation, gels were rinsed with deionized water and stained with staining solution (40% methanol, 10% acetic acid, 0.5% Coomassie Blue), then destained using destaining solution (40% methanol, 10% acetic acid) until clear bands appeared, indicating proteolytic activity.

BMDM Isolation and Culture

Femurs and tibias of sacrificed 8-week-old female C57BL/6 mice were extracted and bone marrow was flushed by centrifugation. Bone marrow was resuspended in DMEM supplemented with 1X Penicillin-Streptomycin, 20% L-cell conditioned media and 10% FBS. Bone marrow progenitor cells were then incubated at 37˚C, 20% CO_2 for one week to differentiate into BMDMs.

BMDM Infection

Differentiated BMDMs were diluted in Trypan Blue, counted, and assessed for viability. 1 x 10^5 cells/chamber were plated in 4-well chamber slides (Thermo Scientific), and incubated overnight at 37˚C, 20% CO_2 to enable adherence. Late log phase promastigotes were inoculated directly into the chamber slide using an MOI of 5:1. Culture media was aspirated and replaced 6-hours post-inoculation to remove non-attached promastigotes. Following timepoints of infection, slides were dried and stained using Diff-Quick (RAL Diagnostics). Using a light microscope, 200 cells per chamber were counted, and infection ratio and number of amastigotes per cell was determined.

Trichloroacetic Acid (TCA) Precipitation of Proteins

Volumes of sample lysates containing 10 µg of protein for downstream proteomic analysis, or 200 µg of protein for subsequent phosphoproteomic analysis, were transferred to Eppendorf tubes and completed with deionized water to a final volume of 100 µL. To each sample, 100 µL of 10X Tris HCl-EDTA buffer, 100 µL of 0.3% sodium deoxycholate and 100 µL of 72% trichloroacetic acid (TCA) were added sequentially. Samples were incubated on ice for 1 hour, then centrifuged at 14,000 rpm for 20 minutes at 4˚C. The supernatant was then removed by aspiration, and the pellet was resuspended in 100 µL of 90% room temperature acetone and incubated at -20˚C overnight. Following incubation, samples were centrifuged at 14,000 rpm for 20 minutes at 4˚C, supernatant was aspirated, and the pellet was left to air dry before being frozen at -80˚C.

Liquid Chromatography-Mass Spectrometry (LC-MS/MS)

Liquid chromatography–Mass spectrometry (LC-MS/MS) was performed at the Institut de Recherches Cliniques de Montréal (IRCM), Montreal, Canada. Trypsin digestion of TCA-precipitated proteins required an overnight incubation at 37˚C using a ratio of 1:25 protease/protein, followed by the addition of formic acid to quench the reaction at 0.2% w/v. For conventional proteomics, peptides were then injected into a Zorbax Extended-C18 desalting column (Agilent) and separated through liquid chromatography on a Biobasic 18 Integrafrit capillary column (Thermo Scientific) on a Nano high-performance LC system (1100 series unit; Agilent). Eluted peptides were electrosprayed while exiting the capillary column and analysed with a QTRAP 4000 linear ion trap mass spectrometer (SCIEX/ABI).

For phosphoproteomic analysis, digested peptides were desalted using an Oasis HLB extraction plate (Water UK), equilibrated with 100% methanol, and lyophilized. TiO_2 phosphopeptide enrichment was then performed using MagReSyn® TiO_2 beads (ReSyn Biosciences). Briefly, TiO_2 beads were suspended in a solubilization solution (1.8 mM 2,5-Dihydroxybenzoic acid (DHB), 80% acetonitrile (ACN), 3% TFA), to which protein tryptic digest was added. Samples were then incubated for 30 minutes at room temperature without agitation and centrifuged. Phosphopeptide-bound beads were then washed in washing solution A (30% ACN, 3% TFA) three times, then with washing solution B (80% ACN, 0.3% TFA) an additional three times on StageTip C8 material (ThermoFisher Scientific). Phosphopeptides were eluted using elution buffer (40% ACN, 17% NH_4OH), and dried using a speed-vac. Phosphopeptides were then resolubilized in 1% ACN/1% formic acid and separated using an Orbitrap Fusion mass spectrometer (Thermo Scientific) by Nanospray Flex Ion Source. LC-MS/MS data was acquired using MS3 scanning upon detection of a neutral loss of phosphoric acid in MS2 scans.

Protein Database search

Peak lists were extracted from MS/MS spectra data sets using Distiller version 2.6.0 software (matrixscience.com/distiller) with the signal-noise ratio cut-off set at 1, and a 0.3 correlation threshold. Peak lists were searched against the *Leishmania braziliensis* protein database (NCBI txid5660; 25,626 proteins) using Mascot software version 2.3.02 (Matrix Science), with fragment ion mass tolerance of 0.50 Da and parent ion tolerance of 1.5 Da. Carbamidomethylation of cysteine was specified as a fixed modification, and oxidation of methionine residues was specified as a variable modification. Scaffold software version 5.2.2 (Proteome Software Inc.) was used to identify peptides and proteins from MS/MS and normalize datasets to the total ion count (TIC) area. Scaffold software calculates protein probabilities using the Protein Prophet Algorithm, and peptide probabilities using a naïve Bayesian classifier [185]. Inclusion criteria for identified peptides were set to a protein probability greater or equal to 95.0% (FDR < 1%), a peptide probability greater or equal to 80.0% (FDR < 5%), and a minimum of two peptides in at least two biological replicates. Proteins that contained similar peptides that could not be differentiated by MS/MS alone were grouped, and data was normalized using TIC area. The final number of peptides identified was represented by the average of all biological replicates.

Phosphoproteomic datasets were similarly analyzed, with the additional specification of phosphorylation of serine, threonine, or tyrosine as variable modifications. Data was then further analyzed using Scaffold PTM software version 4.0.2 (Proteome Software Inc.), which uses the Ascore probabilistic approach to annotate modification sites in MS/MS spectra [186]. Inclusion criteria for identified post-translational modifications were set to unique modified peptides, an MS summary level, and a minimal localization of 95%. The final number of phosphopeptides identified

was represented by the average of all biological replicates, accounting for the specific phosphosites.

Proteomic Analysis

Gene ontology analysis was performed using Blast2GO (version 5.2.5) [187]. Protein sequences were retrieved from UniProt (uniprot.org) using ID mapping, and input into Blast2GO. Local Blast was performed using the Homo Sapiens genome (NCBI txid9606), and hits were mapped to gene ontology terms and annotated with a maximal E value of 1.0E-06 [187,188].

Protein-protein interaction analysis (PPI) was performed using StringDB (string-db.org) [189]. Protein sequences were retrieved from UniProt using ID mapping, and input into StringDB using the Multiple Proteins by Sequence function and the organism identifier set to *Leishmania braziliensis*, requiring a high confidence score (0.700) and an FDR <5%. Disconnected nodes were hidden, and a Markov Clustering Algorithm (MCL) of 3 was used for node clustering. Clusters were annotated using software-integrated GO and KEGG terms.

Pathway analysis was performed using Reactome PADOG and filtered using an FDR < 10% and a FC ≥1.2, and the highest grouping point [190]. Selected pathways of interest were exported from ReactomeDB and supplemented through an extensive literature review. *Leishmania* homologs were obtained using Blast2GO as previously described, and additional annotations were performed manually using TriTryp and UniProt databases [187,188].

Modelling of protein structure was performed with alpha-fold (alphafold.ebi.ac.uk) and with Swiss-Model (swissmodel.expasy.org) [191–193].

Phosphoproteomic Analysis

Phosphoproteomic datasets were mapped to human homologs using Blast2Go [187]. Kinase enrichment analysis (KEA) and transcription factor enrichment analysis (TFEA) were performed

using Expression2Kinase (X2K) (maayanlab.cloud/X2K), which infers upstream regulatory networks from differentially expressed gene sets [194].

Animals and Ethics

Animal experiments were carried out in containment level 2 pathogen-free housing facilities in the Research Institute of the McGill University Health Center (RI-MUHC). Experiments were performed in accordance with the regulations of the Canadian Council of Animal Care Guidelines (CCAC), and McGill University Animal Care Committee (UACC) under ethics protocol number 7791. Mice were housed socially in 3–5 mice per IVC cage, with food, water, and soft bedding, and were euthanized after 8-10 weeks using isoflurane and CO_2 asphyxiation followed by cervical dislocation.

Murine Footpad Infections

Groups of five female BALB/c mice of 6-8 weeks of age (Charles River Laboratories) were infected in the right hind footpad with 5 x 10^6 stationary-phase *Leishmania* promastigotes. Footpad swelling was measured bi-weekly with a metric caliper up to 8 weeks post-infection to monitor lesion development, with uninfected footpads used as a negative control.

Statistical Analysis

Statistical analyses for assays were performed on GraphPad Prism Software using unpaired Student's t-test (one- or two-tailed) or analysis of variance (ANOVA). Statistical analyses of bioinformatic datasets were performed using the Benjamini-Hochberg procedure. Error bars represent SEM. *$P \leq 0.05$, **$P \leq 0.01$, ***$P \leq 0.001$.

Figures

Figures were generated with GraphPad Prism Software and with BioRender [195].

2.6 RESULTS

Treatment of endogenously infected *L. v. guyanensis* with 2-CMA resolves LRV1 infection.

2'-substituted adenosine analogs, which chemically inhibit viral polymerase by chain termination, have demonstrated activity against mammalian viruses such as HCV [1]. As shown in endogenously LRV1-infected *L. v. braziliensis*, treatment with 2'C-methyladenosine (2-CMA) is capable of fully eliminating the virus from *L. v. guyanensis* [176,177]. All *Leishmania* species used in this study were additionally tested for the presence of the Argonaute gene (AGO), which is specific to the Viannia subgenus, and the GP63 gene, which is conserved among all *Leishmania* (See Supplementary Table 1).

Following species validation, we sought to assess the impact of antiviral treatment on the proteome of LRV1-infected *L. v. guyanensis*, which revealed differential protein expression between infected (Lvg^{LRV1+}) and 2-CMA treated (Lvg^{LRV1-}) parasites. While 867 proteins were shared between the groups, 57 were uniquely detected in Lvg^{LRV1+}, and 104 were uniquely detected in Lvg^{LRV1-}. Most of the shared proteins displayed similar levels of expression, apart from 89 proteins that were overexpressed in Lvg^{LRV1+}, and 165 overexpressed in Lvg^{LRV1-} (Fig. 1 A). Of these, proteins with significant differential expression include kinesin and eukaryotic initiation factor 2a (eIF2a), which are upregulated following 2-CMA treatment, and Facilitates Chromatin Transcription protein (FACT) which is downregulated accordingly (Fig. 1 B). Notably, no proteins surpass a 2.8-fold change in expression levels following 2-CMA treatment (Supplemental Table 4). Gene ontology (GO) analysis revealed an increase in ATP binding activity, response to stimulus, biological processes involved in interspecies interactions, reproductive processes, and reproduction in response to 2-CMA treatment (Fig. 1 C). Furthermore, protein-protein interaction analysis showed a larger cluster for vesicle trafficking and a unique cluster for the kinetoplast in

response to treatment, while wildtype parasites displayed larger clusters for the ribosome and replication (Fig. 1 D). Altogether, these data suggest that alterations to the *L. v. guyanensis* proteome treatment with 2-CMA are related to increased intracellular vesicle transport and trafficking and replication, and decreased translation and metabolic functions.

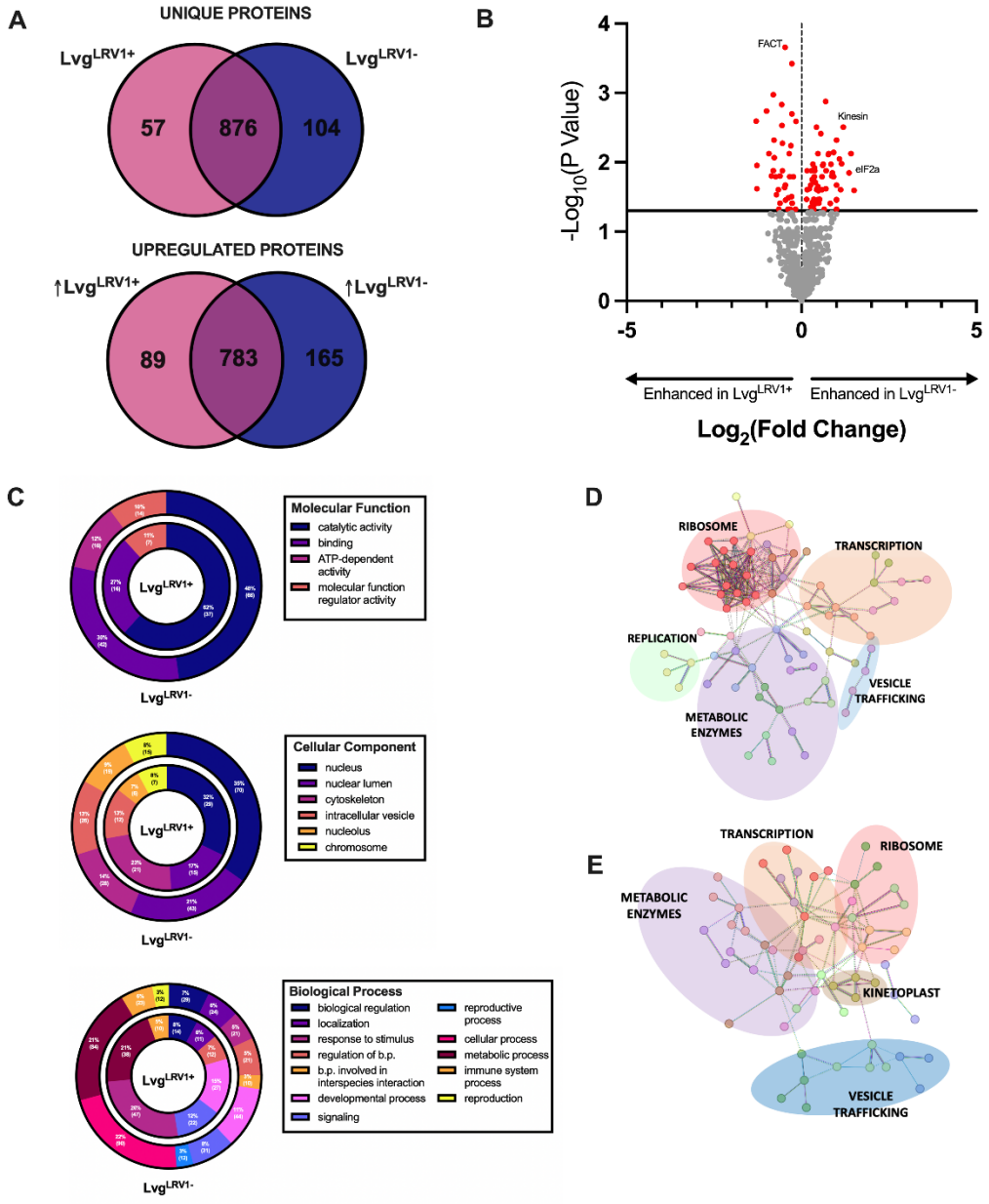

Figure 1. Pharmacological treatment of endogenously LRV1-infected *L. v. guyanensis* alters its proteome.
The protein content of infected (Lvg^{LRV1+}) and treated (Lvg^{LRV1-}) *L. v. guyanensis* parasites was catalogued by mass spectrometry (*L. braziliensis* database). **A.** The distribution of identified

proteins by their (top) presence/absence and by their (bottom) quantitative profiles (*n*=3 for each group analysed. Only proteins that appeared in 2 out of 3 triplicates were included in the final list. See Supplementary Tables 2, 3 and 4). Differential expression was determined based on a positive or negative fold change ≥ 1.2 ($P \leq 0.05$) **B.** The distribution of identified proteins by their fold change and significance visualized by Volcano plot. The threshold for significance ($P \leq 0.05$) delimitates significantly differentially expressed proteins (identified in red). **C.** Gene ontology of differentially expressed proteins was annotated using Blast2GO BlastP function, followed by mapping to Human (e-value ≤ 1.0E-3). **D-E.** Protein-protein interaction networks of differentially expressed proteins were created using STRING with high confidence (0.700) and an MCL parameter of 3, and non-clustered proteins were excluded. Networks are represented for **D.** Lvg^{LRV1+} and **E.** Lvg^{LRV1-}.

Endogenously-infected *L. v. guyanensis* secretes LRV1 through the exosomal pathway.

As previously shown for several *Leishmania* species, promastigotes release extracellular vesicles in culture in response to a temperature shift from 25 to 37˚C [136,137,157]. Extracellular vesicles derived from LRV1-infected (Exo^{LRV1+}), and 2-CMA treated (Exo^{LRV1-}) parasites were characterized by nanoparticle tracking analysis (NTA), to determine size distribution and concentration, and morphology was visualized by transmission electron microscopy (TEM) (Fig. 2 A-B). Exosomes derived from both LRV1-bearing and 2-CMA-treated *L. v. guyanensis* display the cup shape that is characteristic of exosomes visualized by TEM. Further, exosomes in both preparations are similar in size and morphology, apart from LRV1 virions that can be visualized within the exosomes derived from endogenously LRV1-infected *L. v. guyanensis*. The presence of viral material in exosome preparations was additionally assessed by PCR, validating that only exosomes produced by LRV1-bearing *L. v. guyanensis* contained LRV1 viral RNA (Fig. 2 C).

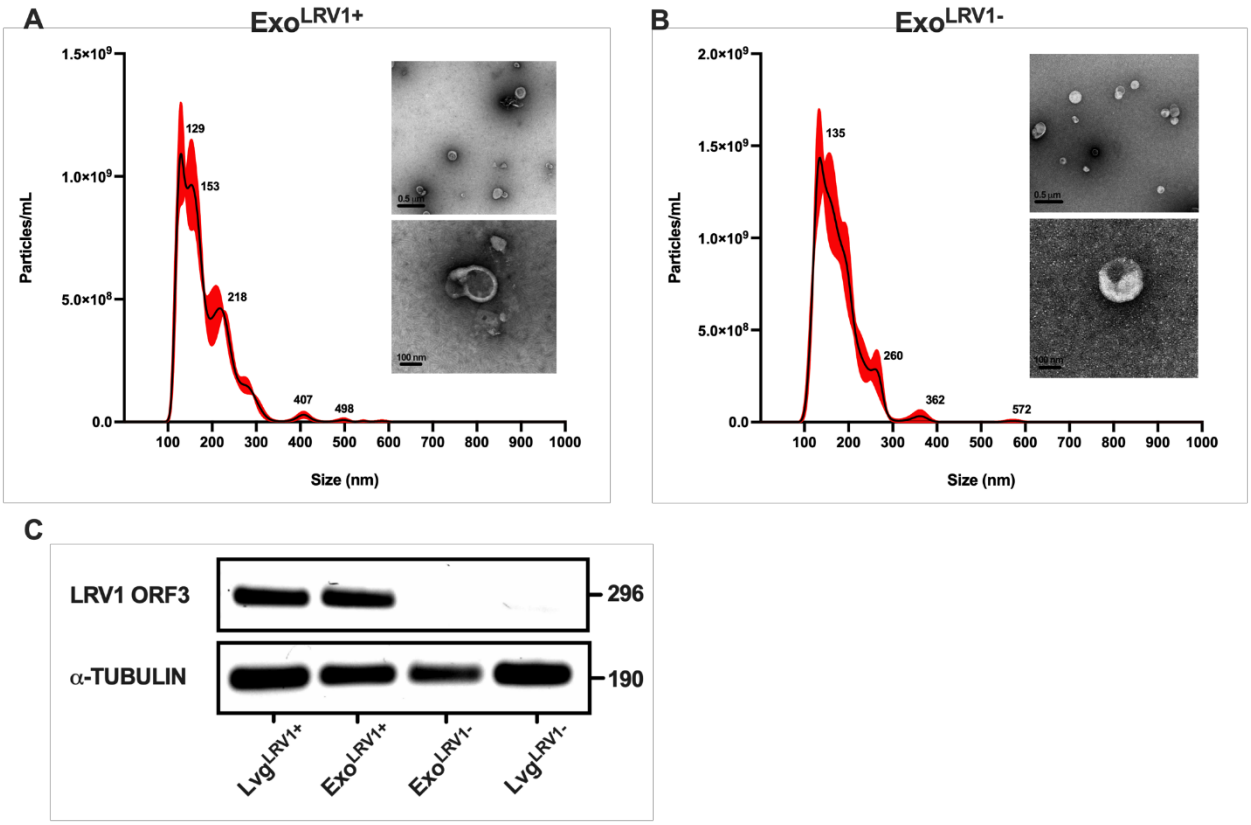

Figure 2. Exosomes produced by LRV1-infected *L. v. guyanensis* contain LRV1.
EVs were isolated from infected (Lvg^{LRV1+}) and treated (Lvg^{LRV1-}) *L. v. guyanensis* parasites using a four-hour temperature shift followed by filtration/ultracentrifugation methodology. Size distribution and quantification of EV preparations was determined by NS300 NTA using a 1:50 dilution in exosome buffer. EVs were prepared for TEM by negative staining and visualized using a FEI Tecnai-12 120kV electron microscope. **A.** EVs isolated from Lvg^{LRV1+} encapsulate characteristic LRV1-like particles. **B.** EVs isolated from Lvg^{LRV1-} do not contain viral-like particles. **C.** Presence of viral RNA in EVs and in parasites, assessed by PCR of total cDNA. Results are representative of at least three independent experiments with similar data.

Exosomal cargo is mostly recapitulative of the cell from which exosomes are derived, though cargo sorting enables the enrichment of certain proteins, nucleic acids, and lipids [113]. We therefore sought to characterize the content of exosomes derived from LRV1-infected (Exo^{LRV1+}) and 2-CMA-treated (Exo^{LRV1-}) *L. v. guyanensis* using proteomic analysis. While 826 proteins were shared between Exo^{LRV1+} and Exo^{LRV1-}, 138 and 91 unique proteins were identified within these respective groups. Moderate variation in expression levels was apparent, with 165 proteins overexpressed in Exo^{LRV1+}, and 89 proteins overexpressed in Exo^{LRV1-}, while the vast majority of

protein expression remained unchanged (Fig. 3 A). Notably, proteins that had significantly altered expression levels include the upregulated microtubule-associated protein Gb4, and the downregulated Isoleucyl tRNA synthetase and Methionine aminopeptidase (Fig. 3 B). In contrast to the parasite's proteome, differential expression of the exoproteome following 2-CMA treatment attained much higher fold changes, notably 7.25 for Gb4, indicating a role for exosomal cargo sorting in enhancing these differences (Supplemental Table 7). When mapped to biological functions using gene ontology analysis, GO terms including molecular function regulator activity, the lysosome, and multicellular organismal processes were only identified in proteins overexpressed in Exo^{LRV1-}, while the nucleolus, response to stimulus and biological processes involved in interspecies interactions were unique to Exo^{LRV1+} (Fig. 3 C). Protein-protein interaction analysis of these data showed a moderate increase in the number of nodes involved in the ribosome, vesicle trafficking and transcription in response to 2-CMA treatment (Fig. 3 D-E). Together, exoproteomic data reveals the role of intracellular vesicle transport and trafficking, translation, metabolic functions, and transcription. While these alterations are similar to that of the parasite's proteome, they are amplified in the exoproteome, reiterating the role of vesicle cargo sorting.

Collectively, these data indicate that exosomes derived from LRV1-infected *L. v. guyanensis* contain LRV1 virions, and that treatment of *L. v. guyanensis* with 2-CMA eliminates the virus, causing alterations to both the proteome and the exoproteome.

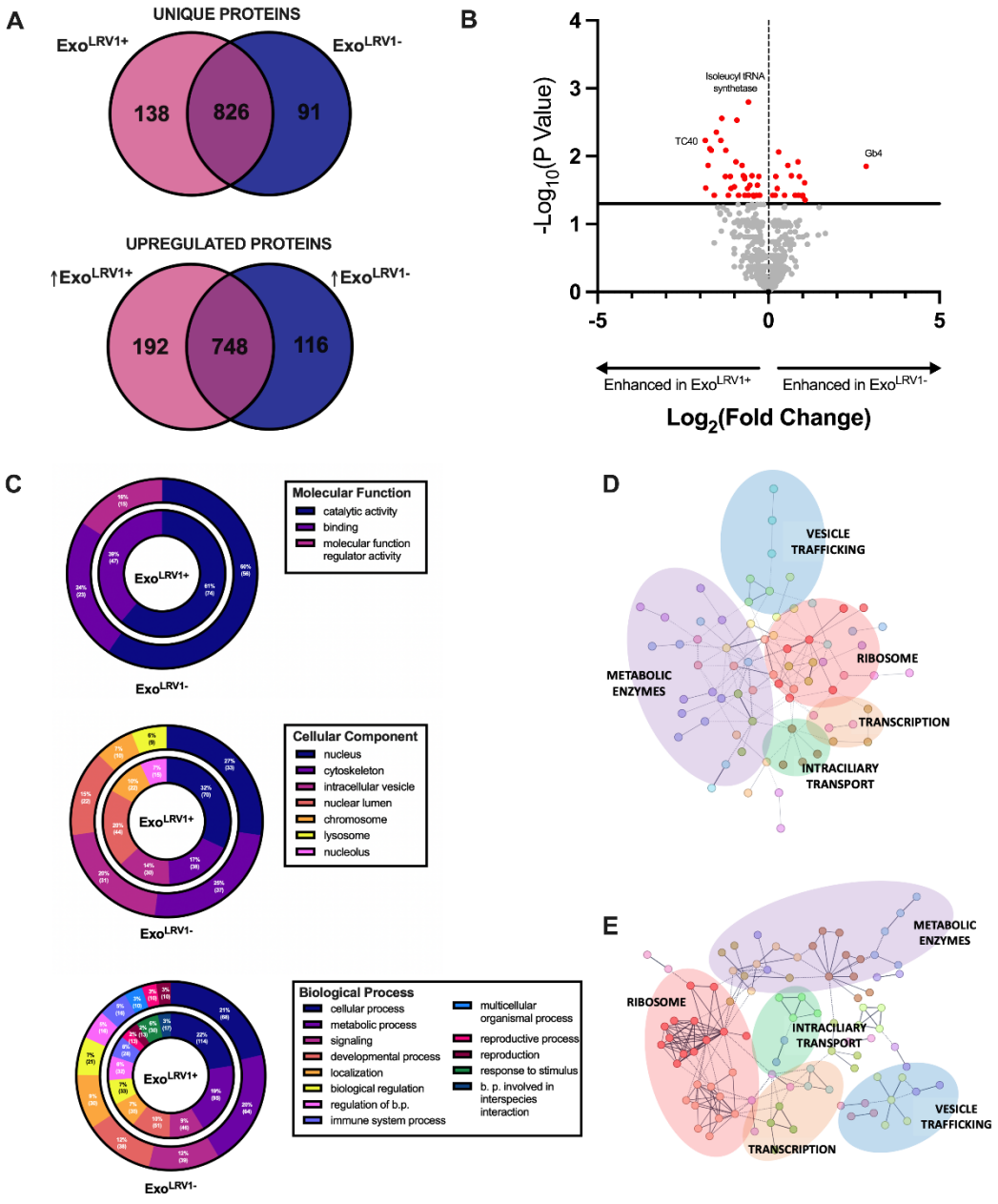

Figure 3. Pharmacological treatment of endogenously LRV1-infected *L. v. guyanensis* alters its exoproteome.

The protein content of exosomes derived from infected (Exo^{LRV1+}) and treated (Exo^{LRV1-}) *L. v. guyanensis* was catalogued by mass spectrometry (*L. braziliensis* database). **A.** The distribution of identified proteins by their (top) presence/absence and by their (bottom) quantitative profiles (n=3 for each group analysed. Only proteins that appeared in 2 out of 3 triplicates were included in the final list. See Supplementary Tables 5, 6 and 7). Differential expression was determined based on a positive or negative fold change ≥ 1.2 ($P \leq 0.05$) **B.** The distribution of identified proteins by their fold change and significance visualized by Volcano plot. The threshold for significance ($P \leq 0.05$) delimitates significantly differentially expressed proteins (identified in red). **C.** Gene ontology of differentially expressed proteins was annotated using Blast2GO BlastP function,

followed by mapping to Human (e-value ≤ 1.0E-3). **D.** Protein-protein interaction networks of differentially expressed proteins were created using STRING with high confidence (0.700) and an MCL parameter of 3, and non-clustered proteins were excluded. Networks are represented for **D.** Exo^{LRV1+} and **E.** Exo^{LRV1-}.

LRV1 infection of *L. v. panamensis* increases parasitic fitness and infectivity.

We have previously shown that exosomes derived from LRV1-infected *L. v. guyanensis* can be used to infect other *Leishmania* species [157]. Herein, we infected *L. v. panamensis*, a closely-related parasite of the *Viannia* subgenus, by direct inoculation of Exo^{LRV1+} into the parasite culture medium (Fig. 4 A). At 2 weeks post-infection, the presence of LRV1 RNA in wildtype (Lpa^{WT}) and in LRV1-infected parasites (Lpa^{LRV1+}) was measured using PCR, corroborating the establishment of LRV1 infection in Lpa^{LRV1+} (Fig. 4 B).

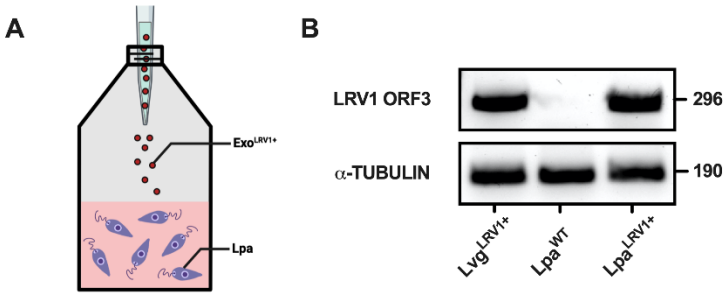

Figure 4. *L. v. panamensis* is infected with LRV1 via exosomes derived from endogenously infected *L. v. guyanensis*.
A. To infect *L. v. panamensis*, 10µg of Exo^{LRV1+} was directly inoculated into logarithmic-phase parasite cultures overnight, then parasites were passaged regularly to maintain logarithmic growth for 2 weeks. **B.** Presence of LRV1 viral RNA in Lpa^{LRV1+}, assessed by PCR at 2 weeks post-infection. Results are representative of at least three independent experiments.

Following previous observation of the modulation of transcriptional profiles of several key *L. v. panamensis* genes in response to LRV1 infection [157], we hypothesized that viral infection would significantly remodel the parasitic proteome. Identification of unique proteins from these groups revealed that only 520 proteins were shared between wildtype and infected *L. v. panamensis*, while

705 were unique to Lpa^{LRV1+} and 42 were unique to Lpa^{WT}. This trend was accentuated when assessing expression levels of proteins, for which 1021 were overexpressed in Lpa^{LRV1+}, and only 54 were overexpressed in Lpa^{WT} (Fig. 5 A). The skewness of protein expression towards infected parasites is striking, and most significantly upregulated proteins include prolyl tRNA synthetase, inositol-3-phosphate synthetase and PKA regulatory subunit, while PKA catalytic subunit is downregulated following LRV1 infection (Fig. 5 B). Further, expression of the metabolic enzyme carboxyeptidase is increased by a fold change of 8.3 in response to LRV1 infection (Supplemental Table 10). Gene ontology analysis of these data revealed an increase in molecular functions including catalytic and binding activity following LRV1 infection, and a decrease in the lysosome cellular component. Most notable changes were visualized using biological process GO terms, for which there is a significant increase in general cellular and metabolic processes in response to infection, while wildtype parasite proteomes displayed unique functions including biological processes involved in interspecies interaction, homeostatic processes, and multicellular organismal processes (Fig. 5 C). When comparing protein-protein interaction analyses between Lpa^{LRV1+} and Lpa^{WT}, it is evident that there is important upregulation of tRNA synthetases, metabolic enzymes, and of proteins involved in vesicle trafficking, the ribosome, the proteasome, the cytoskeleton, replication, translation, and protein folding following LRV1 infection (Fig. 5 D-E). These data suggest important modulation of the parasitic proteome in response to LRV1 infection. This modulation is all the more striking in comparison to that caused by the 2-CMA treatment of *L. v. guyanensis*, for which most proteins detected in the proteome and exoproteome remained unchanged in detection and levels of expression.

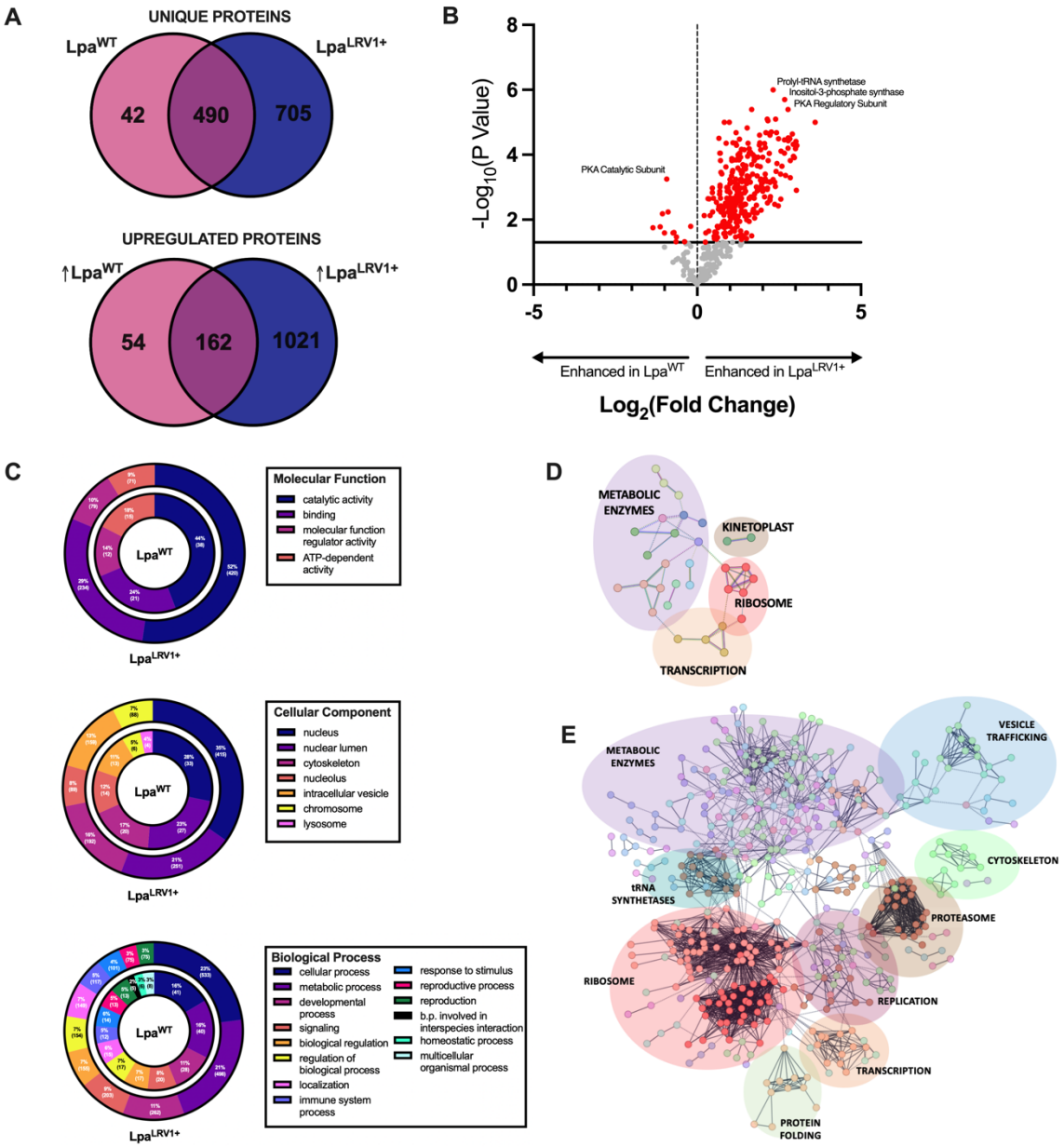

Figure 5. Infection of *Leishmania v. panamensis* with LRV1 induces important changes to the proteic landscape.

The protein content of wildtype (Lpa^{WT}) and LRV1-infected (Lpa^{LRV1+}) *L. v. panamensis* parasites was catalogued by mass spectrometry (*L. braziliensis* database). **A.** The distribution of identified proteins by their (top) presence/absence and by their (bottom) quantitative profiles (n=3 for each group analysed. Only proteins that appeared in 2 out of 3 triplicates were included in the final list. See Supplementary Tables 8, 9 and 10). Differential expression was determined based on a positive or negative fold change ≥ 1.2 (P ≤ 0.05) **B.** The distribution of identified proteins by their fold change and significance visualized by Volcano plot. The threshold for significance (P ≤ 0.05) delimitates significantly differentially expressed proteins (identified in red). **C.** Gene ontology of differentially expressed proteins was annotated using Blast2GO BlastP function, followed by mapping to Human (e-value ≤ 1.0E-3). **D.** Protein-protein interaction networks of differentially

expressed proteins were created using STRING with high confidence (0.700) and an MCL parameter of 3, and non-clustered proteins were excluded. Networks are represented for **D.** Lpa^{WT} and **E.** Lpa^{LRV1+}.

To assess the biological impact of such changes, we identified pathways involved in *Leishmania* infection and survival, and assessed the expression levels of their proteic mediators. Proteins involved in translation, notably for translation initiation/elongation and tRNA aminoacylation were shown to be upregulated in response to infection, as previously visualized by increased ribosomal and translation-associated clusters in PPI analysis (Fig. 6 A). Expression levels of metabolic proteins suggest an increase in most metabolic processes, particularly that of lipid metabolism (Fig. 6 B).

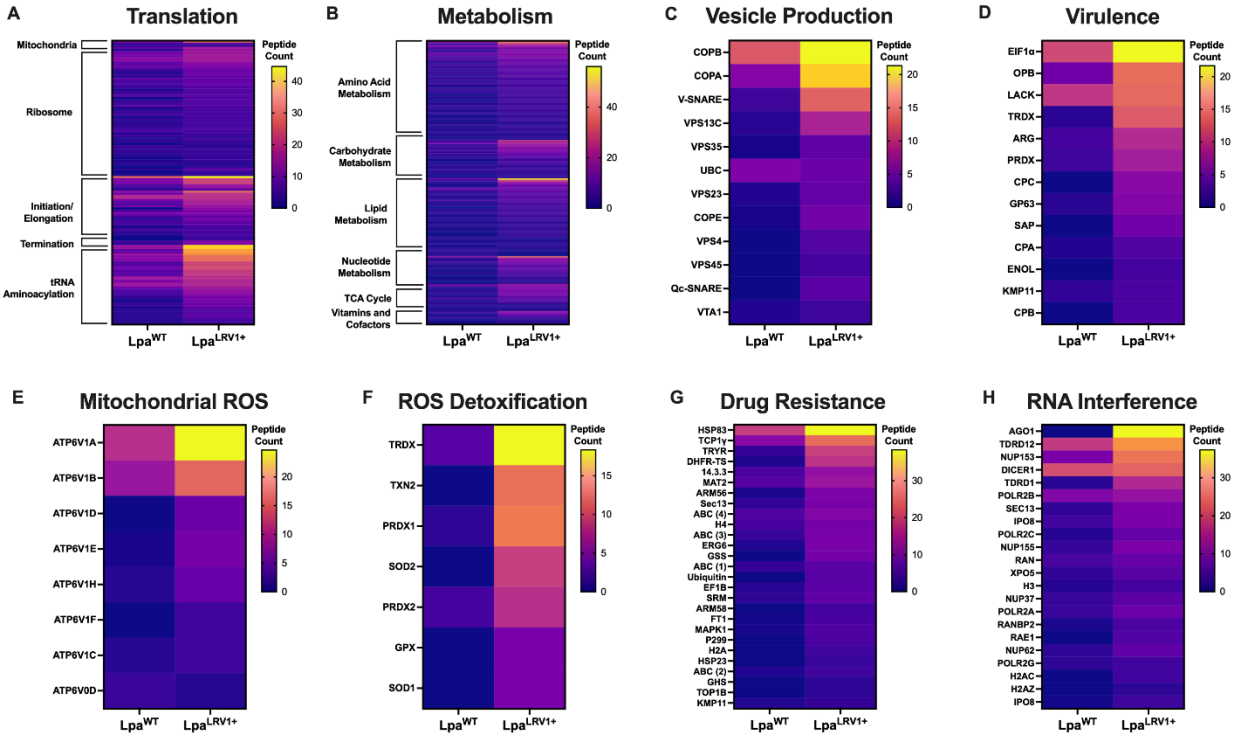

Figure 6. LRV1 infection upregulates the expression of key *L. v. panamensis* infectious and survival assets.
L. braziliensis database proteins were mapped to homologs in *Homo sapiens* and to the Reactome Pathway database using Blast2Go BlastP function and mapping (e-value ≤ 1.0E-3). Lists of homologs were generated and curated manually to integrate additional non-mammalian proteins involved in pathways (See Supplementary Tables 18-25). Identified proteins in wildtype (Lpa^{WT}) and LRV1-infected (Lpa^{LRV1+}) *L. v. panamensis* parasites were then searched against leishmanial homologs and pathway lists, and the expression of peptides involved in **A.** translation (Reactome

ID: R-HSA-72766), **B.** metabolism (Reactome ID: R-HSA-1430728), **C.** vesicle production (Reactome ID: R-HSA-917729), **D.** virulence (Reactome ID: N/A; manually curated), **E.** Mitochondrial ROS production (Reactome ID: R-HSA-1222556), **F.** ROS detoxification (Reactome ID: R-HSA-3299685), **G.** Drug resistance (Reactome ID: N/A; manually curated), and **H.** RNA interference (Reactome ID: R-HSA-211000) were represented using heat maps of identified expression levels.

Having previously reported that LRV1 utilizes the leishmanial exosomal pathway for transmission, we sought to assess expression levels of proteins involved in the endosomal sorting complex required for transport (ESCRT) pathway, which is required for exosome biogenesis [157]. Several key proteins involved in vesicle trafficking were upregulated, including several coatomer subunits (COPA, COPB, COPE), SNAP-receptor proteins (qc-SNARE, v-SNARE), along with multiple vacuolar protein sorting-associated (VPS) proteins (Fig. 6 C). We corroborated the functional impact of ESCRT protein overexpression by measuring the production of extracellular vesicles by Lpa^{WT} and Lpa^{LRV1+}, revealing a decrease in production of vesicles from 60-80nm in size, and an increase in production of vesicles from 100-120nm in size by infected parasites (Fig. 7). This may suggest the biogenesis of slightly larger vesicles in the context of LRV1 infection, to permit the encapsulation of exosomal cargo along with the virion.

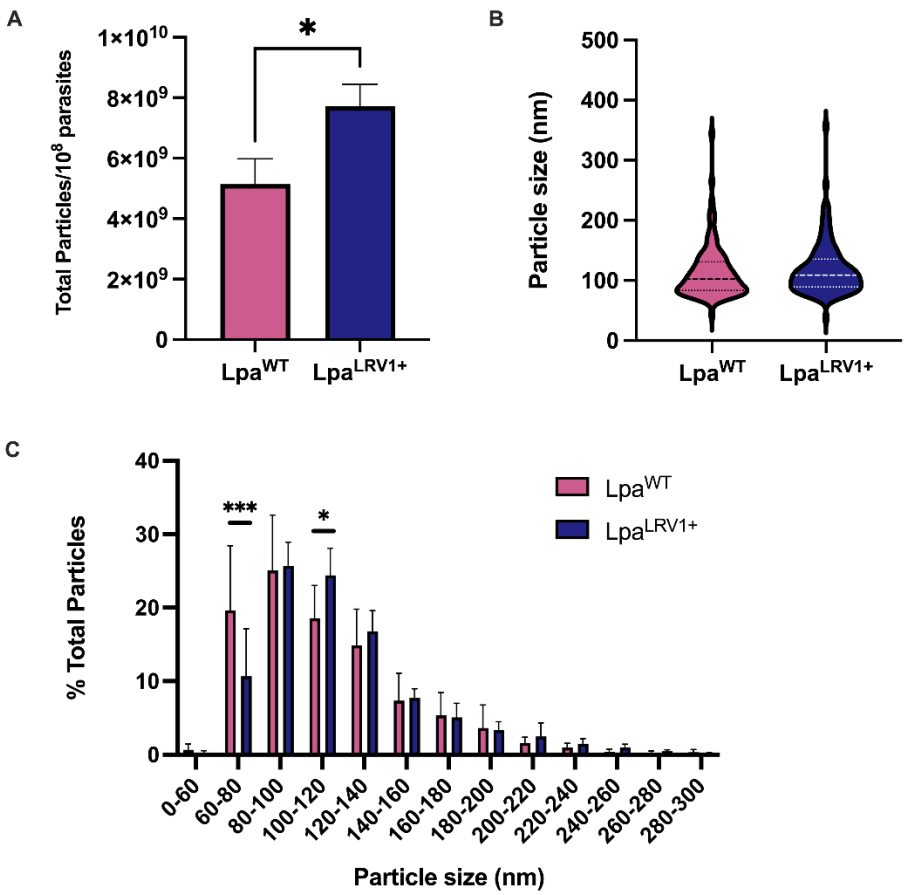

Figure 7. LRV1 infection increases the production of extracellular vesicles by *L. v. panamensis*.
EVs were isolated from wildtype (Lpa^{WT}) and LRV1-infected (Lpa^{LRV1+}) *L. v. panamensis* parasites using a four-hour temperature shift followed by filtration/ultracentrifugation methodology. Size distribution and quantification of EV preparations was determined by NS300 NTA using a 1:50 dilution in exosome buffer (*n*=6 per group). **A.** Total extracellular vesicles produced per 1 x 10^8 Lpa^{WT} and Lpa^{LRV1+} parasites show a significant increase in response to LRV1 infection. **B.** No differences to the mean and median of EV size was apparent. **C.** A decrease in vesicles from 60-80 nm in size and an increase in vesicles from 100-120 nm in size was apparent in Lpa^{LRV1+} comparatively to Lpa^{WT}. Statistical significance was determined using unpaired Student's t-Test with Holm–Sidak's correction, and error bars represent SEM. *$P \leq 0.05$, **$P \leq 0.01$, ***$P \leq 0.001$. Results are representative of three independent experiments performed in duplicate.

Considering the impact of LRV1 on the exacerbation of cutaneous leishmaniasis [157,170,176], we investigated the role of virulence factor expression, which was significantly increased in Lpa^{LRV1+} (Fig. 6 D). Accordingly, an increase in the proteolytic activity of the major surface

metalloprotease GP63, or leishmanolysin, which plays a fundamental role in the subversion of the antileishmanial response, was visualized by gelatin zymography (Fig. 8).

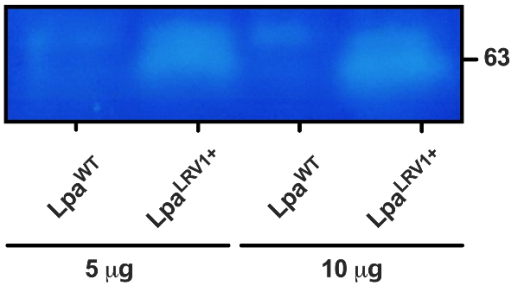

Figure 8. LRV1 infection increases GP63 proteolytic activity.
Lysate of wildtype (Lpa^{WT}) and LRV1-infected (Lpa^{LRV1+}) *L. v. panamensis* parasites was dosed using Bradford protein reagent, and 5μg or 10μg of protein was separated using SDS–PAGE containing gelatin. Following overnight incubation and staining with Coomassie blue, light bands appear where GP63 protease has degraded the gelatin. A significant difference is apparent in GP63 proteolytic activity between Lpa^{WT} and Lpa^{LRV1+}. Results are representative of three independent experiments with similar data.

While the production of reactive oxygen species (ROS) by mitochondria is an evolutionarily-conserved innate antiviral mechanism, several viruses have been reported to manipulate mitochondrial respiratory function and downstream pathways to ensure survival and complete their life cycle [196,197]. We therefore characterized the expression levels of proteins involved in the production of ROS by the mitochondrion/kinetoplast in *Leishmania*, highlighting an important increase in several vacuolar ATPases (Fig. 6 E). Detection of dichlorofluorescein diacetate (DCFDA) fluorescence, which is emitted following oxidization by intracellular ROS, confirmed the increase in ROS production by Lpa^{LRV1+} (Fig. 9).

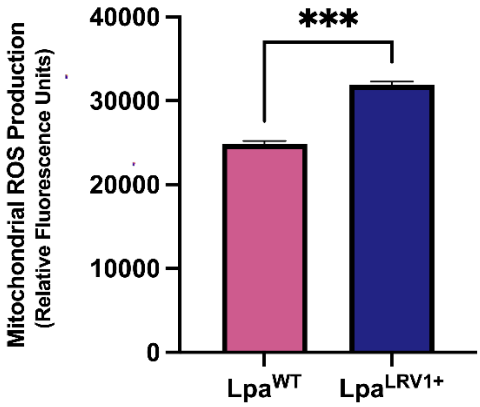

Figure 9. LRV1 infection increases the production of intracellular reactive oxygen species by the *L. v. panamensis* mitochondria/kinetoplast.
5 x 10^6 wildtype (Lpa^{WT}) and LRV1-infected (Lpa^{LRV1+}) *L. v. panamensis* promastigotes were incubated with HEPES-NaCl containing H_2-DCFDA. When oxidized intracellularly, H_2-DCFDA forms a fluorescent compound. Lpa^{LRV1+} has significantly higher levels of intracellular ROS than Lpa^{WT}. Statistical significance was determined using unpaired Student's t-Test with Holm–Sidak's correction, and error bars represent SEM. *$P \leq 0.05$, **$P \leq 0.01$, ***$P \leq 0.001$. Results are representative of three independent experiments performed in duplicate.

In the context of virus-induced ROS production, the antioxidant defense mechanism has been evolved by cells to protect against exposure to free oxygen radicals and ROS-induced apoptosis [197]. Key mediators of this defense in *Leishmania* include superoxide dismutase (SOD1, SOD2), glutathione peroxidase (GPX), thioredoxin (TXN), and the catalase analogs tryparedoxin (TRDX) and peroxiredoxin (PRDX) [197,198], which were all significantly overexpressed in Lpa^{LRV1+} (Fig. 6 F). To determine whether this increase in detoxifying enzymes translated into a greater capacity for survival, we assessed the growth of Lpa^{WT} and Lpa^{LRV1+} in culture media containing increasing concentrations of hydrogen peroxide. LRV1-infected parasites were capable of greater survival at 0.25 and 0.5 mM of H_2O_2, though this trend was lost as higher concentrations of the oxidizing agent (Fig. 10).

It has also been reported that the presence of LRV1 in clinical isolates of *L. v. guyanensis* and *L. v. braziliensis* is predictive of drug treatment failure [167,169,199]. We therefore investigated

expression levels of genes that have been associated to drug resistance, including ABC transporters, which are upregulated in Lpa^{LRV1+} (Fig. 6 G). When assessing resistance to drugs by growing Lpa^{LRV1+} and Lpa^{WT} in increasing concentrations of antimony trioxide, moderate drug resistance is only discernable at 1μM (Fig. 11).

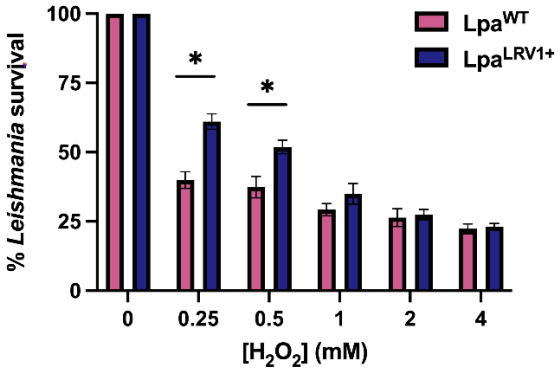

Figure 10. LRV1 infection provides *L. v. panamensis* with greater survival capacity to reactive oxygen species.
Wildtype (Lpa^{WT}) and LRV1-infected (Lpa^{LRV1+}) *L. v. panamensis* parasites were grown in the presence of increasing concentrations of hydrogen peroxide (H_2O_2). Optical density (A=600nm) of parasite culture was measured at day 8 of growth. Lpa^{LRV1+} growth was greater than Lpa^{WT} at both 0.25 and 0.5 mM. Statistical significance was determined using unpaired Student's t-Test with Holm–Sidak's correction, and error bars represent SEM. *P ≤ 0.05, **P ≤ 0.01, ***P ≤ 0.001. Results are representative of three independent experiments performed in duplicate.

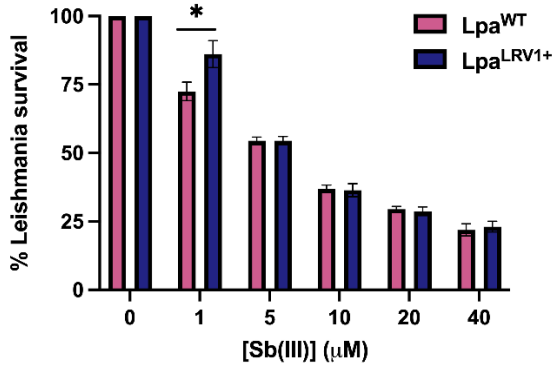

Figure 11. LRV1 infection moderately impacts *L. v. panamensis* drug resistance.
Wildtype (Lpa^{WT}) and LRV1-infected (Lpa^{LRV1+}) *L. v. panamensis* parasites were grown in the presence of increasing concentrations of antimony trioxide (Sb(III)). Optical density (A=600nm) of parasite culture was measured at day 8 of growth. Lpa^{LRV1+} growth was greater than Lpa^{WT} at 1μM. Statistical significance was determined using unpaired Student's t-Test, and error bars represent SEM. *P ≤ 0.05, **P ≤ 0.01, ***P ≤ 0.001. Results are representative of three independent experiments performed in duplicate.

Next, we investigated the RNA interference (RNAi) pathway, which has been suggested to play a key role in the persistence of LRV1 within *Leishmania*, maintaining viral loads under a threshold that would be lytic to the parasite [163]. Most notably, the protein Argonaute 1 (AGO1), a key component of the RNA-induced silencing complex (RISC), is significantly upregulated in Lpa^{LRV1+}, while the expression of the endoribonuclease Dicer1 remains constant (Fig. 6 H).

Thus, the infection of *L. v. panamensis* by LRV1 increases the expression of proteomic mediators of infection and survival. To determine if, altogether, this enabled greater infection *in vitro*, we infected bone-marrow derived macrophages with Lpa^{WT} and Lpa^{LRV1+} for 3 hours at a multiplicity of infection of 5, revealing an increase in the number of amastigotes internalized per infected cell. This trend was maintained over the course of infection, suggesting greater resistance to cellular parasitotoxic functions (Fig. 12).

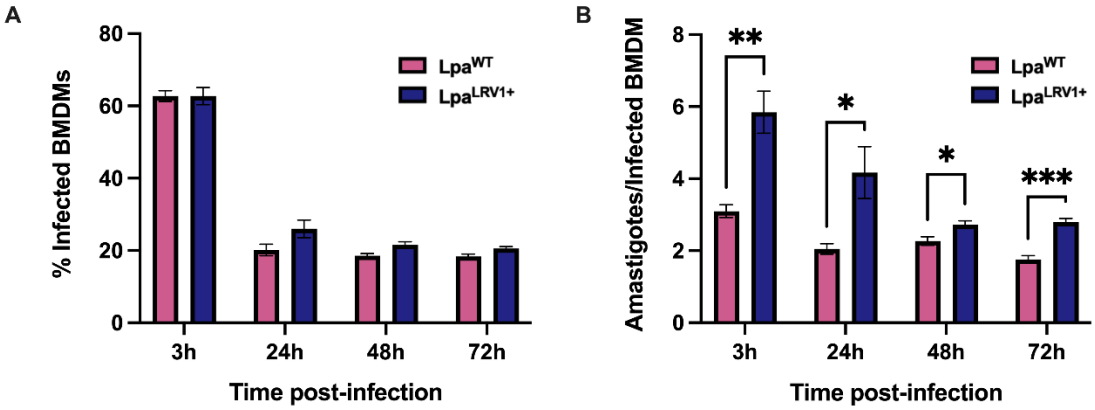

Figure 12. LRV1 infection induces greater infection of BMDMs by *L. v. panamensis*.
BMDMs plated in chamber slides were infected with wildtype (Lpa^{WT}) and LRV1-infected (Lpa^{LRV1+}) *L. v. panamensis* parasites using an MOI of 5 for 3 hours, then washed to remove unattached parasites and maintained for the corresponding time course. Chamber slides were stained using Diff-Quick and 200 cells were counted using a light microscope. **A.** No significant difference in the percentage of infected BMDMs is apparent between Lpa^{WT} and Lpa^{LRV1+} parasites. **B.** The number of amastigotes per 100 infected BMDMs is significantly higher at all timepoint post-infection for Lpa^{LRV1+} parasites. Statistical significance was determined using unpaired Student's t-Test with Holm–Sidak's correction, and error bars represent SEM. *$P \leq 0.05$, **$P \leq 0.01$, ***$P \leq 0.001$. Results are representative of three independent experiments performed in duplicate.

LRV1 Infection of *L. v. panamensis* Alters Signaling

We next aimed to characterize the host-pathogen interaction between LRV1 and *L. v. panamensis*. A significant increase in proteins homologous to those involved in mammalian virus-associated pathways, including that of SARS-CoV2, influenza virus and HIV infection in *Homo sapiens*, was observed in Lpa^{LRV1+} (Fig. 13). Shared expression of key mediators of signaling between these pathways led us to investigate the modulation of signaling cascades.

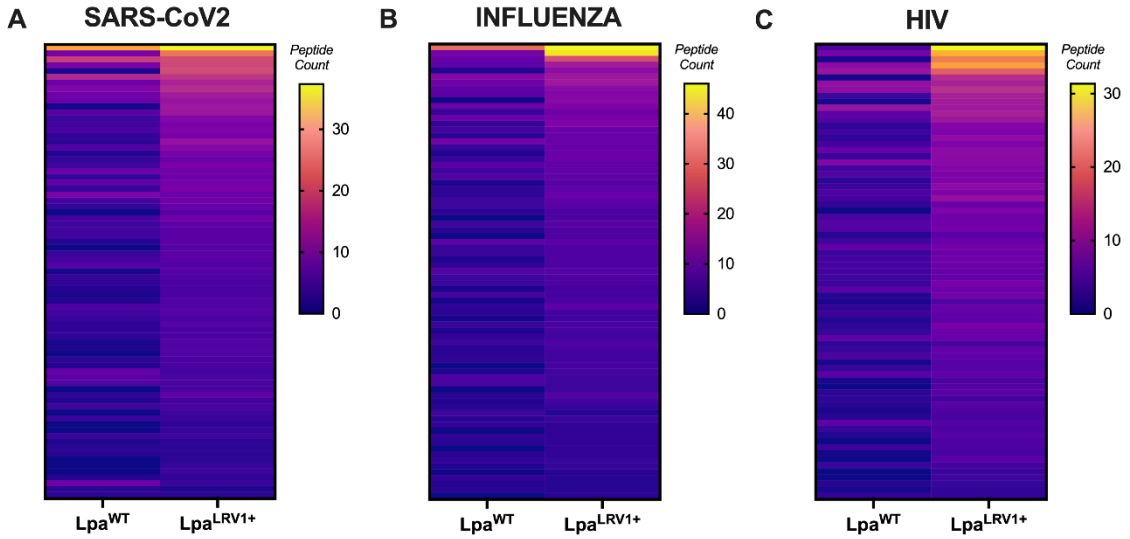

Figure 13. Expression of leishmanial homologs to mediators of mammalian viral infection is increased in response to LRV1 infection.
L. braziliensis database proteins were mapped to homologs in *Homo sapiens* and to the Reactome Pathway database using Blast2Go BlastP function and mapping (e-value ≤ 1.0E-3). Lists of homologs were generated (See Supplementary Table 26). Identified proteins in wildtype (Lpa^{WT}) and LRV1-infected (Lpa^{LRV1+}) *L. v. panamensis* parasites were then searched against leishmanial homologs and pathway lists, and the expression of peptides involved in **A.** SARS-CoV2 infection (Reactome ID: R-HSA-9694516), **B.** Influenza infection (Reactome ID: R-HSA-168255), and **C.,** HIV infection (Reactome ID: R-HSA-162906) were represented using heat maps of identified expression levels.

To better understand signaling events occurring in response to LRV1 infection of *L. v. panamensis*, we performed phosphoproteomic analysis on Lpa^{WT} and Lpa^{LRV1+}. A significantly higher number of phosphopeptides was detected in Lpa^{LRV1+} – 234 uniquely expressed comparatively to 8 unique phosphopeptides in Lpa^{WT} – indicating important post-translational modification of peptides

induced by LRV1 infection. Expression levels of these phosphopeptides varied very little between Lpa^{WT} and Lpa^{LRV1+}, as is expected with transient and relatively rare phosphorylation events (Fig. 14 A, C). The number of post-translational modification sites showed the same trend, with slightly higher values accounting for multiple potential phosphosites per phosphoprotein (Fig. 14 B). Gene ontology analysis provided little insight into variations in phosphoproteome functionality, aside from an increase in molecular function regulator activity and multicellular organismal processes (Fig. 14 C). The low number of phosphopeptides in Lpa^{WT} makes it difficult to infer functionality using GO analysis, which considers the presence of a single peptide as indicative of biological function. Protein-protein interaction analysis provides more robust data in this context, indicating an overexpression of proteins involved in the ribosome, the cilium, vesicle-mediated transport, proton transport and protein ubiquitination in the Lpa^{LRV1+} phosphoproteome, while a single cluster of ribosomal phosphoproteins was present in the Lpa^{WT} phosphoproteome (Fig. 14 D-E).

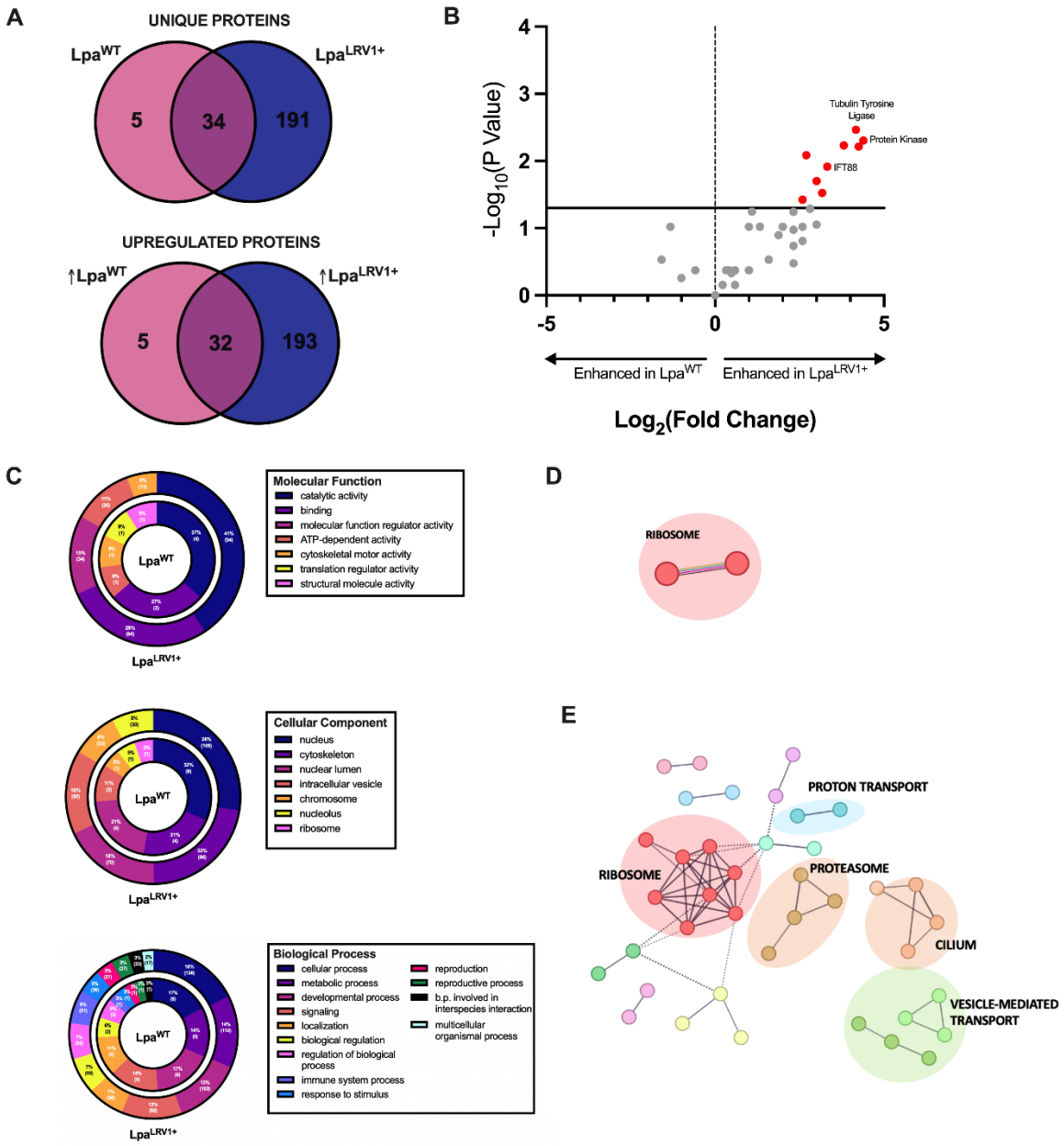

Figure 14. Infection of *L. v. panamensis* with LRV1 induces important changes to the phosphoproteomic landscape.

The phosphoprotein content of wildtype (Lpa^{WT}) and LRV1-infected (Lpa^{LRV1+}) *L. v. panamensis* parasites was catalogued by mass spectrometry (*L. braziliensis* database). **A.** The distribution of identified phosphoproteins by their (top) presence/absence and of identified phosphosites by their (bottom) presence/absence (n=2 for each group analysed. Only proteins that appeared in both duplicates were included in the final list. See Supplementary Tables 11, 12 and 13). Differential expression was determined based on a positive or negative fold change ≥ 1.2 ($P \leq 0.05$) **B.** The distribution of identified proteins by their fold change and significance visualized by Volcano plot. The threshold for significance ($P \leq 0.05$) delimitates significantly differentially expressed proteins (identified in red). **C.** Gene ontology of differentially expressed proteins was annotated using

Blast2GO BlastP function, followed by mapping to Human (e-value ≤ 1.0E-3). **D.** Protein-protein interaction networks of differentially expressed proteins were created using STRING with high confidence (0.700) and an MCL parameter of 3, and non-clustered proteins were excluded. Networks are represented for **D.** Lpa^{WT} and **E.** Lpa^{LRV1+}.

Upstream of phosphopeptides are kinases and transcription factors, which can be inferred from differentially expressed phosphorylated substrates. Expression2Kinase (X2K) analysis of enriched phosphopeptides indicated a notable increase in MAPK signaling and cyclin-dependent pathways in response to LRV1 infection, along with the transcriptional regulators IRF3 (Fig. 15).

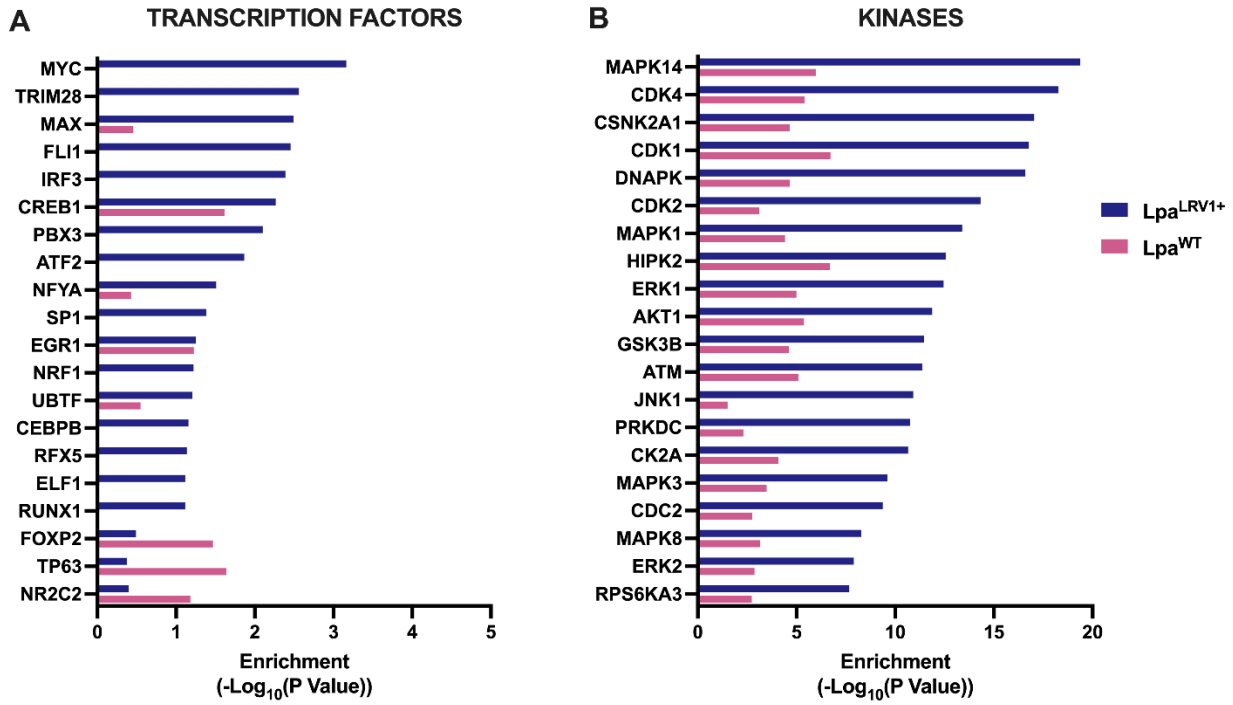

Figure 15. LRV1 infection of *L. v. panamensis* alters upstream regulators of signaling. Identified phosphoproteins (*L. braziliensis* database) in wildtype (Lpa^{WT}) and LRV1-infected (Lpa^{LRV1+}) *L. v. panamensis* parasites were mapped to homologs in *Homo sapiens* (e-value ≤ 1.0E-3) and input into the Expression2Kinase (X2K) database to determine upstream regulators of the phosphoproteome. **A.** Transcription Factor Enrichment Analysis (TFEA) of the top 20 predicted transcription factors regulating input phosphoprotein homologs. **B.** Kinase enrichment analysis (KEA) of the top 20 predicted kinases that regulate the phosphoproteins identified in Lpa^{WT} and Lpa^{LRV1+}.

Though not all pathways have been identified thus far within *Leishmania*, signaling pathways may have been conserved throughout eukaryotic evolution. Analysis of the phosphoproteome therefore provided evidence of pathway modulation in response to LRV1 infection of *L. v. panamensis*.

We next aimed to integrate the modulation of post-translational modification with that of peptide expression, to obtain an overview of the synergistic effect of protein levels and phosphorylation-mediated activation status. Reactome pathway analysis revealed a significant upregulation of the detoxification of reactive oxygen species, RUNX-mediated translational regulation, and mitogen-activated protein (MAP) signaling and cyclin-dependent pathways, among others (Fig. 16).

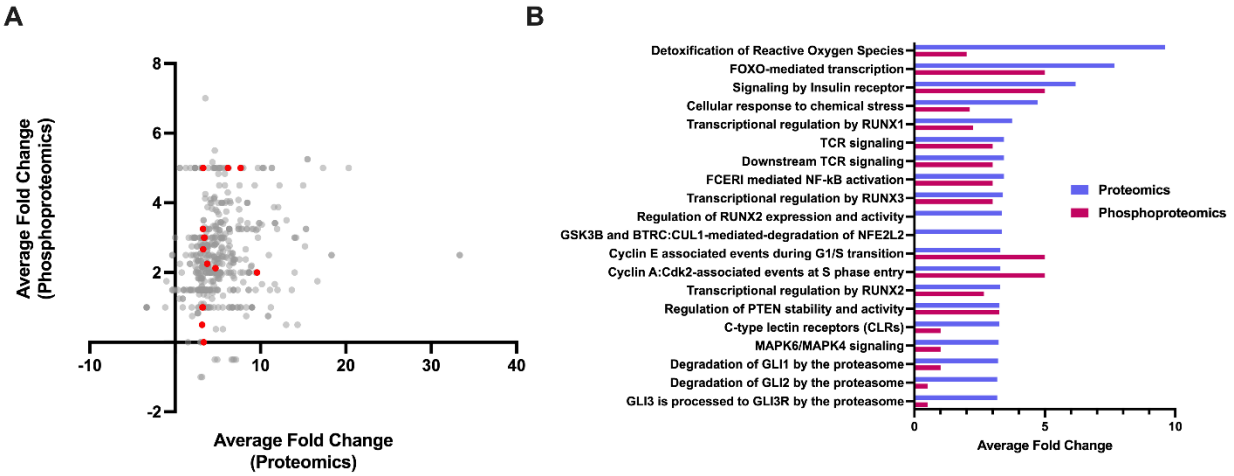

Figure 16. LRV1 infection mediates the modulation of protein expression and phosphorylation.
Identified proteins and phosphoproteins (*L. braziliensis* database) in wildtype (Lpa^{WT}) and LRV1-infected (Lpa^{LRV1+}) *L. v. panamensis* parasites were mapped to homologs in *Homo sapiens* (e-value ≤ 1.0E-3) and input into Reactome Pathway Analysis with Down-weighting of Overlapping Genes (PADOG) gene set analysis. PADOG computes a gene set score for each pathway based on weighted gene set analysis. **A.** Pathway fold changes of the phosphoproteomic dataset plotted against the pathway fold changes for the proteomic pathway dataset indicates 20 significantly altered pathways in Lpa^{LRV1+} comparatively to Lpa^{LRV1-} indicated in red (False discovery rate ≤ 5%). Multiple pathways may overlap. **B.** Significantly altered proteomic and phosphoproteomic pathway average fold change in Lpa^{LRV1+} comparatively to Lpa^{LRV1-} shows that multiple pathways are upregulated in both datasets.

MAP and cyclin-dependent kinases both fall within the CMGC family, which are key effectors of leishmanial MAPK signaling [200]. We further investigated the expression of peptides and phosphopeptides involved in leishmanial MAPK signaling, revealing a notable increase in infected parasites in comparison to their wildtype counterparts (Fig. 17). This is of particular interest, as MAPK signaling is reported to play an important role in *Leishmania* intracellular survival and fitness and multiple effectors have been proposed as potential therapeutic targets [200]. Only four MAPK signaling protein homologs were identified both as peptides and as phosphopeptides: Protein kinase C theta (PRKCQ), Proto-oncogene tyrosine-protein kinase Src (Src), Microtubule Affinity Regulating Kinase 3 (MARK3), and Calmodulin 1 (CALM1).

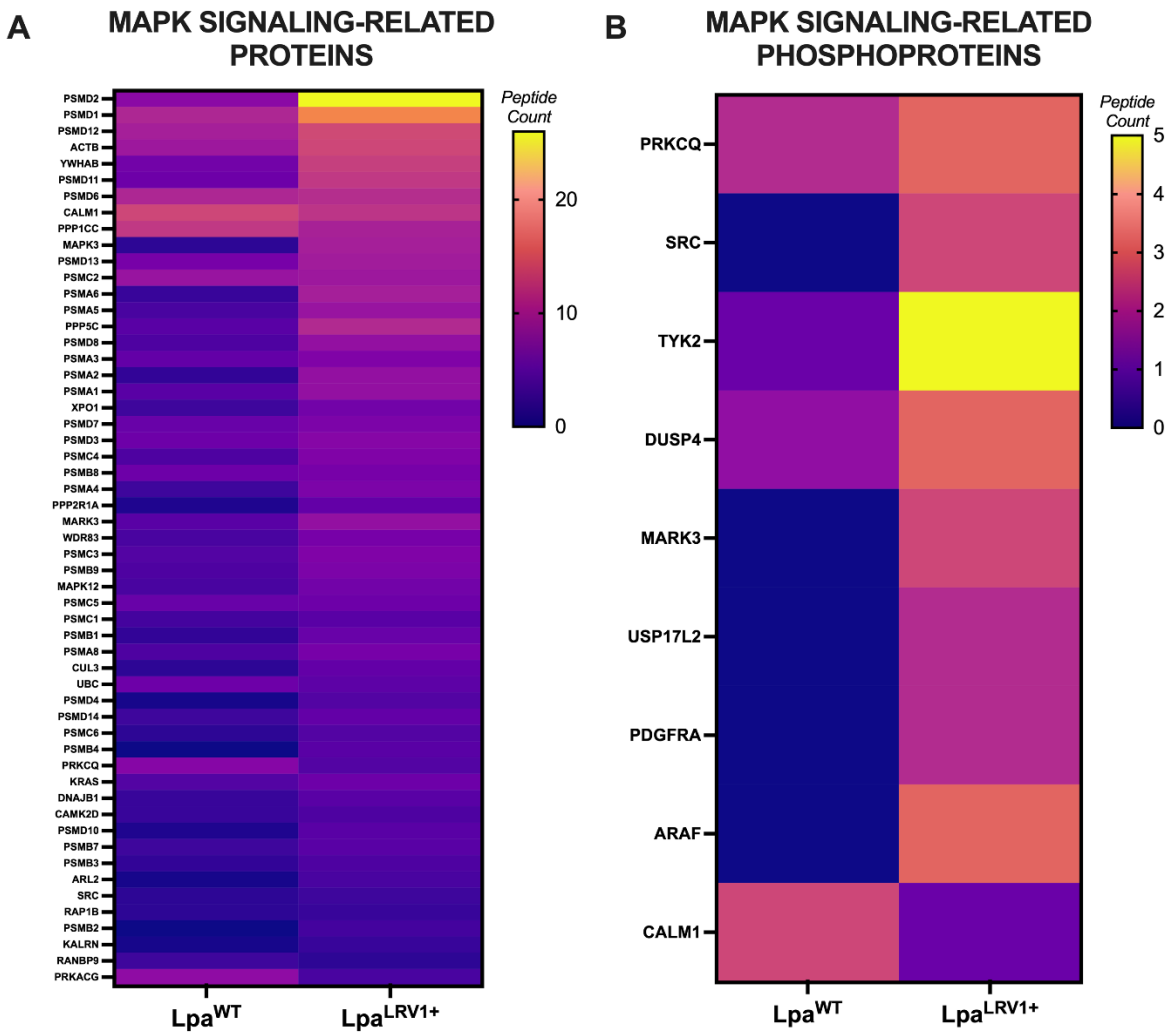

Figure 17. LRV1 infection induces the regulation of peptides and phosphopeptides involved in MAPK signaling.
L. braziliensis database proteins were mapped to homologs in *Homo sapiens* and to the Reactome Pathway database using Blast2Go BlastP function and mapping (e-value ≤ 1.0E-3). A list of MAPK signaling homologs was generated (See Supplementary Table 27). Identified proteins in wildtype (Lpa^{WT}) and LRV1-infected (Lpa^{LRV1+}) *L. v. panamensis* parasites were then searched against leishmanial homologs for MAPK signaling (Reactome ID: R-HSA-5683057). **A.** The expression of peptides involved in MAPK signaling reveals LRV1-mediated modulation. **B.** The expression of phosphopeptides involved in MAPK signaling indicates the phosphorylation of new substrates in Lpa^{LRV1+}.

The upregulation of MAP kinases, which are important downstream effectors of toll-like receptor signaling, and of the transcription factor IRF3, led us to explore the potential role of a homologous pathway to the toll-like-receptor 3 (TLR3) cascade in *Leishmania*. Endosomal TLR3 is a molecular

pattern recognition receptor for mammalian dsRNA viruses, which culminates in an antiviral response [201]. Peptides and phosphopeptides identified as homologs to mediators of the human TLR3 cascade were increased in Lpa^{LRV1+}, revealing a potential ancestral innate immune response mechanism to LRV1 (Figure 18 and 19). Structural homology between leishmanial proteins and mammalian TLR3/TRIF signaling mediators suggest conserved functionality (Figures 20 and 21). The intracellular domain of this potential leishmanial TLR3 homolog is possibly a dissociated enzymatic TIR, as characterized in other TLR-like signaling pathways in lower organisms [202]. Altogether, these data indicate the recognition of LRV1 by *L. v. panamensis*, and potential antiviral mechanisms employed by the parasite against infection.

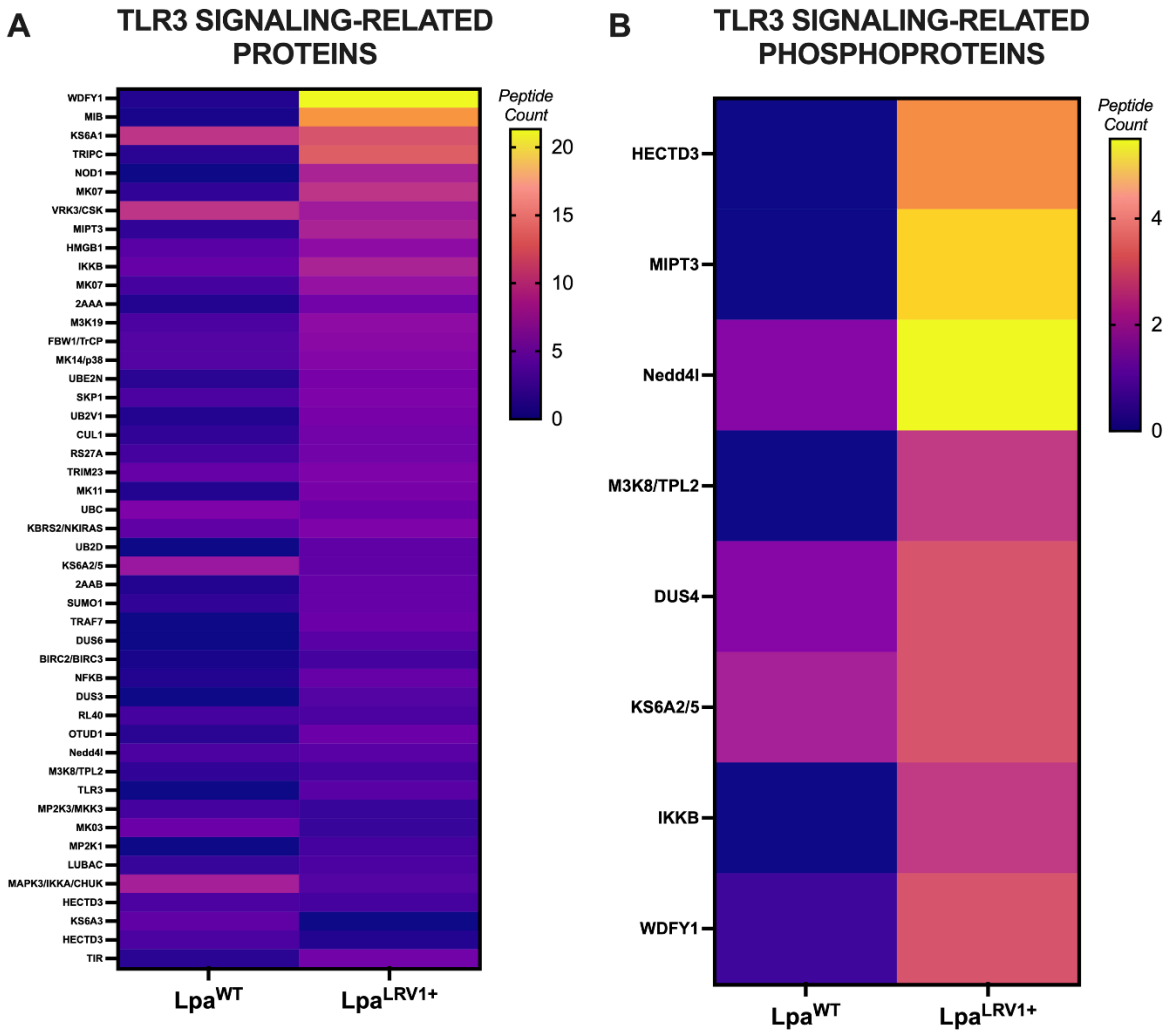

Figure 18. LRV1 infection induces the overexpression of peptide and phosphopeptide homologs of TLR3 signaling.

L. braziliensis database proteins were mapped to homologs in *Homo sapiens* and to the Reactome Pathway database using Blast2Go BlastP function and mapping (e-value ≤ 1.0E-3). A list of TLR3 signaling homologs was generated (See Supplementary Table 28). Identified proteins in wildtype (Lpa^{WT}) and LRV1-infected (Lpa^{LRV1+}) *L. v. panamensis* parasites were then searched against leishmanial homologs for TLR3 signaling (Reactome ID: R-HSA-168164). **A.** The differential expression of peptides involved in TLR3 signaling indicates a role for this pathway. **B.** The expression of phosphopeptides involved in TLR3 signaling suggests activation of the signaling cascade.

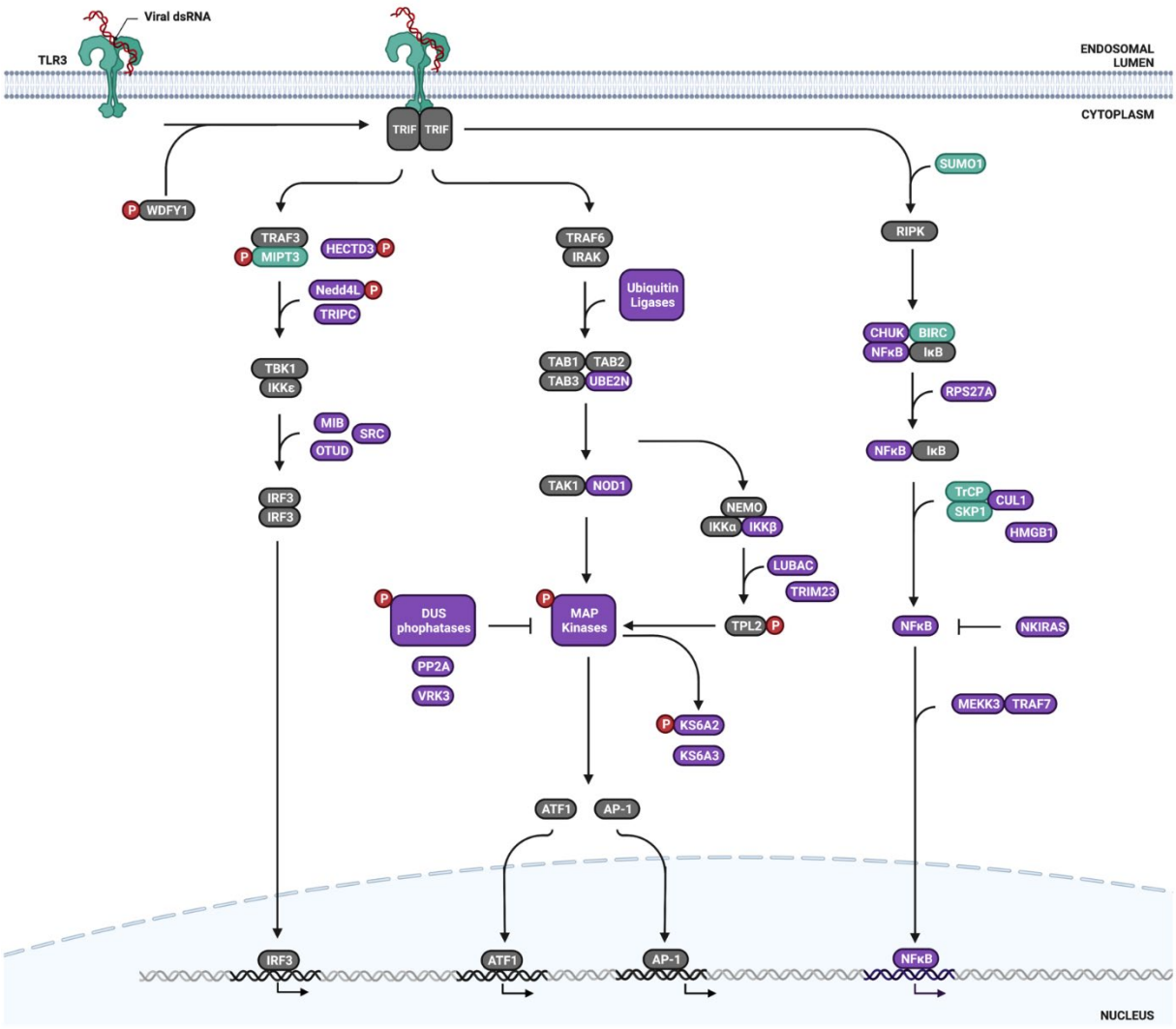

Figure 19. Leishmanial homologs to the canonical TLR3 signaling cascade are upregulated and phosphorylated in response to LRV1 infection.
The TLR3 signaling cascade begins when dsRNA binds to the pattern-recognition domain of TLR3 in the endosome. This induces the recruitment of TRIF to the cytoplasmic domain of TLR3, and the association of TRAF3, TRAF6 or RIPK. Through the action of multiple mediators, TLR3 signaling culminates in the nuclear translocation of transcription factors like IRF3, ATF1, AP-1 and NFκB and downstream antiviral signaling. The TLR3 signaling cascade indicates mammalian effectors in gray. Proteins represented in purple have identified leishmanial homologs in *L. v. panamensis*, obtained using Blast2Go BlastP function and mapping (e-value ≤ 1.0E-3). Red phosphosites indicate the identification of the homologous leishmanial phosphoprotein. Proteins identified in green indicate strong structural homology (See Figure 20) between leishmanial and mammalian proteins.

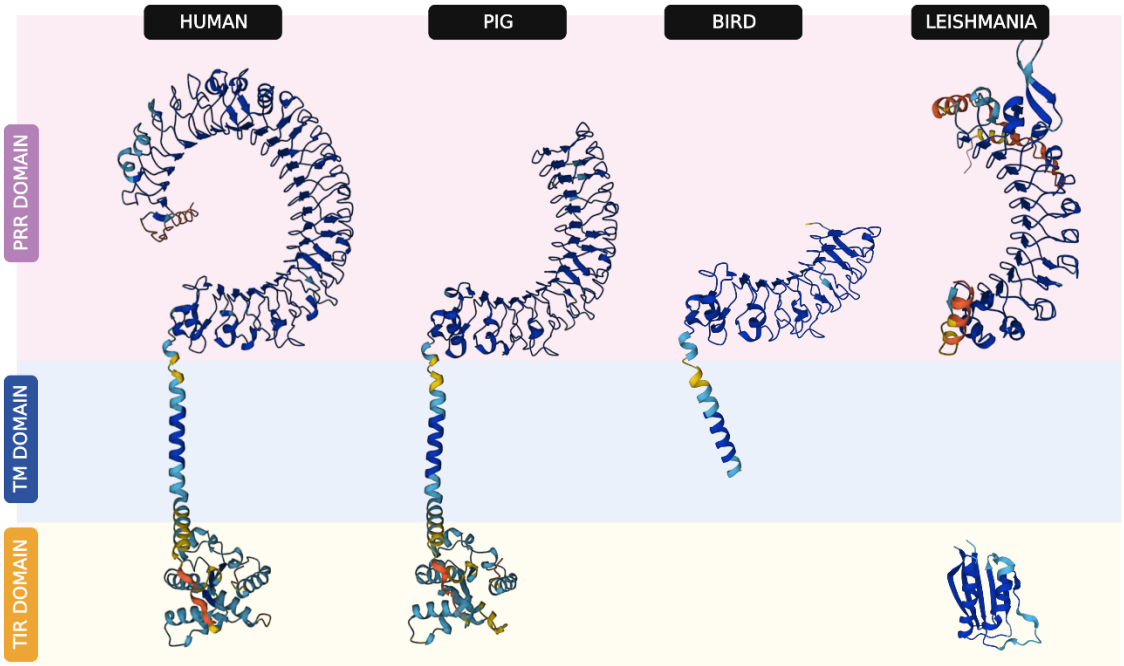

Figure 20. Predicted leishmanial TLR3 homolog shares structural homology with TLR3s from other organisms.
Alpha-fold predictive structures of *Homo sapiens* (Human) TLR3, *Sus scrofa* (Pig) TLR3, *Charadrius alexandrines* (Kentish Plover; bird) TLR3, and *L. v. braziliensis* (*Leishmania*) A0A3P3YXY9. Represented protein domains include the pattern-recognition receptor (PRR) domain, the transmembrane (TM) domain, and the Toll/interleukin-1 receptor (TIR) domain. Structural homology between Human and *Leishmania* proteins is scored with a QMEANDisCo of 0.57 ± 0.05, indicating probable structural and potential functional homology.

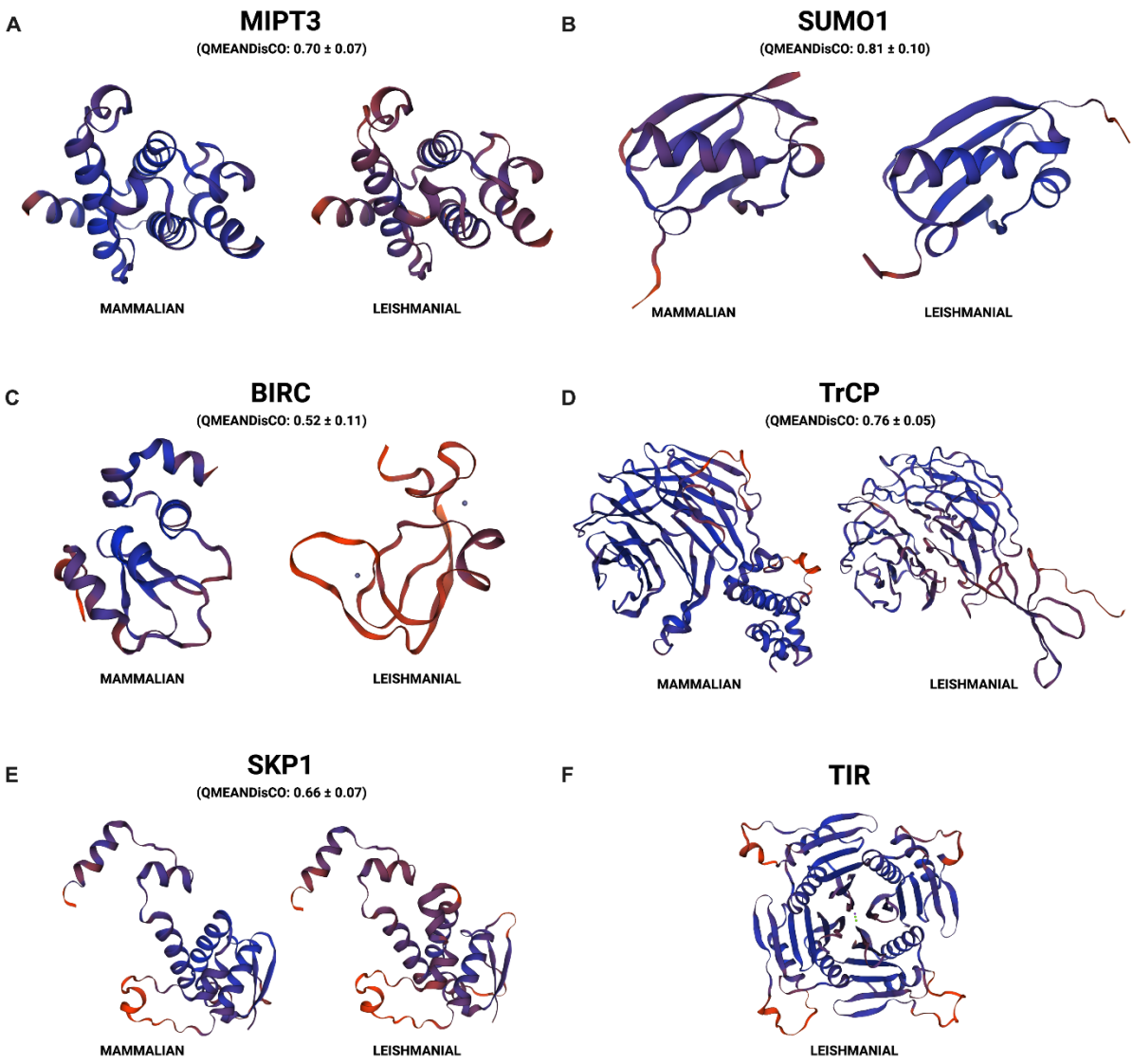

Figure 21. Predicted leishmanial TLR3 downstream effectors share structural homology with mammalian homologs.
Swiss-Model Predictive Structures of TLR3-Mediated Signaling Homologs were created using sequences obtained from UniProt database. Structural homology between Human and *Leishmania* proteins is scored with a QMEANDisCo. A score above 0.70 is considered reliable for structure, and above 0.50 is considered predictive of genetic orthology between different species. Highest probability structures are represented in purple, while lower scoring structures are represented in orange. Models for **A,** TRAF3-interacting protein 1 (MIPT3), **B,** Small Ubiquitin Like Modifier 1 (SUMO1), **C,** Baculoviral IAP Repeat Containing protein (BIRC), **D,** Beta-Transducin Repeat Containing E3 Ubiquitin Protein Ligase (TrCP) and **E,** S-Phase Kinase Associated Protein 1 (SKP1) display significant structural homology to mammalian homologs. **F.** A toll/interleukin-1 (IL-1) receptor (TIR) domain protein that is unique to kinetoplastida organizes as a homotetramer and may act as a dissociated enzymatic TIR domain for leishmanial TLR3.

LRV1 infection can be controlled by *L. v. panamensis.*

Given the identification of homologous antiviral signaling in response to LRV1 infection, we sought to determine whether *L. v. panamensis* could eliminate viral infection. PCR and qPCR detection of viral ORF3 expression revealed a significant diminution of viral RNA over a 10-week course of infection (Fig. 22).

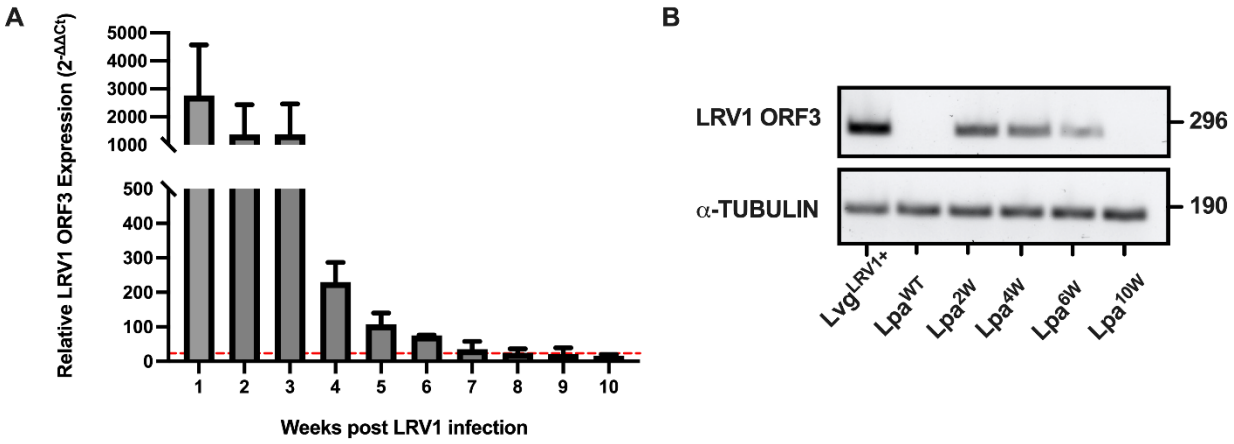

Figure 22. *L. v. panamensis* can control acute LRV1 infection.
LRV1-infected *L. v. panamensis* was cultured continuously for 10 weeks. **A.** qPCR expression of LRV1 ORF3 up to 10 weeks post-infection, analysed by the ΔΔCt method, indicates a decrease in viral RNA expression as of week 4, and elimination by week 10. The limit of detection, indicated in red, was determined using the ΔΔCt of the negative control (Lpa^{WT}). Bars represent SEM. **B.** Presence of LRV1 viral RNA, assessed by PCR up to 10 weeks post-infection. Results are representative of at least three independent experiments.

We selected weeks 2, 4, 6 and 10 post LRV1-infection, and performed proteomic analysis on these parasites to gain insight into mechanisms of viral elimination. While no proteins were significantly overexpressed in any group, 76 peptides were uniquely identified in *L. v. panamensis* at 2 weeks post-infection (Lpa^{2W}), 80 peptides at 4 weeks post-infection (Lpa^{4W}), 9 peptides at 6 weeks post-infection (Lpa^{6W}), and 49 peptides at 10 weeks post-infection (Lpa^{10W}) (Fig. 23 A). Gene ontology analysis revealed a time-dependent decrease in signaling, immune system processes, metabolic processes, and response to stimulus, among others, while homeostatic processes, transporter activity and proteins involved in the lysosome increased following clearance of LRV1 (Fig. 23 B).

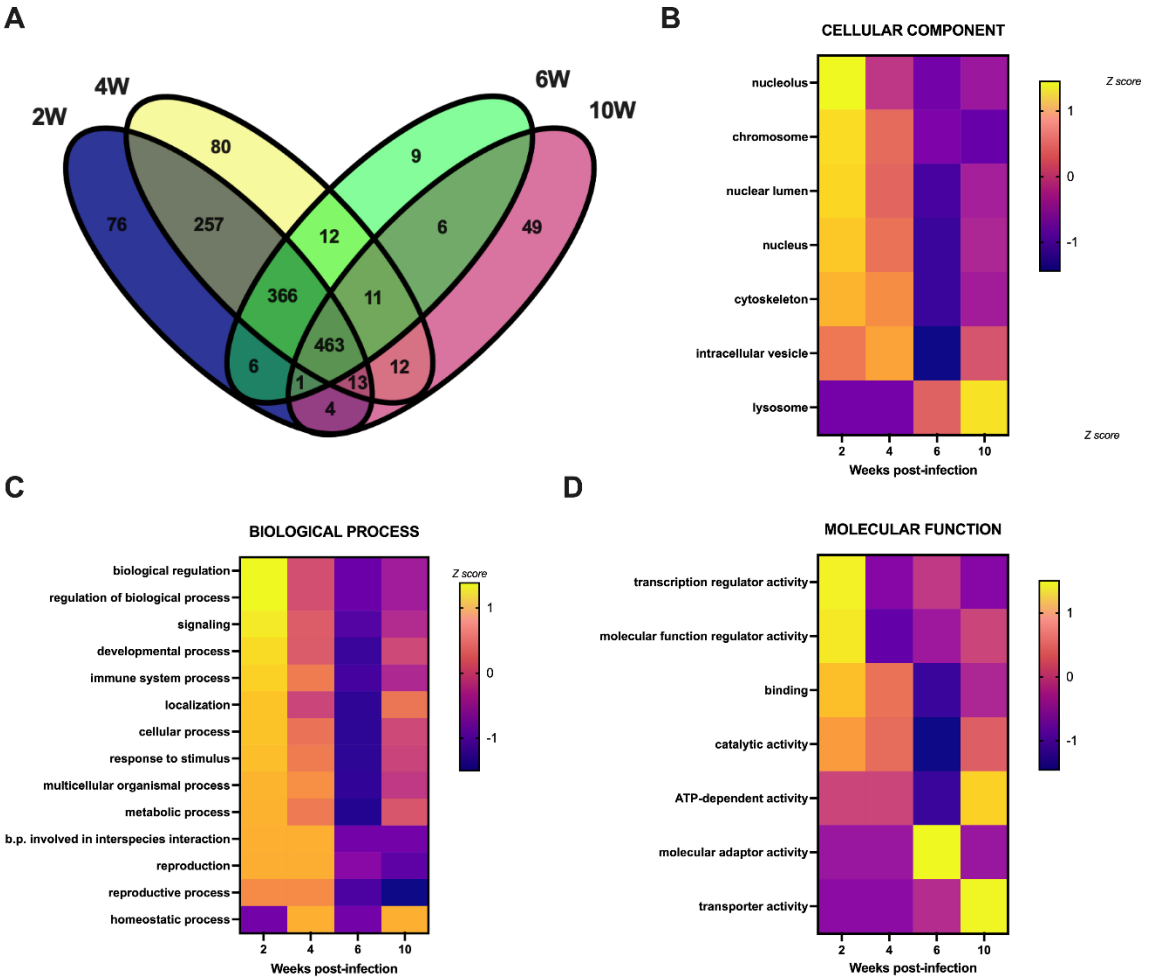

Figure 23. Elimination of LRV1 by *Leishmania v. panamensis* induces important changes to the proteic landscape.
The protein content of LRV1-infected *L. v. panamensis* after 2- (Lpa^{2W}), 4- (Lpa^{4W}), 6- (Lpa^{6W}) and 10- (Lpa^{10W}) weeks post-LRV1 infection was catalogued by mass spectrometry (*L. braziliensis* database). **A.** The distribution of identified proteins by their presence/absence (n=2 for each group analysed. Only proteins that appeared in both duplicates were included in the final list. See Supplementary Tables 28, 29, 30, and 31). No proteins were significantly differentially expressed in only one group. **B.** Gene ontology of differentially expressed proteins was annotated using Blast2GO BlastP function, followed by mapping to Human (e-value ≤ 1.0E-3). Z-scores were calculated to determine relative expression of Gene Ontology categories and represented in heatmaps.

We next assessed the expression of proteins involved in the same pathways previously explored in the comparative study of Lpa^{WT} and Lpa^{LRV1+} (Fig. 24). Notable decreases in the expression of

proteins involved in translation and metabolic processes over the course of infection suggested a return to homeostatic functions (Fig. 24 A-B).

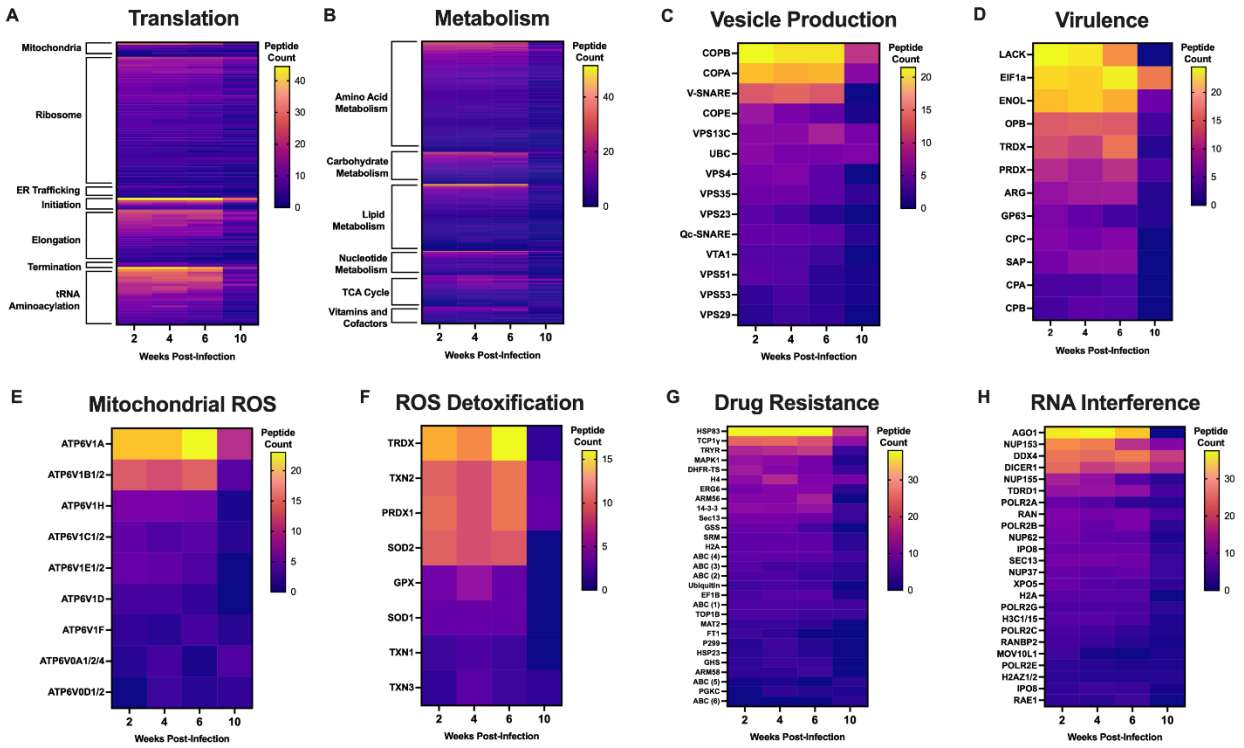

Figure 24. Elimination of LRV1 downregulates the expression of key *L. v. panamensis* infectious and survival assets.
L. braziliensis database proteins were mapped to homologs in *Homo sapiens* and to the Reactome Pathway database using Blast2Go BlastP function and mapping (e-value ≤ 1.0E-3). Lists of homologs were generated and curated manually to integrate additional non-mammalian proteins involved in pathways (See Supplementary Tables 18-25). Identified proteins in *L. v. panamensis* after 2- (Lpa^{2W}), 4- (Lpa^{4W}), 6- (Lpa^{6W}) and 10- (Lpa^{10W}) weeks post-LRV1 infection were then searched against leishmanial homologs and pathway lists, and the expression of peptides involved in **A.** translation (Reactome ID: R-HSA-72766), **B.** metabolism (Reactome ID: R-HSA-1430728), **C.** vesicle production (Reactome ID: R-HSA-917729), **D.** virulence (Reactome ID: N/A; manually curated), **E.** Mitochondrial ROS production (Reactome ID: R-HSA-1222556), **F.** ROS detoxification (Reactome ID: R-HSA-3299685), **G.** Drug resistance (Reactome ID: N/A; manually curated), and **H.** RNA interference (Reactome ID: R-HSA-211000) were represented using heat maps of identified expression levels.

Proteins involved in vesicle production decreased gradually over the course of LRV1 infection (Fig. 24 C). To corroborate this, we assessed the production of vesicles by parasites throughout the course of infection, revealing a time-dependent decrease in EV production beginning

immediately after the height of LRV1 viremia (Fig. 25). The transient increase in vesicle production could indicate that that LRV1 initially hijacks ESCRT machinery to facilitate spread, and that *L. v. panamensis* could rapidly block EV production as a means of viral elimination. The diminution in expression of virulence factors reiterates a potential role for LRV1 in parasitic virulence (Fig. 24 C-D).

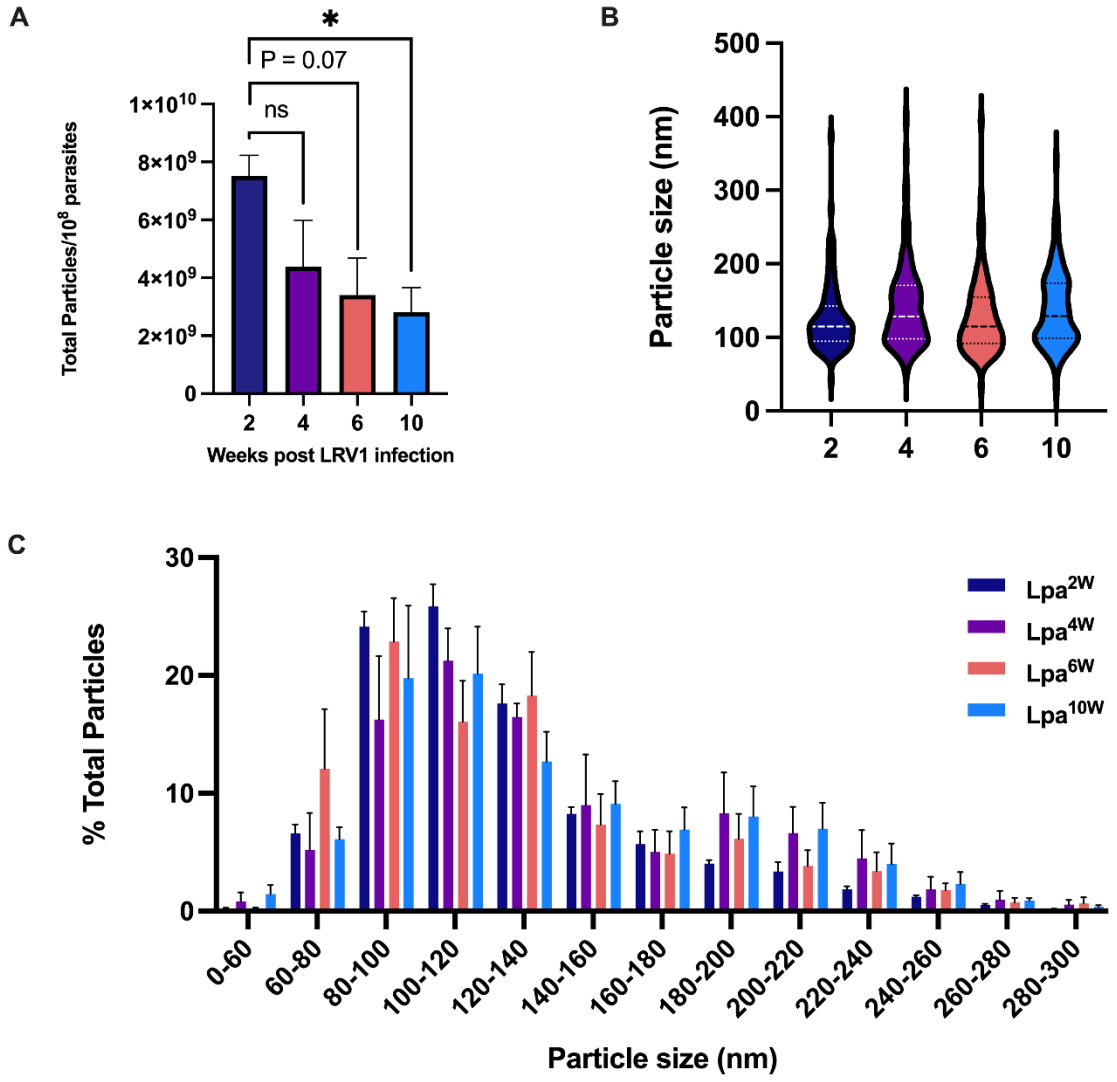

Figure 25. Elimination of LRV1 infection decreases production of extracellular vesicles by *L. v. panamensis*.
EVs were isolated from *L. v. panamensis* after 2- (Lpa^{2W}), 4- (Lpa^{4W}), 6- (Lpa^{6W}) and 10- (Lpa^{10W}) weeks post-LRV1 infection using a four-hour temperature shift followed by filtration/ultracentrifugation methodology. Size distribution and quantification of EV preparations was determined by NS300 NTA using a 1:50 dilution in exosome buffer (n=6 per group). **A.** Total

extracellular vesicles produced per 1 x 10^8 Lpa^{2W}, Lpa^{4W}, Lpa^{6W} and Lpa^{10W} parasites show a significant time-dependent decrease. **B.** No differences to the mean and median of EV size was apparent. **C.** A trend in the increase of EVs from 100-120nm in size in Lpa^{2W} is apparent, though this is not significant. Statistical significance was determined using one-way ANOVA with Holm–Sidak's correction, and error bars represent SEM. *P ≤ 0.05, **P ≤ 0.01, ***P ≤ 0.001. Results are representative of three independent experiments performed in duplicate.

Proteins associated to the production of ROS were also shown to decrease in a time-dependent manner over the course of infection (Fig. 24 E). We corroborated this using H_2DCF-DA, as previously described, revealing a potential decrease in the production of intracellular ROS following viral elimination, though the reduction between weeks 6 and 10 post-infection is not significant (Fig. 26).

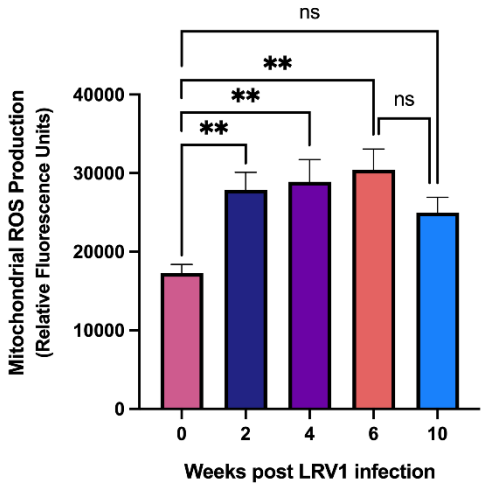

Figure 26. Elimination of LRV1 infection decreases the production of intracellular reactive oxygen species by the *L. v. panamensis* mitochondria/kinetoplast.
5 x 10^6 *L. v. panamensis* promastigotes at 2- (Lpa^{2W}), 4- (Lpa^{4W}), 6- (Lpa^{6W}) and 10- (Lpa^{10W}) post LRV1 infection were incubated with HEPES-NaCl containing H_2-DCFDA. When oxidized intracellularly, H_2-DCFDA forms a fluorescent compound. Lpa^{2W} has significantly higher levels of intracellular ROS than all other timepoints. Statistical significance was determined using one-way ANOVA with Holm–Sidak's correction, and error bars represent SEM. *P ≤ 0.05, **P ≤ 0.01, ***P ≤ 0.001. Results are representative of three independent experiments performed in duplicate.

Peptides involved in the detoxification of ROS and in drug resistance decreased over the course of infection, highlighting the effect of LRV1 on parasitic survival and fitness (Fig. 24 F-G). Finally,

expression of the RNA interference pathway also decreased, with a notable reduction in the expression of AGO1, while expression of Dicer remained constant, suggesting a potential RNAi-dependent mechanism of LRV1 elimination. Similarly, there is a decrease in protein homologs involved in diverse mammalian viral infections over the course of LRV1 infection (Fig. 27).

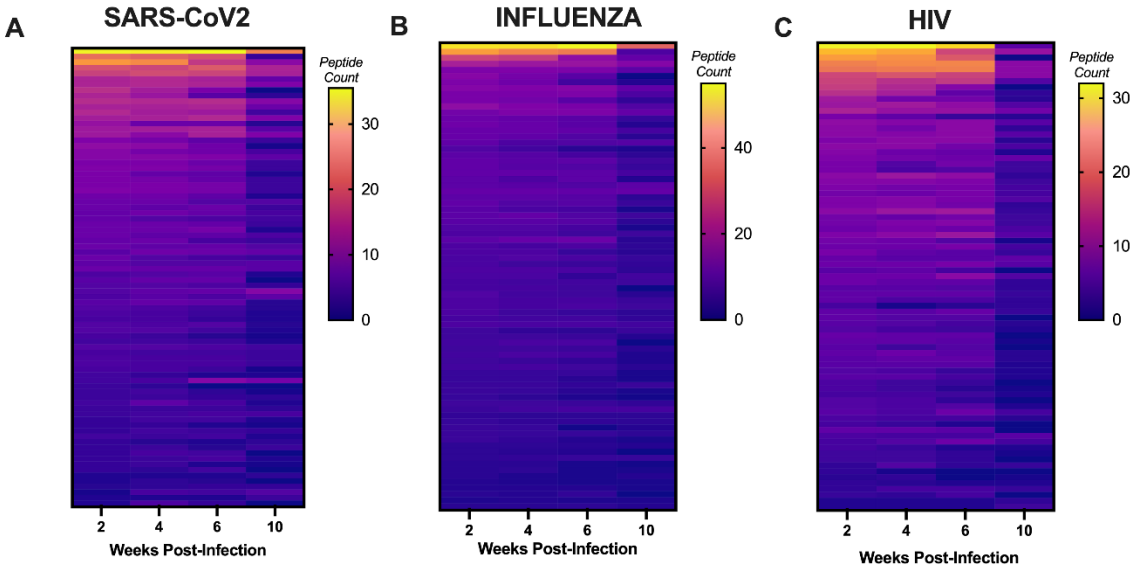

Figure 27. Expression of leishmanial homologs to mediators of mammalian viral infection decreases over the course of LRV1 infection.
L. braziliensis database proteins were mapped to homologs in *Homo sapiens* and to the Reactome Pathway database using Blast2Go BlastP function and mapping (e-value ≤ 1.0E-3). Lists of homologs were generated (See Supplementary Table 26). Identified proteins in *L. v. panamensis* after 2- (Lpa^{2W}), 4- (Lpa^{4W}), 6- (Lpa^{6W}) and 10- (Lpa^{10W}) weeks post-LRV1 infection were then searched against leishmanial homologs and pathway lists, and the expression of peptides involved in **A.** SARS-CoV2 infection (Reactome ID: R-HSA-9694516), **B.** Influenza infection (Reactome ID: R-HSA-168255), and **C.** HIV infection (Reactome ID: R-HSA-162906) were represented using heat maps of identified expression levels.

In addition, given the time-dependent decrease in signaling biological processes indicated by gene ontology analysis, we sought to assess the expression of mediators of MAPK signaling and of potential TLR3 signaling over the course of LRV1 infection in *L. v. panamensis.* This revealed a

modulation of leishmanial signaling pathways, with a general trend of downregulation associated with viral elimination (Fig. 28).

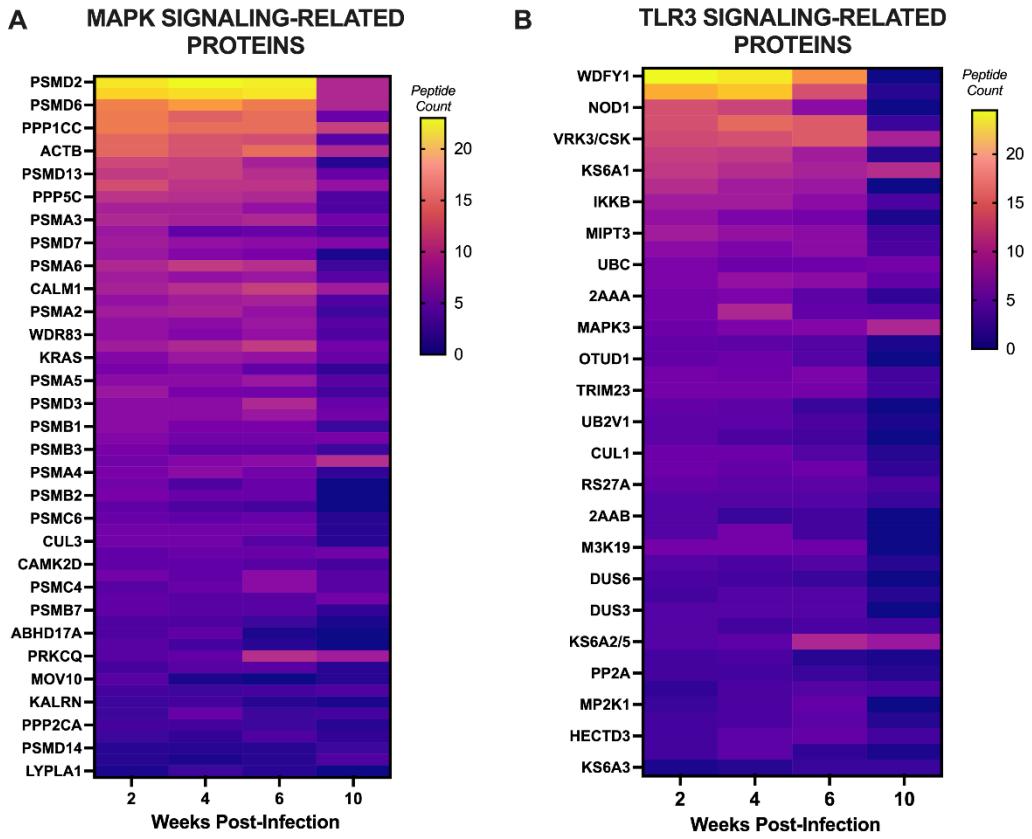

Figure 28. Expression of leishmanial homologs to MAPK and TLR3 signaling decreases over the course of LRV1 infection.
L. braziliensis database proteins were mapped to homologs in *Homo sapiens* and to the Reactome Pathway database using Blast2Go BlastP function and mapping (e-value ≤ 1.0E-3). Lists of MAPK signaling homologs and TLR3 signaling homologs were generated (See Supplementary Tables 27 and 28). Identified proteins in *L. v. panamensis* after 2- (Lpa^{2W}), 4- (Lpa^{4W}), 6- (Lpa^{6W}) and 10- (Lpa^{10W}) weeks post-LRV1 infection were then searched against leishmanial homologs for **A.** MAPK signaling (Reactome ID: R-HSA-5683057) and **B.** TLR3 signaling (Reactome ID: R-HSA-168164).

Considering the decrease of key mediators of leishmanial survival and fitness, we sought to assess the impact on the development of cutaneous leishmaniasis through a murine footpad infection model. Strikingly, lesion size correlated with parasitic viral load, and earlier timepoints post LRV1-infection significantly increased inflammation (Fig. 29).

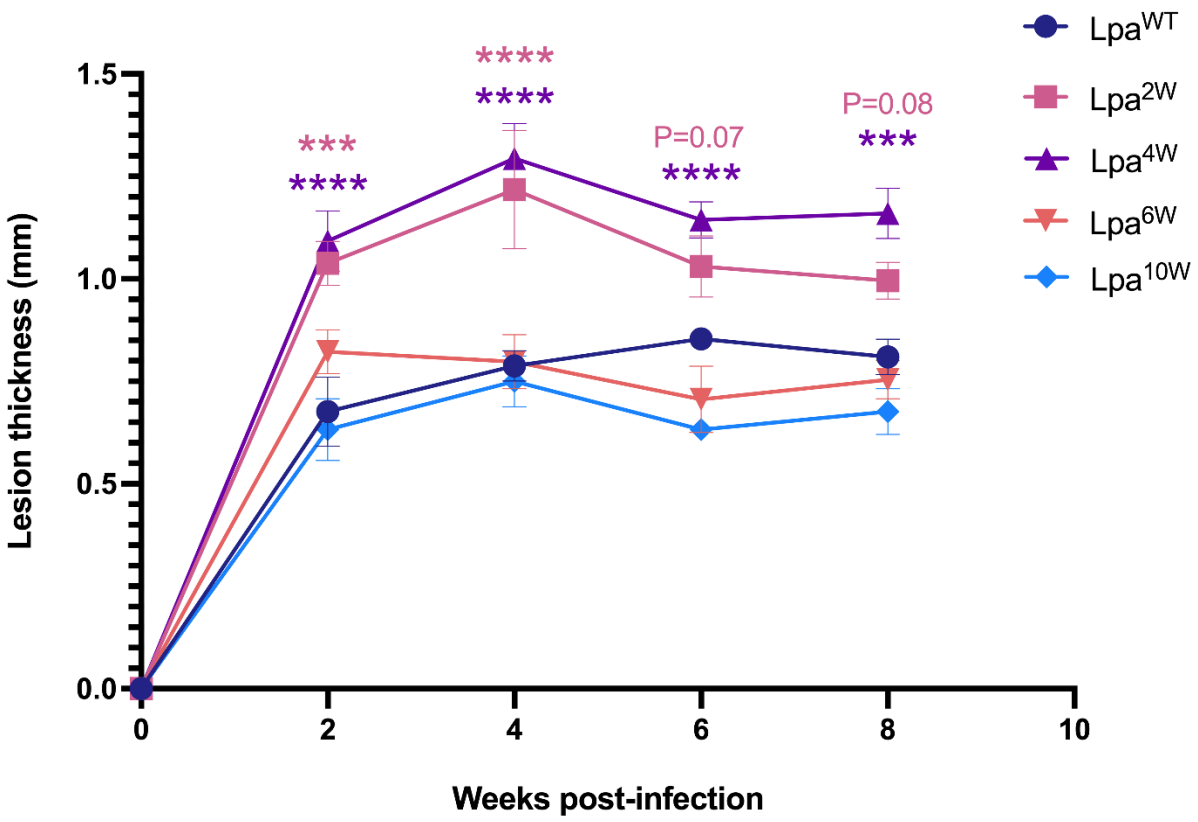

Figure 29. Infection of *L. v. panamensis* by LRV1 exacerbates cutaneous leishmaniasis. *L. v. panamensis* promastigotes at 2- (Lpa^{2W}), 4- (Lpa^{4W}), 6- (Lpa^{6W}) and 10- (Lpa^{10W}) weeks post-LRV1 infection were injected into mice footpads and lesion thickness was monitored up to eight weeks post-infection. Lesion thickness was compared for each mouse between their infected and uninfected footpad, as a control for individual variation. Each data point represents the average ± SEM, n = 5 mice per group. The differences were found to be significant using a one-way analysis of variance with Holm–Sidak's multiple-comparison test. *$P \leq 0.05$, **$P \leq 0.01$, ***$P \leq 0.001$.

Collectively, these data indicate a potential return to baseline for *L. v. panamensis* following the clearance of LRV1 infection, and resulting decrease in viral-mediated fitness, survival, and infectivity.

2.7 DISCUSSION

Several viruses of the *Totiviridae* family endogenously infect parasitic protozoa, including *Giardia spp.*, *Trichomonas vaginalis*, and *Leishmania spp.* [155,170,203]. These unenveloped dsRNA viruses are suspected to have emerged early over the course of evolution, predating the divergence of parasites into distinct lineages, and play diverse roles in parasitic pathogenesis [149,204]. *Leishmania RNA Virus 1*, which has been identified in isolates of *L. v. guyanensis* and *L. v. braziliensis* from South America, has been associated to parasitic metastasis, mucosal involvement, and first-line treatment failure [167,169,170]. Targeting LRV1 has been proposed as a potential therapeutic alternative to classical antileishmanial drugs, and immunization using the LRV1 capsid protein has been reported to confer significant protection against hyperinflammatory phenotypes in a murine model [175]. Chemical agents targeting *Totiviridae* have also been suggested as treatment alternatives, with the adenosine analog 2-CMA, which preferentially inhibits LRV1 replication, permitting full viral elimination *in vitro* [176]. In addition to potential clinical benefits, treatment of LRV1-bearing *L. v. guyanensis* with 2-CMA enables the generation of isogenic LRV1-negative strains for research.

The first research question that we addressed was how pharmacological treatment of LRV1-infected *L. v. guyanensis* impacted the parasite. Previous reports indicated that there was virtually no change to the parasite's transcriptome following treatment, and that growth was unaffected [177,181]. Contrastingly, we observed alterations to the parasite's proteome following 2-CMA treatment, indicating that the modulation of observed functions may occur at the translational and not the transcriptional level. Further, differential protein expression between LRV1-bearing and 2-CMA treated *L. v. guyanensis* was moderate in terms of relative fold change, and modulated functions included translation and vesicle-trafficking, which are intrinsically linked to the LRV1

viral life cycle. Further assessment of the effect of 2-CMA treatment on *L. v. guyanensis* is necessary to fully understand how elimination of LRV1 affects endogenously infected parasites, and to determine potential clinical applications of 2-CMA against metastatic leishmaniasis.

Recently, we showed that LRV1 utilizes leishmanial ESCRT machinery to encapsulate virions within exosomes, forming a pseudo-envelope [157]. Thus, we performed proteomic analysis on exosomes derived from LRV1-bearing and 2-CMA-treated *L. v. guyanensis*, to assess variations in extracellular vesicle cargo content. In comparison to the parasite's proteome, higher levels of differential expression were observed in the exoproteome, highlighting the role of cargo sorting and enrichment within vesicles. Further, functions modulated in the exoproteome were recapitulative of that modulated in the proteome. The inclusion of LRV1 within exosomes derived from endogenously infected *L. v. guyanensis* is the most notable difference. Exosomes containing LRV1 have little supplementary volume to account for additional cargo which may, in part, explain differential cargo sorting. Thus, the proteomic analysis of LRV1-bearing *L. v. guyanensis*, its 2-CMA-treated counterpart, and their respective exosomes, suggested that 2-CMA treatment can eliminate the virus which, in turn, induces changes to the proteome. While it has been suggested that 2-CMA treatment induces few unintended consequences to the parasite, further investigation is required to elucidate the impact of adenosine analogs on *L. v. guyanensis* [177,181].

The biogenesis of an ESCRT-dependent pseudo-envelope by LRV1 enables protection from the extracellular environment and viral transmission to other *Leishmania*. While exosome-enveloped LRV1 can cause acute infection of *L. v. panamensis*, it is unable to establish infection within the *Leishmania* subgenus species *L. mexicana* [157]. It has been hypothesized that this is due to the unique presence of functional RNA interference machinery, including Argonaute and Dicer, in the *Viannia* subgenus, maintaining viral loads under a lytic threshold [163]. Interestingly, though

LRV1 can establish acute infection, *L. v. panamensis* is not a natural endosymbiotic host for LRV1 and eliminates the virus over a 10-week course of infection.

To further understand the host-pathogen interaction between LRV1 and *L. v. panamensis*, we next addressed how LRV1 modulates parasitic fitness, survival, and infectivity. Proteomic analysis of naïve and LRV1-infected *L. v. panamensis* indicated important changes to gene expression, with a significant increase of metabolic functions. This modulation is significantly greater than that observed in 2-CMA treated *L. v. guyanensis*, indicating a complex *Leishmania/*LRV1 host-pathogen interaction.

Manipulation of host cell metabolism by mammalian viruses is well-established, with viruses such as HCV, HCMV and DENV inducing glycolysis and fatty acid synthesis [205]. Viruses require fatty acids and glycolysis at different stages of their lifecycle, and viral replication is an energy-dependent process [205]. Viruses must also hijack host cell translational machinery for replication, recruiting translation initiation factors and ribosomal subunits, accounting for the notable increase in translational and ribosomal proteins in LRV1-infected *L. v. panamensis* [206]. Finally, to complete their life cycle, viruses must exit their host cell for transmission. The overexpression of vesicle-production-related proteins and of vesicles in infected parasites, suggests the induction of exosomes by LRV1 as a potential means of increased viral shedding and transmission. The role of viral hijacking of leishmanial functions to complete their life cycle is further suggested by the decrease in metabolic and translational proteins, and in the reduction of exosome production over the course of viral clearance, indicating a return to baseline homeostatic function.

Infection of *L. v. panamensis* by LRV1 provides the parasite with additional virulence and fitness advantages, which culminate in an increased capability of both infiltrating macrophages and maintaining infection. The increase in virulence factor expression, notably of the surface

metalloprotease GP63, can enable parasites to migrate through extracellular matrix and abrogate canonical leishmanicidal macrophage signaling [142,207]. In response to viral infection, *L. v. panamensis* increases its production of intracellular ROS – a highly conserved antiviral defense mechanism among eukarya [197]. In the context of bacterial or viral infections, phagocytes have been reported to increase the production of antioxidant molecules to inhibit cellular damage caused by free oxygen radicals and ROS-mediated cell death [197]. The upregulation of antioxidant enzymes and associated increase in resistance to ROS observed in LRV1-infected *L. v. panamensis* is therefore possibly an unintended consequence of viral infection. Thus, through this antiviral response, parasites may become more capable of withstanding the oxidative burst within macrophages, increasing infectivity. Though moderate resistance to trivalent antimonials was observed experimentally in LRV1-infected parasites, significant overexpression of proteins associated to drug-resistance indicate potential resistance to different chemotherapeutics. In fact, in addition to trivalent antimony, LRV1-associated treatment failure has been reported in response to pentamidine, pentavalent antimony and amphotericin B [167,169]. Once *L. v. panamensis* overcomes LRV1 infection, however, virulence factor expression, antioxidants and drug-resistance proteins significantly decrease. The production of intracellular ROS also decreases over the course of infection, corroborating the potential role of oxidative stress in a leishmanial antiviral response. The importance of LRV1 in this acquired fitness advantage is further demonstrated by the exacerbation of cutaneous leishmaniasis lesions, which correlates directly with the viral load. Considering the characteristic hyperinflammatory phenotype caused by LRV1-bearing *Leishmania* is dependent on mammalian endosomal TLR3, it follows that the exacerbation of cutaneous lesions requires the presence of viral dsRNA [54,179].

In addition, potential mechanisms of viral elimination by *L. v. panamensis* can be inferred from our data. Initially during infection, there is an important increase in RNA interference machinery, notably of the RISC component Argonaute 1 (AGO1), which subsequently decreases over the course of infection. Argonaute proteins are key players in both viral persistence or tolerance, and in viral clearance, in a context-dependent manner [208]. As previously discussed, AGO1 is suspected to play a role in maintaining LRV1 within its endosymbiotic host, though its transient upregulated expression in LRV1-infected *L. v. panamensis* suggests an antiviral function.

However, our most striking evidence of ancient antiviral immune mechanisms conserved in *Leishmania* was revealed by phosphoproteomic and proteomic analysis of signaling pathways. The upregulation of MAPK signaling, and of TLR3 signaling homologs in response to infection indicates the role of signal transduction in viral clearance. The TLR family encompasses multiple pathogen-associated molecular pattern recognition receptors that have been characterized in diverse vertebrates and invertebrates along the evolutionary spectrum [209,210]. Though evolutionary pressure on TLRs has caused significant divergence between TLR orthologue sequences between species, structural similarity between a potential leishmanial TLR3 and its mammalian counterpart may indicate functional conservation [202,210]. The upregulation of several homologs to downstream mediators of TLR3 signalling further indicates a role for a potential TLR-dependent antiviral response in *Leishmania*.

Collectively, findings stemming from our study describe a host-pathogen interaction between a virus and a unicellular eukaryote, which provides parasites with a fitness advantage and additional pathogenicity. Our study further indicates potential antiviral immune mechanisms evolutionarily-conserved in lower eukaryotes, including ancestral TLR-mediated signaling, RNA interference, and antiviral oxidative stress. Previously characterized ancestral immune mechanisms, including

restriction enzymes and CRISPR-Cas within prokaryotic organisms, suggest diverse forms of immunity along the evolutionary spectrum. Further elucidation of potential leishmanial antiviral immunity may enable the discovery of mammalian immune mechanisms and provide further understanding of the evolution of complex immune systems.

CONCLUDING REMARKS

Leishmaniasis remains a major cause of morbidity and mortality throughout LMICs, placing an important financial burden on both individuals and healthcare systems. Climate change-mediated migration of *Lutzomyia* and *Phlebotomus* sandfly vectors, expected to cause a significant expansion of endemic regions over the next decade, along with an increased incidence of resistance to therapeutics, pose a growing threat to global health. To properly combat this neglected tropical disease, elucidation of pathogenesis and drug resistance mechanisms is required. Presence of the endogenous *Totivirus* LRV1 within *L. (Viannia)* species, endemic to South America, has been associated with first-line treatment failure, disease relapse, and parasitic metastasis to the nasopharyngeal mucosa. To this effect, understanding the host/pathogen interaction between *Leishmania* and LRV1 is fundamental to the treatment of mucocutaneous leishmaniasis.

Our study, based on our previous elucidation of the role of the leishmanial exosomal pathway in the LRV1 life cycle, assessed the impact of acute viral infection of *L. v. panamensis*. Through bioinformatic analyses and functional assays, we revealed that LRV1 infection confers additional virulence and survival assets to *L. v. panamensis*, potentially explaining drug resistance and pathology exacerbation in the presence of the virus. Moreover, we identified multiple pathways that were hijacked by LRV1 to enable their replication, notably metabolic and translational machinery. Finally, we proposed potential mechanisms by which *L. v. panamensis* can eventually overcome infection, including ROS-mediated antiviral activity, RNA interference, and potential ancestral toll-like signaling. To further elucidate these mechanisms, analysis of the transcriptome and of the metabolome may provide information pertaining to additional levels of regulation, and analysis of early moments post-infection may help identify leishmanial antiviral signaling pathways.

FUNDING

MO is supported by the Canadian Institutes of Health Research (CIHR, grant number PJT-159765) and The Natural Sciences and Engineering Research Council of Canada (NSERC). AL is supported by a MSc studentship from Fonds de Recherche du Québec en Santé (FRQS).

APPENDIX

Table S1. Sanger sequencing *Leishmania* species validation.

Species	GP63		AGO1	
	Identified Gene	ID (%)	Identified Gene	ID (%)
Leishmania (Viannia) guyanensis metastatic clone 21 (MHOM/BR/75/M4147)	*L. v. g.* strain M4147 GP63	*99.10*	*L. v. g.* strain AGO1	99.42
Leishmania (Viannia) guyanensis 2-CMA treated (MHOM/BR/75/M4147)	*L. v. g.* strain M4147 GP63	*99.40*	*L. v. g.* strain AGO1	99.28
Leishmania (Viannia) panamensis (MHOM/87/CO/UA140)	*L. v. p.* strain UA140 GP63	*98.49*	*L. v. p.* AGO/DCL gene	99.28
Leishmania mexicana (MHOM/GT/2001/U1103)	*L. m.* strain U1103 GP63	*98.08*	No Amplicon	N/A
GP63 and AGO1 genes amplified by PCR and sequenced using Sanger Sequencing.				

Table S2. Unique proteins identified in Lvg^{LRV1-} relative to Lvg^{LRV1+}
View complete table.

Table S3. Unique proteins identified in Lvg^{LRV1+} relative to Lvg^{LRV1-}
View complete table.

Table S4. Differentially expressed proteins identified in Lvg^{LRV1-} and Lvg^{LRV1+}
View complete table.

Table S5. Unique proteins identified in Exo^{LRV1+} relative to Exo^{LRV1-}
View complete table.

Table S6. Unique proteins identified in Exo^{LRV1-} relative to Exo^{LRV1+}
View complete table.

Table S7. Differentially expressed proteins identified in Exo^{LRV1-} and Exo^{LRV1+}
View complete table.

Table S8. Unique proteins identified in Lpa^{WT} relative to Lpa^{LRV1+}
View complete table.

Table S9. Unique proteins identified in Lpa^{LRV1+} relative to Lpa^{WT}
View complete table.

Table S10. Differentially expressed proteins identified in Lpa^{WT} and Lpa^{LRV1+}
View complete table.

Table S11. Unique phosphoproteins identified in Lpa^{WT} relative to Lpa^{LRV1+}
View complete table.

Table S12. Unique phosphoproteins identified in Lpa^{LRV1+} relative to Lpa^{WT}
View complete table.

Table S13. Differentially expressed phosphoproteins identified in Lpa^{WT} and Lpa^{LRV1+}
View complete table.

Table S14. Uniquely expressed proteins in Lpa^{2W} relative to other weeks post LRV1-infection
View complete table.

Table S15. Uniquely expressed proteins in Lpa^{4W} relative to other weeks post LRV1-infection
View complete table.

Table S16. Uniquely expressed proteins in Lpa^{6W} relative to other weeks post LRV1-infection
View complete table.

Table S17. Uniquely expressed proteins in Lpa^{10W} relative to other weeks post LRV1-infection
View complete table.

Table S18. Leishmanial homologs of proteins involved in translation.
View complete table.

Table S19. Leishmanial homologs of proteins involved in metabolic processes.
View complete table.

Table S20. Leishmanial homologs of proteins involved in vesicle production.
View complete table.

Table S21. Leishmanial proteins involved in parasitic virulence.
View complete table.

Table S22. Leishmanial homologs of proteins involved in ROS production.
View complete table.

Table S23. Leishmanial homologs of proteins involved in detoxification of ROS.
View complete table.

Table S24. Leishmanial proteins involved in drug resistance.
View complete table.

Table S25. Leishmanial homologs of proteins involved in RNA interference.
View complete table.

Table S26. Leishmanial homologs of proteins involved in mammalian viral infections.
View complete table.

Table S27. Leishmanial homologs of proteins involved in MAPK signaling.
View complete table.

Table S28. Leishmanial homologs of proteins involved in TLR3 signaling.
View complete table.

WORKS CITED

1. Reithinger R, Dujardin J-C, Louzir H, Pirmez C, Alexander B, Brooker S. Cutaneous leishmaniasis. Lancet Infect Dis. 2007;7: 581–596. doi:10.1016/S1473-3099(07)70209-8

2. Mitra AK, Mawson AR. Neglected Tropical Diseases: Epidemiology and Global Burden. Trop Med Infect Dis. 2017;2: 36. doi:10.3390/tropicalmed2030036

3. Maurício IL. Leishmania Taxonomy. In: Bruschi F, Gradoni L, editors. The Leishmaniases: Old Neglected Tropical Diseases. Cham: Springer International Publishing; 2018. pp. 15–30. doi:10.1007/978-3-319-72386-0_2

4. Desjeux P. Leishmaniasis: current situation and new perspectives. Comp Immunol Microbiol Infect Dis. 2004;27: 305–318. doi:10.1016/j.cimid.2004.03.004

5. Kevric I, Cappel MA, Keeling JH. New World and Old World Leishmania Infections: A Practical Review. Dermatol Clin. 2015;33: 579–593. doi:10.1016/j.det.2015.03.018

6. Sunter J, Gull K. Shape, form, function and Leishmania pathogenicity: from textbook descriptions to biological understanding. Open Biol. 2017;7: 170165. doi:10.1098/rsob.170165

7. Cantacessi C, Dantas-Torres F, Nolan MJ, Otranto D. The past, present, and future of Leishmania genomics and transcriptomics. Trends Parasitol. 2015;31: 100–108. doi:10.1016/j.pt.2014.12.012

8. Kazemi B. Genomic Organization of Leishmania Species. Iran J Parasitol. 2011;6: 1–18.

9. Dolinski K, Botstein D. Orthology and Functional Conservation in Eukaryotes. Annu Rev Genet. 2007;41: 465–507. doi:10.1146/annurev.genet.40.110405.090439

10. Lye L-F, Owens K, Shi H, Murta SMF, Vieira AC, Turco SJ, et al. Retention and Loss of RNA Interference Pathways in Trypanosomatid Protozoans. PLoS Pathog. 2010;6: e1001161. doi:10.1371/journal.ppat.1001161

11. Ticha L, Kykalova B, Sadlova J, Gramiccia M, Gradoni L, Volf P. Development of Various Leishmania (Sauroleishmania) tarentolae Strains in Three Phlebotomus Species. Microorganisms. 2021;9: 2256. doi:10.3390/microorganisms9112256

12. World Health Organization. Leishmaniasis. [cited 12 Jan 2023]. Available: https://www.who.int/news-room/fact-sheets/detail/leishmaniasis

13. Mann S, Frasca K, Scherrer S, Henao-Martínez AF, Newman S, Ramanan P, et al. A Review of Leishmaniasis: Current Knowledge and Future Directions. Curr Trop Med Rep. 2021;8: 121–132. doi:10.1007/s40475-021-00232-7

14. Burza S, Croft SL, Boelaert M. Leishmaniasis. The Lancet. 2018;392: 951–970. doi:10.1016/S0140-6736(18)31204-2

15. Zijlstra EE, Musa AM, Khalil E a. G, Hassan IE, El-Hassan AM. Post-kala-azar dermal leishmaniasis. Lancet Infect Dis. 2003;3: 87–98. doi:10.1016/S1473-3099(03)00517-6

16. Ramesh V, Mukherjee A. Post-kala-azar dermal leishmaniasis. Int J Dermatol. 1995;34: 85–91. doi:10.1111/j.1365-4362.1995.tb03584.x

17. Zijlstra EE, Khalil EA, Kager PA, El-Hassan AM. Post-kala-azar dermal leishmaniasis in the Sudan: clinical presentation and differential diagnosis. Br J Dermatol. 2000;143: 136–143. doi:10.1046/j.1365-2133.2000.03603.x

18. David CV, Craft N. Cutaneous and mucocutaneous leishmaniasis. Dermatol Ther. 2009;22: 491–502. doi:10.1111/j.1529-8019.2009.01272.x

19. Hashiguchi Y, Gomez EL, Kato H, Martini LR, Velez LN, Uezato H. Diffuse and disseminated cutaneous leishmaniasis: clinical cases experienced in Ecuador and a brief review. Trop Med Health. 2016;44: 2. doi:10.1186/s41182-016-0002-0

20. Gitari JW, Nzou SM, Wamunyokoli F, Kinyeru E, Fujii Y, Kaneko S, et al. Leishmaniasis recidivans by Leishmania tropica in Central Rift Valley Region in Kenya. Int J Infect Dis. 2018;74: 109–116. doi:10.1016/j.ijid.2018.07.008

21. Pan American Health Organization WHO. Leishmaniasis in the Americas. Recommendations for the treatment. 2018. Available: https://www.paho.org/en/documents/leishmaniasis-americas-recommendations-treatment-2018

22. Georgiadou SP, Makaritsis KP, Dalekos GN. Leishmaniasis revisited: Current aspects on epidemiology, diagnosis and treatment. J Transl Intern Med. 2015;3: 43–50. doi:10.1515/jtim-2015-0002

23. Ibarra-Meneses AV, Corbeil A, Wagner V, Onwuchekwa C, Fernandez-Prada C. Identification of asymptomatic Leishmania infections: a scoping review. Parasit Vectors. 2022;15: 5. doi:10.1186/s13071-021-05129-y

24. Srivastava P, Gidwani K, Picado A, Van der Auwera G, Tiwary P, Ostyn B, et al. Molecular and serological markers of Leishmania donovani infection in healthy individuals from endemic areas of Bihar, India. Trop Med Int Health TM IH. 2013;18: 548–554. doi:10.1111/tmi.12085

25. World Health Organization, Alvar J. Report of the consultative meeting on cutaneous leishmaniasis. Geneva; 2008 Mar p. 36. Available: https://www.who.int/publications-detail-redirect/WHO-HTM-NTD-IDM-2008.7

26. Eltoum IA, Zijlstra EE, Ali MS, Ghalib HW, Satti MM, Eltoum B, et al. Congenital kala-azar and leishmaniasis in the placenta. Am J Trop Med Hyg. 1992;46: 57–62. doi:10.4269/ajtmh.1992.46.57

27. Dey A, Singh S. Transfusion transmitted leishmaniasis: a case report and review of literature. Indian J Med Microbiol. 2006;24: 165–170.

28. Antinori S, Cascio A, Parravicini C, Bianchi R, Corbellino M. Leishmaniasis among organ transplant recipients. Lancet Infect Dis. 2008;8: 191–199. doi:10.1016/S1473-3099(08)70043-4

29. Alvar J, Cañavate C, Gutiérrez-Solar B, Jiménez M, Laguna F, López-Vélez R, et al. Leishmania and human immunodeficiency virus coinfection: the first 10 years. Clin Microbiol Rev. 1997;10: 298–319. doi:10.1128/CMR.10.2.298

30. Strazzulla A, Cocuzza S, Pinzone MR, Postorino MC, Cosentino S, Serra A, et al. Mucosal Leishmaniasis: An Underestimated Presentation of a Neglected Disease. BioMed Res Int. 2013;2013: 805108. doi:10.1155/2013/805108

31. Singh OP, Hasker E, Sacks D, Boelaert M, Sundar S. Asymptomatic Leishmania Infection: A New Challenge for Leishmania Control. Clin Infect Dis Off Publ Infect Dis Soc Am. 2014;58: 1424–1429. doi:10.1093/cid/ciu102

32. Ezra N, Ochoa MT, Craft N. Human Immunodeficiency Virus and Leishmaniasis. J Glob Infect Dis. 2010;2: 248–257. doi:10.4103/0974-777X.68528

33. González C, Wang O, Strutz SE, González-Salazar C, Sánchez-Cordero V, Sarkar S. Climate Change and Risk of Leishmaniasis in North America: Predictions from Ecological Niche Models of Vector and Reservoir Species. PLoS Negl Trop Dis. 2010;4: e585. doi:10.1371/journal.pntd.0000585

34. Koch LK, Kochmann J, Klimpel S, Cunze S. Modeling the climatic suitability of leishmaniasis vector species in Europe. Sci Rep. 2017;7: 13325. doi:10.1038/s41598-017-13822-1

35. Chaves LF, Pascual M. Climate Cycles and Forecasts of Cutaneous Leishmaniasis, a Nonstationary Vector-Borne Disease. PLOS Med. 2006;3: e295. doi:10.1371/journal.pmed.0030295

36. Curtin JM, Aronson NE. Leishmaniasis in the United States: Emerging Issues in a Region of Low Endemicity. Microorganisms. 2021;9: 578. doi:10.3390/microorganisms9030578

37. Rostamian M, Rezaeian S, Hamidouche M, Bahrami F, Ghadiri K, Chegeneh Lorestani R, et al. The effects of natural disasters on leishmaniases frequency: A global systematic review and meta-analysis. Acta Trop. 2021;217: 105855. doi:10.1016/j.actatropica.2021.105855

38. Mackenzie JS, Jeggo M. The One Health Approach—Why Is It So Important? Trop Med Infect Dis. 2019;4: 88. doi:10.3390/tropicalmed4020088

39. Bates PA. Transmission of Leishmania metacyclic promastigotes by phlebotomine sand flies. Int J Parasitol. 2007;37: 1097–1106. doi:10.1016/j.ijpara.2007.04.003

40. Torres-Guerrero E, Quintanilla-Cedillo MR, Ruiz-Esmenjaud J, Arenas R. Leishmaniasis: a review. F1000Research. 2017;6. doi:10.12688/f1000research.11120.1

41. Killick-Kendrick R. The life-cycle of Leishmania in the sandfly with special reference to the form infective to the vertebrate host. Ann Parasitol Hum Comparée. 1990;65: 37–42. doi:10.1051/parasite/1990651037

42. Ueno N, Wilson ME. Receptor-mediated phagocytosis of Leishmania: implications for intracellular survival. Trends Parasitol. 2012;28: 335–344. doi:10.1016/j.pt.2012.05.002

43. Volpedo G, Pacheco-Fernandez T, Holcomb EA, Cipriano N, Cox B, Satoskar AR. Mechanisms of Immunopathogenesis in Cutaneous Leishmaniasis And Post Kala-azar Dermal Leishmaniasis (PKDL). Front Cell Infect Microbiol. 2021;11. Available: https://www.frontiersin.org/articles/10.3389/fcimb.2021.685296

44. Ritter U, Frischknecht F, Zandbergen G van. Are neutrophils important host cells for Leishmania parasites? Trends Parasitol. 2009;25: 505–510. doi:10.1016/j.pt.2009.08.003

45. Silveira FT, Lainson R, De Castro Gomes CM, Laurenti MD, Corbett CEP. Immunopathogenic competences of Leishmania (V.) braziliensis and L. (L.) amazonensis in American cutaneous leishmaniasis. Parasite Immunol. 2009;31: 423–431. doi:10.1111/j.1365-3024.2009.01116.x

46. Liu D, Uzonna JE. The early interaction of Leishmania with macrophages and dendritic cells and its influence on the host immune response. Front Cell Infect Microbiol. 2012;2: 83. doi:10.3389/fcimb.2012.00083

47. Olivier M, Minguez-Menendez A, Fernandez-Prada C. Leishmania Viannia guyanensis. Trends Parasitol. 2019;35: 1018–1019. doi:10.1016/j.pt.2019.06.008

48. Atayde VD, Hassani K, da Silva Lira Filho A, Borges AR, Adhikari A, Martel C, et al. Leishmania exosomes and other virulence factors: Impact on innate immune response and macrophage functions. Cell Immunol. 2016;309: 7–18. doi:10.1016/j.cellimm.2016.07.013

49. Olivier M, Zamboni DS. Leishmania Viannia guyanensis, LRV1 virus and extracellular vesicles: a dangerous trio influencing the faith of immune response during muco-cutaneous leishmaniasis. Curr Opin Immunol. 2020;66: 108–113. doi:10.1016/j.coi.2020.08.004

50. Scott P, Novais FO. Cutaneous leishmaniasis: immune responses in protection and pathogenesis. Nat Rev Immunol. 2016;16: 581–592. doi:10.1038/nri.2016.72

51. Soong L, Henard CA, Melby PC. Immunopathogenesis of non-healing American cutaneous leishmaniasis and progressive visceral leishmaniasis. Semin Immunopathol. 2012;34: 735–751. doi:10.1007/s00281-012-0350-8

52. Tomiotto-Pellissier F, Bortoleti BT da S, Assolini JP, Gonçalves MD, Carloto ACM, Miranda-Sapla MM, et al. Macrophage Polarization in Leishmaniasis: Broadening Horizons. Front Immunol. 2018;9. Available: https://www.frontiersin.org/articles/10.3389/fimmu.2018.02529

53. Zamboni DS, Sacks DL. Inflammasomes and Leishmania: in good times or bad, in sickness or in health. Curr Opin Microbiol. 2019;52: 70–76. doi:10.1016/j.mib.2019.05.005

54. de Carvalho RVH, Lima-Junior DS, da Silva MVG, Dilucca M, Rodrigues TS, Horta CV, et al. Leishmania RNA virus exacerbates Leishmaniasis by subverting innate immunity via TLR3-mediated NLRP3 inflammasome inhibition. Nat Commun. 2019;10: 5273. doi:10.1038/s41467-019-13356-2

55. Gupta AK, Ghosh K, Palit S, Barua J, Das PK, Ukil A. Leishmania donovani inhibits inflammasome-dependent macrophage activation by exploiting the negative regulatory proteins A20 and UCP2. FASEB J. 2017;31: 5087–5101. doi:10.1096/fj.201700407R

56. Hartley M-A, Eren RO, Rossi M, Prevel F, Castiglioni P, Isorce N, et al. Leishmania guyanensis parasites block the activation of the inflammasome by inhibiting maturation of IL-1β. Microb Cell Graz Austria. 2018;5: 137–149. doi:10.15698/mic2018.03.619

57. Kihel A, Hammi I, Darif D, Lemrani M, Riyad M, Guessous F, et al. The different faces of the NLRP3 inflammasome in cutaneous Leishmaniasis: A review. Cytokine. 2021;147: 155248. doi:10.1016/j.cyto.2020.155248

58. Hartley M-A, Kohl K, Ronet C, Fasel N. The therapeutic potential of immune cross-talk in leishmaniasis. Clin Microbiol Infect. 2013;19: 119–130. doi:10.1111/1469-0691.12095

59. Faria DR, Souza PEA, Durães FV, Carvalho EM, Gollob KJ, Machado PR, et al. Recruitment of CD8+ T cells expressing granzymeA is associated with lesion progression in human cutaneous leishmaniasis. Parasite Immunol. 2009;31: 432–439. doi:10.1111/j.1365-3024.2009.01125.x

60. Crosby EJ, Goldschmidt MH, Wherry EJ, Scott P. Engagement of NKG2D on Bystander Memory CD8 T Cells Promotes Increased Immunopathology following Leishmania major Infection. PLOS Pathog. 2014;10: e1003970. doi:10.1371/journal.ppat.1003970

61. Boaventura VS, Santos CS, Cardoso CR, de Andrade J, Dos Santos WLC, Clarêncio J, et al. Human mucosal leishmaniasis: Neutrophils infiltrate areas of tissue damage that express high levels of Th17-related cytokines. Eur J Immunol. 2010;40: 2830–2836. doi:10.1002/eji.200940115

62. Nylén S, Eidsmo L. Tissue damage and immunity in cutaneous leishmaniasis. Parasite Immunol. 2012;34: 551–561. doi:10.1111/pim.12007

63. Olivier M, Gregory DJ, Forget G. Subversion Mechanisms by Which Leishmania Parasites Can Escape the Host Immune Response: a Signaling Point of View. Clin Microbiol Rev. 2005;18: 293–305. doi:10.1128/CMR.18.2.293-305.2005

64. Gupta AK, Das S, Kamran M, Ejazi SA, Ali N. The pathogenicity and virulence of Leishmania - interplay of virulence factors with host defenses. Virulence. 13: 903–935. doi:10.1080/21505594.2022.2074130

65. Olivier M, Atayde VD, Isnard A, Hassani K, Shio MT. Leishmania virulence factors: focus on the metalloprotease GP63. Microbes Infect. 2012;14: 1377–1389. doi:10.1016/j.micinf.2012.05.014

66. Carvalho LP, Passos S, Dutra WO, Soto M, Alonso C, Gollob KJ, et al. Effect of LACK and KMP11 on IFN-γ Production by Peripheral Blood Mononuclear Cells from Cutaneous and Mucosal Leishmaniasis Patients. Scand J Immunol. 2005;61: 337–342. doi:10.1111/j.1365-3083.2005.01581.x

67. de Menezes JP, Saraiva EM, da Rocha-Azevedo B. The site of the bite: Leishmania interaction with macrophages, neutrophils and the extracellular matrix in the dermis. Parasit Vectors. 2016;9: 264. doi:10.1186/s13071-016-1540-3

68. Swenerton RK, Zhang S, Sajid M, Medzihradszky KF, Craik CS, Kelly BL, et al. The Oligopeptidase B of Leishmania Regulates Parasite Enolase and Immune Evasion *. J Biol Chem. 2011;286: 429–440. doi:10.1074/jbc.M110.138313

69. Suman SS, Amit A, Singh KP, Gupta P, Equbal A, Kumari A, et al. Cytosolic tryparedoxin of Leishmania donovani modulates host immune response in visceral leishmaniasis. Cytokine. 2018;108: 1–8. doi:10.1016/j.cyto.2018.03.010

70. Malvolti S, Malhame M, Mantel CF, Rutte EAL, Kaye PM. Human leishmaniasis vaccines: Use cases, target population and potential global demand. PLoS Negl Trop Dis. 2021;15: e0009742. doi:10.1371/journal.pntd.0009742

71. Nassif PW, Mello TFPD, Navasconi TR, Mota CA, Demarchi IG, Aristides SMA, et al. Safety and efficacy of current alternatives in the topical treatment of cutaneous leishmaniasis: a systematic review. Parasitology. 2017;144: 995–1004. doi:10.1017/S0031182017000385

72. Sasidharan S, Saudagar P. Leishmaniasis: where are we and where are we heading? Parasitol Res. 2021;120: 1541–1554. doi:10.1007/s00436-021-07139-2

73. David CV, Craft N. Cutaneous and mucocutaneous leishmaniasis. Dermatol Ther. 2009;22: 491–502. doi:10.1111/j.1529-8019.2009.01272.x

74. Tuon FF, Amato VS, Graf ME, Siqueira AM, Nicodemo AC, Amato Neto V. Treatment of New World cutaneous leishmaniasis--a systematic review with a meta-analysis. Int J Dermatol. 2008;47: 109–124. doi:10.1111/j.1365-4632.2008.03417.x

75. Douanne N, Dong G, Amin A, Bernardo L, Blanchette M, Langlais D, et al. Leishmania parasites exchange drug-resistance genes through extracellular vesicles. Cell Rep. 2022;40: 111121. doi:10.1016/j.celrep.2022.111121

76. Callahan HL, Roberts WL, Rainey PM, Beverley SM. The PGPA gene of Leishmania major mediates antimony (SbIII) resistance by decreasing influx and not by increasing efflux. Mol Biochem Parasitol. 1994;68: 145–149. doi:10.1016/0166-6851(94)00154-5

77. The LABCG2 Transporter from the Protozoan Parasite Leishmania Is Involved in Antimony Resistance. [cited 22 Jan 2023]. doi:10.1128/AAC.02813-15

78. Castanys-Muñoz E, Alder-Baerens N, Pomorski T, Gamarro F, Castanys S. A novel ATP-binding cassette transporter from Leishmania is involved in transport of phosphatidylcholine analogues and resistance to alkyl-phospholipids. Mol Microbiol. 2007;64: 1141–1153. doi:10.1111/j.1365-2958.2007.05653.x

79. Characterization of an ABCG-Like Transporter from the Protozoan Parasite Leishmania with a Role in Drug Resistance and Transbilayer Lipid Movement. [cited 22 Jan 2023]. doi:10.1128/AAC.00587-08

80. A New ABC Half-Transporter in Leishmania major Is Involved in Resistance to Antimony. [cited 22 Jan 2023]. doi:10.1128/AAC.00211-13

81. Purkait B, Kumar A, Nandi N, Sardar AH, Das S, Kumar S, et al. Mechanism of amphotericin B resistance in clinical isolates of Leishmania donovani. Antimicrob Agents Chemother. 2012;56: 1031–1041. doi:10.1128/AAC.00030-11

82. Haimeur A, Guimond C, Pilote S, Mukhopadhyay R, Rosen BP, Poulin R, et al. Elevated levels of polyamines and trypanothione resulting from overexpression of the ornithine decarboxylase gene in arsenite-resistant Leishmania. Mol Microbiol. 1999;34: 726–735. doi:10.1046/j.1365-2958.1999.01634.x

83. Coelho AC, Beverley SM, Cotrim PC. Functional genetic identification of PRP1, an ABC transporter superfamily member conferring pentamidine resistance in Leishmania major. Mol Biochem Parasitol. 2003;130: 83–90. doi:10.1016/S0166-6851(03)00162-2

84. Heterogeneity of Molecular Resistance Patterns in Antimony-Resistant Field Isolates of Leishmania Species from the Western Mediterranean Area. [cited 22 Jan 2023]. Available: https://journals.asm.org/doi/epdf/10.1128/AAC.02521-13?src=getftr

85. Kazemi-Rad E, Mohebali M, Khadem-Erfan MB, Hajjaran H, Hadighi R, Khamesipour A, et al. Overexpression of Ubiquitin and Amino Acid Permease Genes in Association with Antimony Resistance in <italic>Leishmania tropica</italic> Field Isolates. Korean J Parasitol. 2013;51: 413–419. doi:10.3347/kjp.2013.51.4.413

86. A Telomeric Cluster of Antimony Resistance Genes on Chromosome 34 of Leishmania infantum. [cited 22 Jan 2023]. doi:10.1128/AAC.00544-16

87. Gourbal B, Sonuc N, Bhattacharjee H, Legare D, Sundar S, Ouellette M, et al. Drug Uptake and Modulation of Drug Resistance in Leishmania by an Aquaglyceroporin *. J Biol Chem. 2004;279: 31010–31017. doi:10.1074/jbc.M403959200

88. Marquis N, Gourbal B, Rosen BP, Mukhopadhyay R, Ouellette M. Modulation in aquaglyceroporin AQP1 gene transcript levels in drug-resistant Leishmania. Mol Microbiol. 2005;57: 1690–1699. doi:10.1111/j.1365-2958.2005.04782.x

89. Baker N, Glover L, Munday JC, Aguinaga Andrés D, Barrett MP, de Koning HP, et al. Aquaglyceroporin 2 controls susceptibility to melarsoprol and pentamidine in African trypanosomes. Proc Natl Acad Sci. 2012;109: 10996–11001. doi:10.1073/pnas.1202885109

90. Ponte-Sucre A, Gamarro F, Dujardin J-C, Barrett MP, López-Vélez R, García-Hernández R, et al. Drug resistance and treatment failure in leishmaniasis: A 21st century challenge. PLoS Negl Trop Dis. 2017;11. doi:10.1371/journal.pntd.0006052

91. Pourshafie M, Morand S, Virion A, Rakotomanga M, Dupuy C, Loiseau PM. Cloning of S-Adenosyl-l-Methionine:C-24-Δ-Sterol-Methyltransferase (ERG6) from Leishmania donovani and Characterization of mRNAs in Wild-Type and Amphotericin B-Resistant Promastigotes. Antimicrob Agents Chemother. 2004;48: 2409–2414. doi:10.1128/AAC.48.7.2409-2414.2004

92. Ning Y, Frankfater C, Hsu F-F, Soares RP, Cardoso CA, Nogueira PM, et al. Lathosterol Oxidase (Sterol C-5 Desaturase) Deletion Confers Resistance to Amphotericin B and Sensitivity to Acidic Stress in Leishmania major. mSphere. 2020;5: e00380-20. doi:10.1128/mSphere.00380-20

93. Bagher KHADEM ERFAN M, MOHEBALI M, KAZEMI-RAD E, HAJJARAN H, EDRISSIAN G, MAMISHI S, et al. Downregulation of Calcineurin Gene Is Associated with Glucantime® Resiatance in Leishmania infantum. Iran J Parasitol. 2013;8: 359–366.

94. Guimond C, Trudel N, Brochu C, Marquis N, Fadili AE, Peytavi R, et al. Modulation of gene expression in Leishmania drug resistant mutants as determined by targeted DNA microarrays. Nucleic Acids Res. 2003;31: 5886–5896. doi:10.1093/nar/gkg806

95. Rosa-Teijeiro C, Wagner V, Corbeil A, d'Annessa I, Leprohon P, do Monte-Neto RL, et al. Three different mutations in the DNA topoisomerase 1B in Leishmania infantum contribute to resistance to antitumor drug topotecan. Parasit Vectors. 2021;14: 438. doi:10.1186/s13071-021-04947-4

96. Tj V, Ah F. Trypanothione S-transferase activity in a trypanosomatid ribosomal elongation factor 1B. J Biol Chem. 2004;279. doi:10.1074/jbc.M311039200

97. Richard D, Leprohon P, Drummelsmith J, Ouellette M. Growth Phase Regulation of the Main Folate Transporter of Leishmania infantum and Its Role in Methotrexate Resistance*. J Biol Chem. 2004;279: 54494–54501. doi:10.1074/jbc.M409264200

98. Goyeneche-Patino DA, Valderrama L, Walker J, Saravia NG. Antimony Resistance and Trypanothione in Experimentally Selected and Clinical Strains of Leishmania panamensis. Antimicrob Agents Chemother. 2008;52: 4503–4506. doi:10.1128/AAC.01075-08

99. Hombach A, Ommen G, MacDonald A, Clos J. A small heat shock protein is essential for thermotolerance and intracellular survival of Leishmania donovani. J Cell Sci. 2014;127: 4762–4773. doi:10.1242/jcs.157297

100. Vergnes B, Gourbal B, Girard I, Sundar S, Drummelsmith J, Ouellette M. A Proteomics Screen Implicates HSP83 and a Small Kinetoplastid Calpain-related Protein in Drug Resistance in Leishmania donovani Clinical Field Isolates by Modulating Drug-induced Programmed Cell Death*. Mol Cell Proteomics. 2007;6: 88–101. doi:10.1074/mcp.M600319-MCP200

101. Kumar D, Singh R, Bhandari V, Kulshrestha A, Negi NS, Salotra P. Biomarkers of antimony resistance: need for expression analysis of multiple genes to distinguish resistance phenotype in clinical isolates of Leishmania donovani. Parasitol Res. 2012;111: 223–230. doi:10.1007/s00436-012-2823-z

102. Singh R, Kumar D, Duncan RC, Nakhasi HL, Salotra P. Overexpression of histone H2A modulates drug susceptibility in Leishmania parasites. Int J Antimicrob Agents. 2010;36: 50–57. doi:10.1016/j.ijantimicag.2010.03.012

103. MAPK1 of Leishmania donovani Modulates Antimony Susceptibility by Downregulating P-Glycoprotein Efflux Pumps. [cited 22 Jan 2023]. doi:10.1128/AAC.04816-14

104. Pérez-Victoria FJ, Castanys S, Gamarro F. Leishmania donovani Resistance to Miltefosine Involves a Defective Inward Translocation of the Drug. Antimicrob Agents Chemother. 2003;47: 2397–2403. doi:10.1128/AAC.47.8.2397-2403.2003

105. de Souza Moreira D, Ferreira RF, Murta SMF. Molecular characterization and functional analysis of pteridine reductase in wild-type and antimony-resistant Leishmania lines. Exp Parasitol. 2016;160: 60–66. doi:10.1016/j.exppara.2015.12.009

106. Fernandez-Prada C, Sharma M, Plourde M, Bresson E, Roy G, Leprohon P, et al. High-throughput Cos-Seq screen with intracellular Leishmania infantum for the discovery of novel drug-resistance mechanisms. Int J Parasitol Drugs Drug Resist. 2018;8: 165–173. doi:10.1016/j.ijpddr.2018.03.004

107. Yadav S, Ali V, Singh Y, Kanojia S, Goyal N. Leishmania donovani chaperonin TCP1γ subunit protects miltefosine induced oxidative damage. Int J Biol Macromol. 2020;165: 2607–2620. doi:10.1016/j.ijbiomac.2020.10.134

108. Zabala-Peñafiel A, Dias-Lopes G, Souza-Silva F, Miranda LFC, Conceição-Silva F, Alves CR. Assessing the effect of antimony pressure on trypanothione reductase activity in Leishmania (Viannia) braziliensis. Biochimie. 2022 [cited 22 Jan 2023]. doi:10.1016/j.biochi.2022.12.010

109. Mukhopadhyay R, Dey S, Xu N, Gage D, Lightbody J, Ouellette M, et al. Trypanothione overproduction and resistance to antimonials and arsenicals in Leishmania. Proc Natl Acad Sci. 1996;93: 10383–10387. doi:10.1073/pnas.93.19.10383

110. Salari S, Bamorovat M, Sharifi I, Almani PGN. Global distribution of treatment resistance gene markers for leishmaniasis. J Clin Lab Anal. 2022;36: e24599. doi:10.1002/jcla.24599

111. Théry C, Witwer KW, Aikawa E, Alcaraz MJ, Anderson JD, Andriantsitohaina R, et al. Minimal information for studies of extracellular vesicles 2018 (MISEV2018): a position statement of the International Society for Extracellular Vesicles and update of the MISEV2014 guidelines. J Extracell Vesicles. 2018;7: 1535750. doi:10.1080/20013078.2018.1535750

112. Doyle LM, Wang MZ. Overview of Extracellular Vesicles, Their Origin, Composition, Purpose, and Methods for Exosome Isolation and Analysis. Cells. 2019;8: 727. doi:10.3390/cells8070727

113. Akers JC, Gonda D, Kim R, Carter BS, Chen CC. Biogenesis of extracellular vesicles (EV): exosomes, microvesicles, retrovirus-like vesicles, and apoptotic bodies. J Neurooncol. 2013;113: 1–11. doi:10.1007/s11060-013-1084-8

114. Keller S, Ridinger J, Rupp A-K, Janssen JW, Altevogt P. Body fluid derived exosomes as a novel template for clinical diagnostics. J Transl Med. 2011;9: 86. doi:10.1186/1479-5876-9-86

115. De Toro J, Herschlik L, Waldner C, Mongini C. Emerging Roles of Exosomes in Normal and Pathological Conditions: New Insights for Diagnosis and Therapeutic Applications. Front Immunol. 2015;6: 203. doi:10.3389/fimmu.2015.00203

116. Théry C, Duban L, Segura E, Véron P, Lantz O, Amigorena S. Indirect activation of naïve CD4+ T cells by dendritic cell–derived exosomes. Nat Immunol. 2002;3: 1156–1162. doi:10.1038/ni854

117. Lugini L, Cecchetti S, Huber V, Luciani F, Macchia G, Spadaro F, et al. Immune Surveillance Properties of Human NK Cell-Derived Exosomes. J Immunol. 2012;189: 2833–2842. doi:10.4049/jimmunol.1101988

118. Clayton A, Mitchell JP, Court J, Mason MD, Tabi Z. Human Tumor-Derived Exosomes Selectively Impair Lymphocyte Responses to Interleukin-2. Cancer Res. 2007;67: 7458–7466. doi:10.1158/0008-5472.CAN-06-3456

119. Szajnik M, Czystowska M, Szczepanski MJ, Mandapathil M, Whiteside TL. Tumor-Derived Microvesicles Induce, Expand and Up-Regulate Biological Activities of Human

Regulatory T Cells (Treg). PLOS ONE. 2010;5: e11469. doi:10.1371/journal.pone.0011469

120. Kalluri R, LeBleu VS. The biology, function, and biomedical applications of exosomes. Science. 2020;367. doi:10.1126/science.aau6977

121. Saad MH, Badierah R, Redwan EM, El-Fakharany EM. A Comprehensive Insight into the Role of Exosomes in Viral Infection: Dual Faces Bearing Different Functions. Pharmaceutics. 2021;13: 1405. doi:10.3390/pharmaceutics13091405

122. Lenassi M, Cagney G, Liao M, Vaupotič T, Bartholomeeusen K, Cheng Y, et al. HIV Nef is secreted in exosomes and triggers apoptosis in bystander CD4+ T cells. Traffic Cph Den. 2010;11: 110–122. doi:10.1111/j.1600-0854.2009.01006.x

123. Ahmed W, Philip PS, Attoub S, Khan G. Epstein–Barr virus-infected cells release Fas ligand in exosomal fractions and induce apoptosis in recipient cells via the extrinsic pathway. J Gen Virol. 2015;96: 3646–3659. doi:10.1099/jgv.0.000313

124. Dreux M, Garaigorta U, Boyd B, Décembre E, Chung J, Whitten-Bauer C, et al. Short-Range Exosomal Transfer of Viral RNA from Infected Cells to Plasmacytoid Dendritic Cells Triggers Innate Immunity. Cell Host Microbe. 2012;12: 558–570. doi:10.1016/j.chom.2012.08.010

125. Pleet ML, Mathiesen A, DeMarino C, Akpamagbo YA, Barclay RA, Schwab A, et al. Ebola VP40 in Exosomes Can Cause Immune Cell Dysfunction. Front Microbiol. 2016;7. Available: https://www.frontiersin.org/articles/10.3389/fmicb.2016.01765

126. Wang J, Chen S, Bihl J. Exosome-Mediated Transfer of ACE2 (Angiotensin-Converting Enzyme 2) from Endothelial Progenitor Cells Promotes Survival and Function of Endothelial Cell. Oxid Med Cell Longev. 2020;2020: e4213541. doi:10.1155/2020/4213541

127. Martins S de T, Alves LR. Extracellular Vesicles in Viral Infections: Two Sides of the Same Coin? Front Cell Infect Microbiol. 2020;10. Available: https://www.frontiersin.org/articles/10.3389/fcimb.2020.593170

128. Nagashima S, Jirintai S, Takahashi M, Kobayashi T, Tanggis, Nishizawa T, et al. Hepatitis E virus egress depends on the exosomal pathway, with secretory exosomes derived from multivesicular bodies. J Gen Virol. 2014;95: 2166–2175. doi:10.1099/vir.0.066910-0

129. Nolte-‘t Hoen E, Cremer T, Gallo RC, Margolis LB. Extracellular vesicles and viruses: Are they close relatives? Proc Natl Acad Sci. 2016;113: 9155–9161. doi:10.1073/pnas.1605146113

130. Gioseffi A, Edelmann MJ, Kima PE. Intravacuolar Pathogens Hijack Host Extracellular Vesicle Biogenesis to Secrete Virulence Factors. Front Immunol. 2021;12. Available: https://www.frontiersin.org/articles/10.3389/fimmu.2021.662944

131. Cecil JD, Sirisaengtaksin N, O'Brien-Simpson NM, Krachler AM. Outer Membrane Vesicle—Host Cell Interactions. Microbiol Spectr. 2019;7: 10.1128/microbiolspec.PSIB-0001–2018. doi:10.1128/microbiolspec.PSIB-0001-2018

132. Torrecilhas AC, Soares RP, Schenkman S, Fernández-Prada C, Olivier M. Extracellular Vesicles in Trypanosomatids: Host Cell Communication. Front Cell Infect Microbiol. 2020;10. Available: https://www.frontiersin.org/articles/10.3389/fcimb.2020.602502

133. Oliveira DL, Freire-de-Lima CG, Nosanchuk JD, Casadevall A, Rodrigues ML, Nimrichter L. Extracellular Vesicles from Cryptococcus neoformans Modulate Macrophage Functions. Infect Immun. 2010;78: 1601–1609. doi:10.1128/IAI.01171-09

134. Trocoli Torrecilhas AC, Tonelli RR, Pavanelli WR, da Silva JS, Schumacher RI, de Souza W, et al. Trypanosoma cruzi: parasite shed vesicles increase heart parasitism and generate an intense inflammatory response. Microbes Infect. 2009;11: 29–39. doi:10.1016/j.micinf.2008.10.003

135. Atayde VD, Suau HA, Townsend S, Hassani K, Kamhawi S, Olivier M. Exosome secretion by the parasitic protozoan Leishmania within the sand fly midgut. Cell Rep. 2015;13: 957–967. doi:10.1016/j.celrep.2015.09.058

136. Hassani K, Antoniak E, Jardim A, Olivier M. Temperature-Induced Protein Secretion by Leishmania mexicana Modulates Macrophage Signalling and Function. PLOS ONE. 2011;6: e18724. doi:10.1371/journal.pone.0018724

137. Silverman JM, Clos J, de'Oliveira CC, Shirvani O, Fang Y, Wang C, et al. An exosome-based secretion pathway is responsible for protein export from Leishmania and communication with macrophages. J Cell Sci. 2010;123: 842–852. doi:10.1242/jcs.056465

138. Santarém N, Racine G, Silvestre R, Cordeiro-da-Silva A, Ouellette M. Exoproteome dynamics in Leishmania infantum. J Proteomics. 2013;84: 106–118. doi:10.1016/j.jprot.2013.03.012

139. Silverman JM, Clos J, Horakova E, Wang AY, Wiesgigl M, Kelly I, et al. Leishmania Exosomes Modulate Innate and Adaptive Immune Responses through Effects on Monocytes and Dendritic Cells. J Immunol. 2010;185: 5011–5022. doi:10.4049/jimmunol.1000541

140. Lopez Kostka S, Dinges S, Griewank K, Iwakura Y, Udey MC, von Stebut E. IL-17 Promotes Progression of Cutaneous Leishmaniasis in Susceptible Mice1. J Immunol. 2009;182: 3039–3046. doi:10.4049/jimmunol.0713598

141. Silverman JM, Reiner NE. Leishmania Exosomes Deliver Preemptive Strikes to Create an Environment Permissive for Early Infection. Front Cell Infect Microbiol. 2012;1: 26. doi:10.3389/fcimb.2011.00026

142. da Silva Lira Filho A, Fajardo EF, Chang KP, Clément P, Olivier M. Leishmania Exosomes/Extracellular Vesicles Containing GP63 Are Essential for Enhance Cutaneous

Leishmaniasis Development Upon Co-Inoculation of Leishmania amazonensis and Its Exosomes. Front Cell Infect Microbiol. 2022;11. Available: https://www.frontiersin.org/articles/10.3389/fcimb.2021.709258

143. Hassani K, Shio MT, Martel C, Faubert D, Olivier M. Absence of Metalloprotease GP63 Alters the Protein Content of Leishmania Exosomes. PLOS ONE. 2014;9: e95007. doi:10.1371/journal.pone.0095007

144. Bruenn JA. 7 - Viruses of Fungi and Protozoans: Is Everyone Sick? In: Hurst CJ, editor. Viral Ecology. San Diego: Academic Press; 2000. pp. 297–317. doi:10.1016/B978-012362675-2/50008-2

145. Jagdale SS, Joshi RS. Enemies with benefits: mutualistic interactions of viruses with lower eukaryotes. Arch Virol. 2018;163: 821–830. doi:10.1007/s00705-017-3686-5

146. Bell PJL. Evidence supporting a viral origin of the eukaryotic nucleus. Virus Res. 2020;289: 198168. doi:10.1016/j.virusres.2020.198168

147. Cavalier-Smith T. Origin of mitochondria by intracellular enslavement of a photosynthetic purple bacterium. Proc R Soc B Biol Sci. 2006;273: 1943–1952. doi:10.1098/rspb.2006.3531

148. Grybchuk D, Akopyants NS, Kostygov AY, Konovalovas A, Lye L-F, Dobson DE, et al. Viral discovery and diversity in trypanosomatid protozoa with a focus on relatives of the human parasite Leishmania. Proc Natl Acad Sci. 2018;115: E506–E515. doi:10.1073/pnas.1717806115

149. Lafleur A, Olivier M. Viral endosymbiotic infection of protozoan parasites: How it influences the development of cutaneous leishmaniasis. PLOS Pathog. 2022;18: e1010910. doi:10.1371/journal.ppat.1010910

150. Jenkins MC, Higgins J, Abrahante JE, Kniel KE, O'Brien C, Trout J, et al. Fecundity of Cryptosporidium parvum is correlated with intracellular levels of the viral symbiont CPV. Int J Parasitol. 2008;38: 1051–1055. doi:10.1016/j.ijpara.2007.11.005

151. He D, Pengtao G, Ju Y, Jianhua L, He L, Guocai Z, et al. Differential Protein Expressions in Virus-Infected and Uninfected *Trichomonas vaginalis*. Korean J Parasitol. 2017;55: 121–128. doi:10.3347/kjp.2017.55.2.121

152. Khoshnan A, Alderete JF. Trichomonas vaginalis with a double-stranded RNA virus has upregulated levels of phenotypically variable immunogen mRNA. J Virol. 1994;68: 4035–4038. doi:10.1128/jvi.68.6.4035-4038.1994

153. Lye L-F, Akopyants NS, Dobson DE, Beverley SM. A Narnavirus-Like Element from the Trypanosomatid Protozoan Parasite Leptomonas seymouri. Genome Announc. 2016;4: e00713-16. doi:10.1128/genomeA.00713-16

154. Akopyants NS, Lye L-F, Dobson DE, Lukeš J, Beverley SM. A Narnavirus in the Trypanosomatid Protist Plant Pathogen Phytomonas serpens. Genome Announc. 2016;4: e00711-16. doi:10.1128/genomeA.00711-16

155. Wang AL, Wang CC. Discovery of a specific double-stranded RNA virus in Giardia lamblia. Mol Biochem Parasitol. 1986;21: 269–276. doi:10.1016/0166-6851(86)90132-5

156. Zhao Z, Li X, Zhang N, Li J, Zhao N, Gao M, et al. Multiple Regulations of Parasitic Protozoan Viruses: A Double-Edged Sword for Protozoa. mBio. 2023;0: e02642-22. doi:10.1128/mbio.02642-22

157. Atayde VD, da Silva Lira Filho A, Chaparro V, Zimmermann A, Martel C, Jaramillo M, et al. Exploitation of the Leishmania exosomal pathway by Leishmania RNA virus 1. Nat Microbiol. 2019;4: 714–723. doi:10.1038/s41564-018-0352-y

158. Kleschenko Y, Grybchuk D, Matveeva NS, Macedo DH, Ponirovsky EN, Lukashev AN, et al. Molecular Characterization of Leishmania RNA virus 2 in Leishmania major from Uzbekistan. Genes. 2019;10: 830. doi:10.3390/genes10100830

159. Hillman BI, Cohen AB. Totiviruses (Totiviridae)1. In: Bamford DH, Zuckerman M, editors. Encyclopedia of Virology (Fourth Edition). Oxford: Academic Press; 2021. pp. 648–657. doi:10.1016/B978-0-12-809633-8.21347-2

160. El-Gayar EK, Mokhtar AB, Hassan WA. Molecular characterization of double-stranded RNA virus in Trichomonas vaginalis Egyptian isolates and its association with pathogenicity. Parasitol Res. 2016;115: 4027–4036. doi:10.1007/s00436-016-5174-3

161. Fichorova RN, Lee Y, Yamamoto HS, Takagi Y, Hayes GR, Goodman RP, et al. Endobiont Viruses Sensed by the Human Host – Beyond Conventional Antiparasitic Therapy. PLOS ONE. 2012;7: e48418. doi:10.1371/journal.pone.0048418

162. Pu X, Li X, Cao L, Yue K, Zhao P, Wang X, et al. Giardia duodenalis Induces Proinflammatory Cytokine Production in Mouse Macrophages via TLR9-Mediated p38 and ERK Signaling Pathways. Front Cell Dev Biol. 2021;9: 694675. doi:10.3389/fcell.2021.694675

163. Brettmann EA, Shaik JS, Zangger H, Lye L-F, Kuhlmann FM, Akopyants NS, et al. Tilting the balance between RNA interference and replication eradicates Leishmania RNA virus 1 and mitigates the inflammatory response. Proc Natl Acad Sci. 2016;113: 11998–12005. doi:10.1073/pnas.1615085113

164. Grybchuk D, Kostygov AY, Macedo DH, Votýpka J, Lukeš J, Yurchenko V. RNA Viruses in Blechomonas (Trypanosomatidae) and Evolution of Leishmaniavirus. mBio. 2018;9: e01932-18. doi:10.1128/mBio.01932-18

165. Shita EY, Semegn EN, Wubetu GY, Abitew AM, Andualem BG, Alemneh MG. Prevalence of Leishmania RNA virus in Leishmania parasites in patients with tegumentary

leishmaniasis: A systematic review and meta-analysis. PLoS Negl Trop Dis. 2022;16: e0010427. doi:10.1371/journal.pntd.0010427

166. Ginouvès M, Simon S, Bourreau E, Lacoste V, Ronet C, Couppié P, et al. Prevalence and Distribution of Leishmania RNA Virus 1 in Leishmania Parasites from French Guiana. Am J Trop Med Hyg. 2016;94: 102–106. doi:10.4269/ajtmh.15-0419

167. Bourreau E, Ginouves M, Prévot G, Hartley M-A, Gangneux J-P, Robert-Gangneux F, et al. Presence of Leishmania RNA Virus 1 in Leishmania guyanensis Increases the Risk of First-Line Treatment Failure and Symptomatic Relapse. J Infect Dis. 2016;213: 105–111. doi:10.1093/infdis/jiv355

168. Hartley M-A, Bourreau E, Rossi M, Castiglioni P, Eren RO, Prevel F, et al. Leishmaniavirus-Dependent Metastatic Leishmaniasis Is Prevented by Blocking IL-17A. PLOS Pathog. 2016;12: e1005852. doi:10.1371/journal.ppat.1005852

169. Adaui V, Lye L-F, Akopyants NS, Zimic M, Llanos-Cuentas A, Garcia L, et al. Association of the Endobiont Double-Stranded RNA Virus LRV1 With Treatment Failure for Human Leishmaniasis Caused by Leishmania braziliensis in Peru and Bolivia. J Infect Dis. 2016;213: 112–121. doi:10.1093/infdis/jiv354

170. A I, C R, F P, G R, S F-M, F S, et al. Leishmania RNA virus controls the severity of mucocutaneous leishmaniasis. Science. 2011;331. doi:10.1126/science.1199326

171. Ronet C, Beverley SM, Fasel N. Muco-cutaneous leishmaniasis in the New World. Virulence. 2011;2: 547–552. doi:10.4161/viru.2.6.17839

172. Rossi M, Castiglioni P, Hartley M-A, Eren RO, Prével F, Desponds C, et al. Type I interferons induced by endogenous or exogenous viral infections promote metastasis and relapse of leishmaniasis. Proc Natl Acad Sci. 2017;114: 4987–4992. doi:10.1073/pnas.1621447114

173. Eren RO, Reverte M, Rossi M, Hartley M-A, Castiglioni P, Prevel F, et al. Mammalian Innate Immune Response to a Leishmania-Resident RNA Virus Increases Macrophage Survival to Promote Parasite Persistence. Cell Host Microbe. 2016;20: 318–328. doi:10.1016/j.chom.2016.08.001

174. de Carvalho RVH, Lima-Júnior DS, de Oliveira CV, Zamboni DS. Endosymbiotic RNA virus inhibits Leishmania-induced caspase-11 activation. iScience. 2021;24: 102004. doi:10.1016/j.isci.2020.102004

175. Castiglioni P, Hartley M-A, Rossi M, Prevel F, Desponds C, Utzschneider DT, et al. Exacerbated Leishmaniasis Caused by a Viral Endosymbiont can be Prevented by Immunization with Its Viral Capsid. PLoS Negl Trop Dis. 2017;11: e0005240. doi:10.1371/journal.pntd.0005240

176. Kuhlmann FM, Robinson JI, Bluemling GR, Ronet C, Fasel N, Beverley SM. Antiviral screening identifies adenosine analogs targeting the endogenous dsRNA Leishmania RNA

virus 1 (LRV1) pathogenicity factor. Proc Natl Acad Sci. 2017;114: E811–E819. doi:10.1073/pnas.1619114114

177. Saura A, Zakharova A, Klocek D, Gerasimov ES, Butenko A, Macedo DH, et al. Elimination of LRVs Elicits Different Responses in Leishmania spp. mSphere. 2022;7: e00335-22. doi:10.1128/msphere.00335-22

178. Robinson JI, Beverley SM. Concentration of 2′C-methyladenosine triphosphate by Leishmania guyanensis enables specific inhibition of Leishmania RNA virus 1 via its RNA polymerase. J Biol Chem. 2018;293: 6460–6469. doi:10.1074/jbc.RA117.001515

179. Hartley M-A, Ronet C, Zangger H, Beverley SM, Fasel N. Leishmania RNA virus: when the host pays the toll. Front Cell Infect Microbiol. 2012;2. doi:10.3389/fcimb.2012.00099

180. Kariyawasam R, Lau R, Valencia BM, Llanos-Cuentas A, Boggild AK. Leishmania RNA Virus 1 (LRV-1) in Leishmania (Viannia) braziliensis Isolates from Peru: A Description of Demographic and Clinical Correlates. Am J Trop Med Hyg. 2020;102: 280–285. doi:10.4269/ajtmh.19-0147

181. Zakharova A, Albanaz ATS, Opperdoes FR, Škodová-Sveráková I, Zagirova D, Saura A, et al. Leishmania guyanensis M4147 as a new LRV1-bearing model parasite: Phosphatidate phosphatase 2-like protein controls cell cycle progression and intracellular lipid content. PLoS Negl Trop Dis. 2022;16: e0010510. doi:10.1371/journal.pntd.0010510

182. Martínez JE, Valderrama L, Gama V, Leiby DA, Saravia NG. CLONAL DIVERSITY IN THE EXPRESSION AND STABILITY OF THE METASTATIC CAPABILITY OF LEISHMANIA GUYANENSIS IN THE GOLDEN HAMSTER. J Parasitol. 2000;86: 792–799. doi:10.1645/0022-3395(2000)086[0792:CDITEA]2.0.CO;2

183. Altschul SF, Gish W, Miller W, Myers EW, Lipman DJ. Basic local alignment search tool. J Mol Biol. 1990;215: 403–410. doi:10.1016/S0022-2836(05)80360-2

184. Vucetic A, Filho ADSL, Dong G, Olivier M. Isolation of Extracellular Vesicles from Leishmania spp. In: Michels PAM, Ginger ML, Zilberstein D, editors. Trypanosomatids: Methods and Protocols. New York, NY: Springer US; 2020. pp. 555–574. doi:10.1007/978-1-0716-0294-2_33

185. Searle BC. Scaffold: A bioinformatic tool for validating MS/MS-based proteomic studies. PROTEOMICS. 2010;10: 1265–1269. doi:10.1002/pmic.200900437

186. Vincent-Maloney N, Searle BC, Turner M. Probabilistically Assigning Sites of Protein Modification with Scaffold PTM. J Biomol Tech JBT. 2011;22: S36–S37.

187. Conesa A, Götz S, García-Gómez JM, Terol J, Talón M, Robles M. Blast2GO: a universal tool for annotation, visualization and analysis in functional genomics research. Bioinformatics. 2005;21: 3674–3676. doi:10.1093/bioinformatics/bti610

188. Apweiler R, Bairoch A, Wu CH, Barker WC, Boeckmann B, Ferro S, et al. UniProt: the Universal Protein knowledgebase. Nucleic Acids Res. 2004;32: D115–D119. doi:10.1093/nar/gkh131

189. Szklarczyk D, Kirsch R, Koutrouli M, Nastou K, Mehryary F, Hachilif R, et al. The STRING database in 2023: protein-protein association networks and functional enrichment analyses for any sequenced genome of interest. Nucleic Acids Res. 2023;51: D638–D646. doi:10.1093/nar/gkac1000

190. Gillespie M, Jassal B, Stephan R, Milacic M, Rothfels K, Senff-Ribeiro A, et al. The reactome pathway knowledgebase 2022. Nucleic Acids Res. 2022;50: D687–D692. doi:10.1093/nar/gkab1028

191. Varadi M, Anyango S, Deshpande M, Nair S, Natassia C, Yordanova G, et al. AlphaFold Protein Structure Database: massively expanding the structural coverage of protein-sequence space with high-accuracy models. Nucleic Acids Res. 2022;50: D439–D444. doi:10.1093/nar/gkab1061

192. Waterhouse A, Bertoni M, Bienert S, Studer G, Tauriello G, Gumienny R, et al. SWISS-MODEL: homology modelling of protein structures and complexes. Nucleic Acids Res. 2018;46: W296–W303. doi:10.1093/nar/gky427

193. Studer G, Rempfer C, Waterhouse AM, Gumienny R, Haas J, Schwede T. QMEANDisCo—distance constraints applied on model quality estimation. Bioinformatics. 2020;36: 1765–1771. doi:10.1093/bioinformatics/btz828

194. Clarke DJB, Kuleshov MV, Schilder BM, Torre D, Duffy ME, Keenan AB, et al. eXpression2Kinases (X2K) Web: linking expression signatures to upstream cell signaling networks. Nucleic Acids Res. 2018;46: W171–W179. doi:10.1093/nar/gky458

195. Aoki S, Shteyn K, Marien R. BioRender. https://www.biorender.com/; 2017.

196. Foo J, Bellot G, Pervaiz S, Alonso S. Mitochondria-mediated oxidative stress during viral infection. Trends Microbiol. 2022;30: 679–692. doi:10.1016/j.tim.2021.12.011

197. Reshi ML, Su Y-C, Hong J-R. RNA Viruses: ROS-Mediated Cell Death. Int J Cell Biol. 2014;2014: 467452. doi:10.1155/2014/467452

198. Castro H, Teixeira F, Romao S, Santos M, Cruz T, Flórido M, et al. Leishmania Mitochondrial Peroxiredoxin Plays a Crucial Peroxidase-Unrelated Role during Infection: Insight into Its Novel Chaperone Activity. PLOS Pathog. 2011;7: e1002325. doi:10.1371/journal.ppat.1002325

199. Abtahi M, Eslami G, Cavallero S, Vakili M, Hosseini SS, Ahmadian S, et al. Relationship of Leishmania RNA Virus (LRV) and treatment failure in clinical isolates of Leishmania major. BMC Res Notes. 2020;13: 126. doi:10.1186/s13104-020-04973-y

200. Raj S, Saha G, Sasidharan S, Dubey VK, Saudagar P. Biochemical characterization and chemical validation of Leishmania MAP Kinase-3 as a potential drug target. Sci Rep. 2019;9: 16209. doi:10.1038/s41598-019-52774-6

201. Matsumoto M, Oshiumi H, Seya T. Antiviral responses induced by the TLR3 pathway. Rev Med Virol. 2011;21: 67–77. doi:10.1002/rmv.680

202. Nimma S, Gu W, Maruta N, Li Y, Pan M, Saikot FK, et al. Structural Evolution of TIR-Domain Signalosomes. Front Immunol. 2021;12. Available: https://www.frontiersin.org/articles/10.3389/fimmu.2021.784484

203. Kd S, R W, L G, Pj M. Molecular organization of Leishmania RNA virus 1. Proc Natl Acad Sci U S A. 1992;89. doi:10.1073/pnas.89.18.8596

204. Widmer G, Dooley S. Phylogenetic analysis of Leishmania RNA virus and Leishmania suggests ancient virus-parasite association. Nucleic Acids Res. 1995;23: 2300–2304. doi:10.1093/nar/23.12.2300

205. Sanchez EL, Lagunoff M. Viral activation of cellular metabolism. Virology. 2015;479–480: 609–618. doi:10.1016/j.virol.2015.02.038

206. Bushell M, Sarnow P. Hijacking the translation apparatus by RNA viruses. J Cell Biol. 2002;158: 395–399. doi:10.1083/jcb.200205044

207. Olivier M, Atayde VD, Isnard A, Hassani K, Shio MT. Leishmania virulence factors: focus on the metalloprotease GP63. Microbes Infect. 2012;14: 1377–1389. doi:10.1016/j.micinf.2012.05.014

208. Hutvagner G, Simard MJ. Argonaute proteins: key players in RNA silencing. Nat Rev Mol Cell Biol. 2008;9: 22–32. doi:10.1038/nrm2321

209. Nie L, Cai S-Y, Shao J-Z, Chen J. Toll-Like Receptors, Associated Biological Roles, and Signaling Networks in Non-Mammals. Front Immunol. 2018;9. Available: https://www.frontiersin.org/articles/10.3389/fimmu.2018.01523

210. Roach JC, Glusman G, Rowen L, Kaur A, Purcell MK, Smith KD, et al. The evolution of vertebrate Toll-like receptors. Proc Natl Acad Sci. 2005;102: 9577–9582. doi:10.1073/pnas.0502272102